The Thesis Committee for Vincent Anthony Clause
Certifies that this is the approved version of the following thesis:

Integrating Geologic and SRTM Data to Identify Geomorphologic Landforms in the Eastern Amazon River Valley

APPROVED BY
SUPERVISING COMMITTEE:

Supervisor:

Edgardo M. Latrubesse

Carlos E. Ramos Scharrón

Mark A. Helper

Integrating Geologic and SRTM Data to Identify Geomorphologic Landforms in the Eastern Amazon River Valley

by

Vincent Anthony Clause, B.A.

Thesis

Presented to the Faculty of the Graduate School of

The University of Texas at Austin

in Partial Fulfillment

of the Requirements

for the Degree of

Master of Arts

The University of Texas at Austin

August 2014

Dedication

I would like to dedicate this thesis to my beautiful wife, Blaire Clause. Thank you for your support and tender love. I am very blessed to have you in my life.

Acknowledgements

First and above all, I praise God for providing me this opportunity and granting me the capability to succeed. I would like to acknowledge and offer my sincerest gratitude to my supervisor, Edgardo M. Latrubesse, for his assistance, mentoring and support throughout my studies. I owe many thanks to my committee members Mark A. Helper and Carlos E. Ramos Scharrón for their assistance and valuable comments. The support from everyone in the Department of Geography and The Environment at The University of Texas at Austin made obtaining a Masters of Arts possible. I am very grateful for my parents who have provided me guidance throughout my life, and my grandparents, Tony and Sheila Clause who have always believed in me. I would like to give a final thanks to everyone in the Large Rivers group for their help and support throughout my studies.

Abstract

Integrating Geologic and SRTM Data to Identify Geomorphologic Landforms in the Eastern Amazon River Valley

Vincent Anthony Clause, M.A.

The University of Texas at Austin, 2014

Supervisor: Edgardo M. Latrubesse

Studies of the Amazon drainage network have primarily focused on the Western Basin and the Amazon Cone, but they have neglected the integration between these areas. Data presents a time gap in the Amazon's development and the forces responsible for the organization of the drainage network are poorly understood. A key element towards gaining an improved awareness of the Amazon is the Eastern Amazon River Valley. The focus of this study is an 80,000 km² portion of this area. An integrated method is adopted that combines terrain information derived from a digital elevation model with geologic data. The interpretation of DEM data is unique to this study. Seven distinct surfaces were identified, along with numerous erosional environments. This observation supports a geomorphologic record of numerous erosional events starting in the Miocene. This finding is significant as it rejects previous models for staircase-like terraces for the Amazon, and establishes a timeline for the development of geomorphologic landforms in the study area. In addition, neotectonics provide an alternative explanation to the

generation of topography in the study area. It was concluded that geomorphology in the study area is the result of physical and chemical weathering, and modified by neotectonics. These findings provide alternative means for Amazon landscape evolution.

Table of Contents

List of Tables

List of Figures

Chapter 1: Introduction

The Amazon is a well-studied system, however, gaps in our knowledge of how it developed over time remain. Studies have primarily focused on the Western Basin (Hoorn, 1993; Hoorn, 1994; Räsänen et al., 1995; Rossetti et al., 2005)) and the Amazon Cone (Dobson et al., 2001; Figueiredo et al., 2009, Gorini et al., 2014), while neglecting to identify how integration between these two areas occurred. Data presents a time gap in the Amazon's development (Latrubesse et al, 2010). Interpretations of events in the Andean zone, and changes in deposition patterns within the Amazon Cone promote an age for the system that ranges from the Middle Miocene (Figueiredo et al., 2009; Hoorn, 1994) to the Miocene-Pliocene (Gorini et al, 2014, Latrubesse et al., 2007). Forces responsible for the basins organization are also uncertain, both Andean uplift (Hoorn et al., 2010) and intraplate tectonics have been cited as contributing to this progression (Braun, 2010; Costa et al., 2001). Theory that pertains to the Amazon is also challenged by staircase terraces found in the Lower Amazon Region (Klammer 1984) that are not known to exist elsewhere in the system. A key element towards gaining an improved awareness of the Amazon basin is the Eastern Amazon River Valley (EAV) (Latrubesse et al., 2010). The EAV serves as a link between the Western Amazon and the marine cone, and can provide supplementary evidence to events that promoted the organization of the present Amazon Drainage System. By enhancing our knowledge of the EAV, current gaps in the evolution of the Amazon System can be better understood.

The EAV's Cenozoic history is currently hindered by a divergence in the timing of depositional events, and environmental changes that have contributed to the development of the geomorphologic units in the landscape. Primary contributors to this problem are a plateau landscape, and the detection of staircase terraces, as recently acknowledged by Mertes and Dunne (2008). Theory related to the plateau landscape supports multiple geologic interpretations (Caputo, 2011; Daemon and Contreiras, 1971; Sombroek, 1966) of depositional events in the EAV as well as several environmental changes that have led to their development (Costa, 1991; 1966 Irion, 1995; Radambrasil, 1977; Sombroek, 1966; Truckenbrodt et al., 1991). The staircase terraces are a controversial topic because they provide evidence for a period of deposition during the Late Cenozoic that has not been found elsewhere in the Amazon Region. The plan for this thesis is to identify and characterize these specific units while simultaneously relating them to others unit in the landscape. A more robust understanding of how the EAV landscape formed provides a better account of depositional and environmental histories for the region, and can also enrich current theory for the Amazon System.

Improving current models for the Amazon system requires an updated analysis and review of geomorphologic landforms in the EAV (Latrubesse, 2010). Toward this end, I examined a 80,000 km² area that encompasses a large portion of the Amazon River Valley in Eastern Brazil (Figure 1.1). This portion of the Amazon is unique because it includes plateaus and terraces.

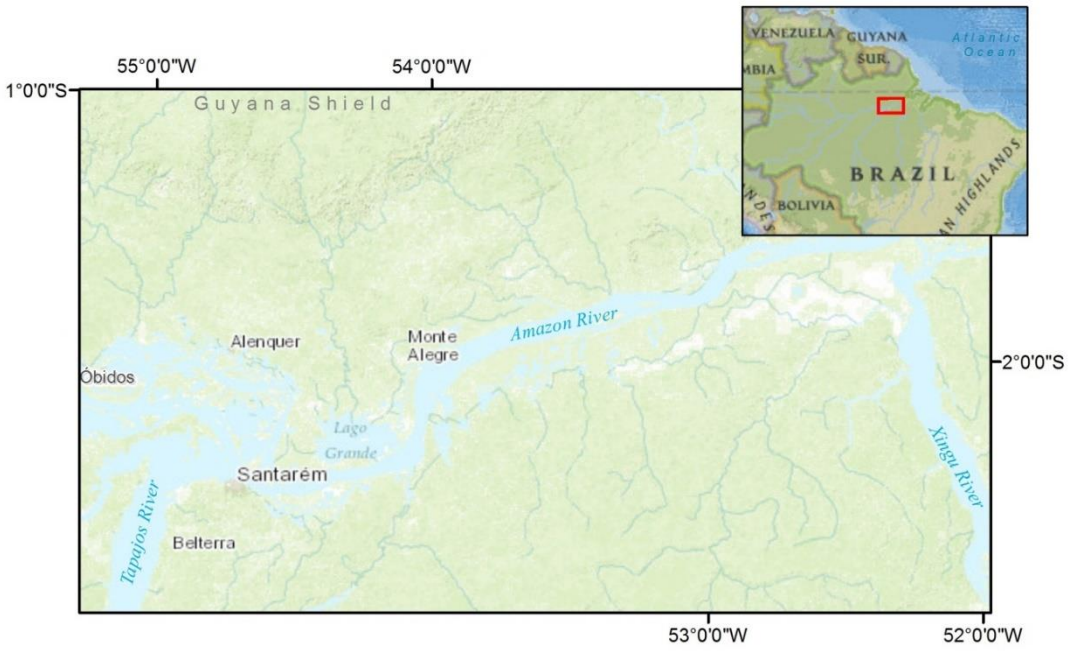

Figure 1.1. Location of 80,000 km² study area in E. Brazil.

Digital terrain modeling (DTM) techniques and geologic and regional data are used in this study to identify and contribute information that can help resolve contradictory interpretations of EAV development. The specific objectives of this study are to (1) identify and map geomorphologic units in the EAV. This objective is achieved by the creation of a geomorphologic map that identifies both erosional and depositional units. (2) Reconcile and resolve differences mapped here with those of other studies. (3) Identify influences of climate and/or neotectonics on the development of topography. This objective is achieved by viewing the units identified in the study area in relation to tectonic lineaments and climatic data found in the literature.

The data presented in this report will ultimately serve as a link by incorporating new information with old to fill gaps in the literature, while concurrently increasing awareness of geomorphic unit locations and their magnitude. To fully understand events that affected the modern Amazon River, we must first better understand the fundamental parts of the system, which this research intends to accomplish.

Chapter 2: Background

Introduction

The Amazon River System has developed over a mosaic of geological provinces (Almeida et al., 1981). The underlying lithology and structural controls that define these provinces not only provides information on temporal changes in the basin (Potter, 1977), but research has shown that many current landforms in the Amazon system are a product of these features (Almeida et al., 1981; Costa et al., 2001; Latrubesse, 2012; Potter, 1977). Because of this, any study of Amazonian geomorphology must be considered in relation to the surrounding geologic structures that may have impacted their development (Riccomini and Assumpção, 1999).

Published interpretations of EAV geomorphology are contradictory (Ab'Saber, 1967; Irion, 1984; Klammer, 1984; Truckenbrodt et al., 1991). Regional and geologic contexts provide a basis for evaluating the development of EAV geomorphologic units. After defining the study area and presenting the regional setting the study area is divided into four geologic domains. These are described in relation to the underlying geology and present geomorphology.

Regional Context

The study area is a 400 km long segment of the Amazon River Valley located primarily in the state of Pará, Brazil. The landscape is dominated by plateaus (Truckenbrodt et al., 1991), and a system of hills primarily drained by trellis and rectangular drainage networks (Costa et al., 2001). The landscape is blanketed by a dense vegetative cover as a result of being within a tropical wet climate zone, and receiving

rainfall of ~2000 mm/yr (Salati and Vose, 1984). The mean annual temperature and relative humidity ranges from 23.5° C to 26.9° C and 73% and 94% respectively (Guerra, 1959). The western boundary of the study is immediately east of Óbidos (~55°), where the easternmost gauging station in the Amazon River system exists due to tidal fluctuations that affect the downstream area (Mertes et al., 1996). The eastern boundary is 52° W, where the landscape transitions to an area of relatively low-lying relief (Costa et al., 2002). The northern and southern extents of the research area are confined within the 1° and 3° S latitudes (Figure 1.1).

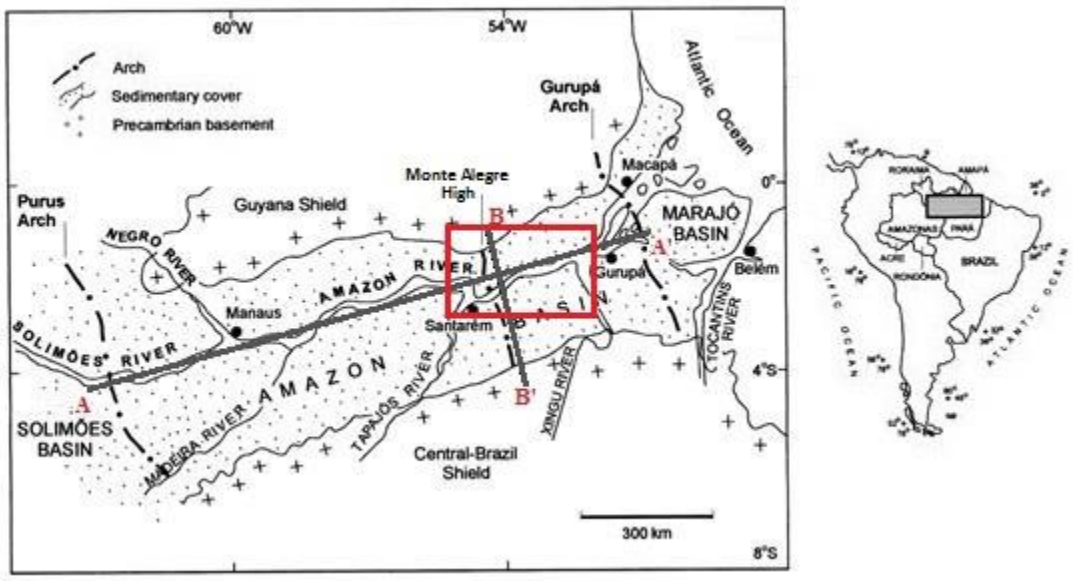

Figure 2.1. Amazon Sedimentary Basin and study area (red outline). Transects A-A' and B-B' correspond to figures 2.2 and 2.3 respectively (modified from Costa et al., 2001).

A large part of the study area is contained within the Amazon Sedimentary Basin (Figure 2.1), which underlies the area east of Manaus to the city of Gurupá, and is bounded by the Guyana Shield to the north and Brazilian Shield to the south (Figure 2.1).

In addition to being constrained between the two shields, it has also been suggested that the basins development was strongly influenced by structural highs, which are believed to impact depositional patterns (Almedia et al., 1981). The study area contains one of these features, the Monte Alegre High, which forms the divide between the Middle and Lower Amazon Basin (Mosmon et al., 1986) (Figure 2.2).

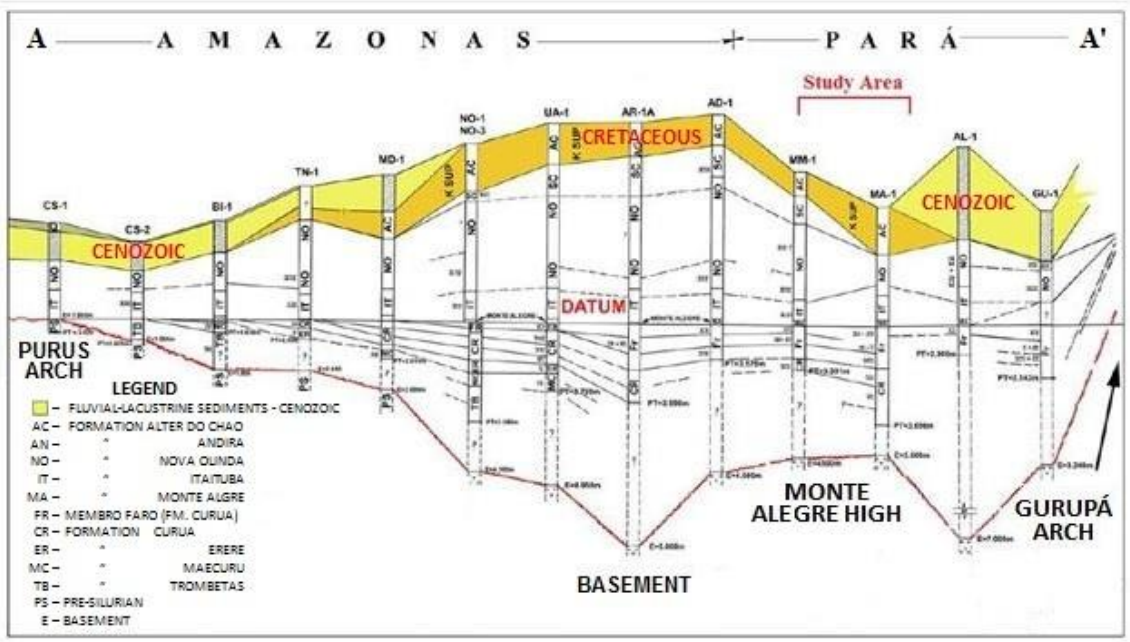

Figure 2.2. Stratigraphic cross section A-A' (see Figure 2.1 for location) of the Middle and Lower Amazon Basin, showing sedimentary thickness variations associated with basement highs. Study area is indicated (modified from Caputo, 2011).

The Amazon Sedimentary Basin has a record of being a depositional setting that dates to the Paleozoic when thick sequences of marine and fluvial-lacustrine deposits accumulated in a Paleozoic basin (Almedia et al., 1981). These units crop out in narrow belts along the Brazilian and Guyana Shields, and are present at basin depths of 4.5 km in the center of the basin (Figure 2.3). These basin depths are a consequence of Paleozoic and Mesozoic rifting and the development of graben structures associated with the early

stages of the breakup of Gondwana (Mosmann et al., 1986; Potter, 1997). During the Triassic, the separation event not only produced rifting along the Atlantic coast and Amazon Valley, it also produced uplift of the Guyana shield, and intrusion of igneous dikes and sills in Paleozoic rocks on the northern edge of the Middle Amazon Basin (Potter, 1997). These changes were enhanced by Late Jurassic basin extension and a period of strike-slip faulting that further helped develop the basin's axis (Costa et al., 2001). The combination of Paleozoic and Mesozoic rifting events produced subsidence of the underlying Precambrian rocks (Potter, 1997), allowing the basin to develop as a syneclise (Mosmann et al., 1986) (Figure 2.3). More recently, the basin has been influenced by neotectonic forces that enhanced the Amazon Sedimentary Basin axis (Costa et al., 2001).

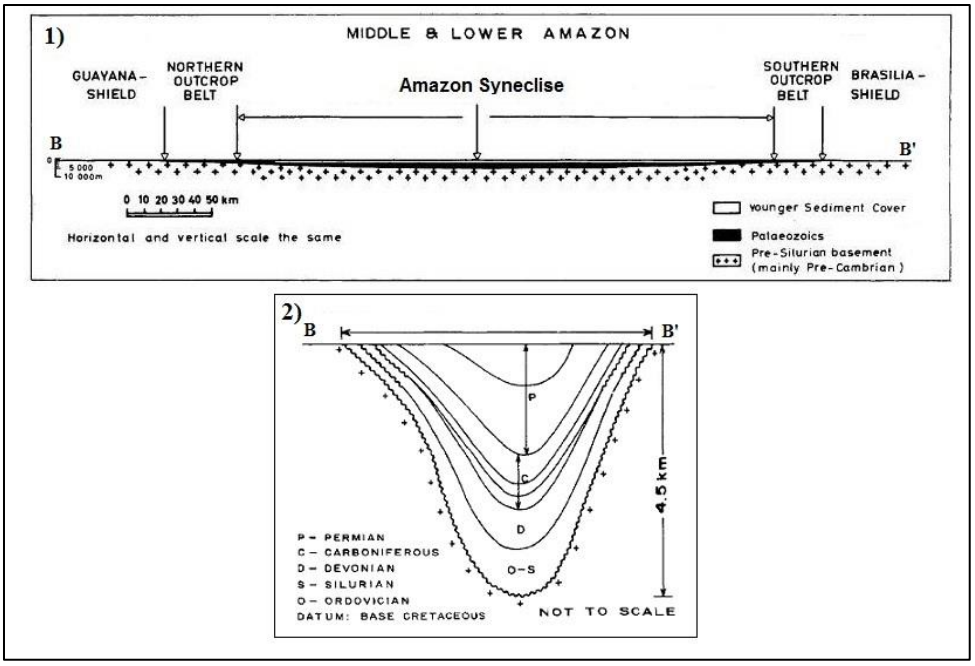

Figure 2.3. Stratigraphic cross section B-B' (see Figure 2.1 for location). Image 1 represents the shallow syneclise that is present in the Middle and Lower Amazon Basin. Image 2 displays a vertically exaggerated view of sedimentary fill (modified from Kroemmelbein, 1967; Mosmann et al., 1986).

Geologic Setting

The study area contains outcrops of Precambrian, Paleozoic, Mesozoic and Cenozoic rocks (Figure 2.4), and is primarily controlled by a E-W rift, E-W strike-slip faults and NE/SW normal faults (Costa et al., 2001). On the basis of geomorphic expression, this report segregates the study area into four distinct domains. The following section examines the geology and geomorphology of each domain. The section begins with the oldest rocks in the study area, the Guyana shield domain, followed by an examination of the Paleozoic Belt, Meso-Cenozoic Fill and Holocene floodplain. By understanding where these different units exist and the complex patterns associated with each, a better understanding of the geomorphology in the EAV can be obtained.

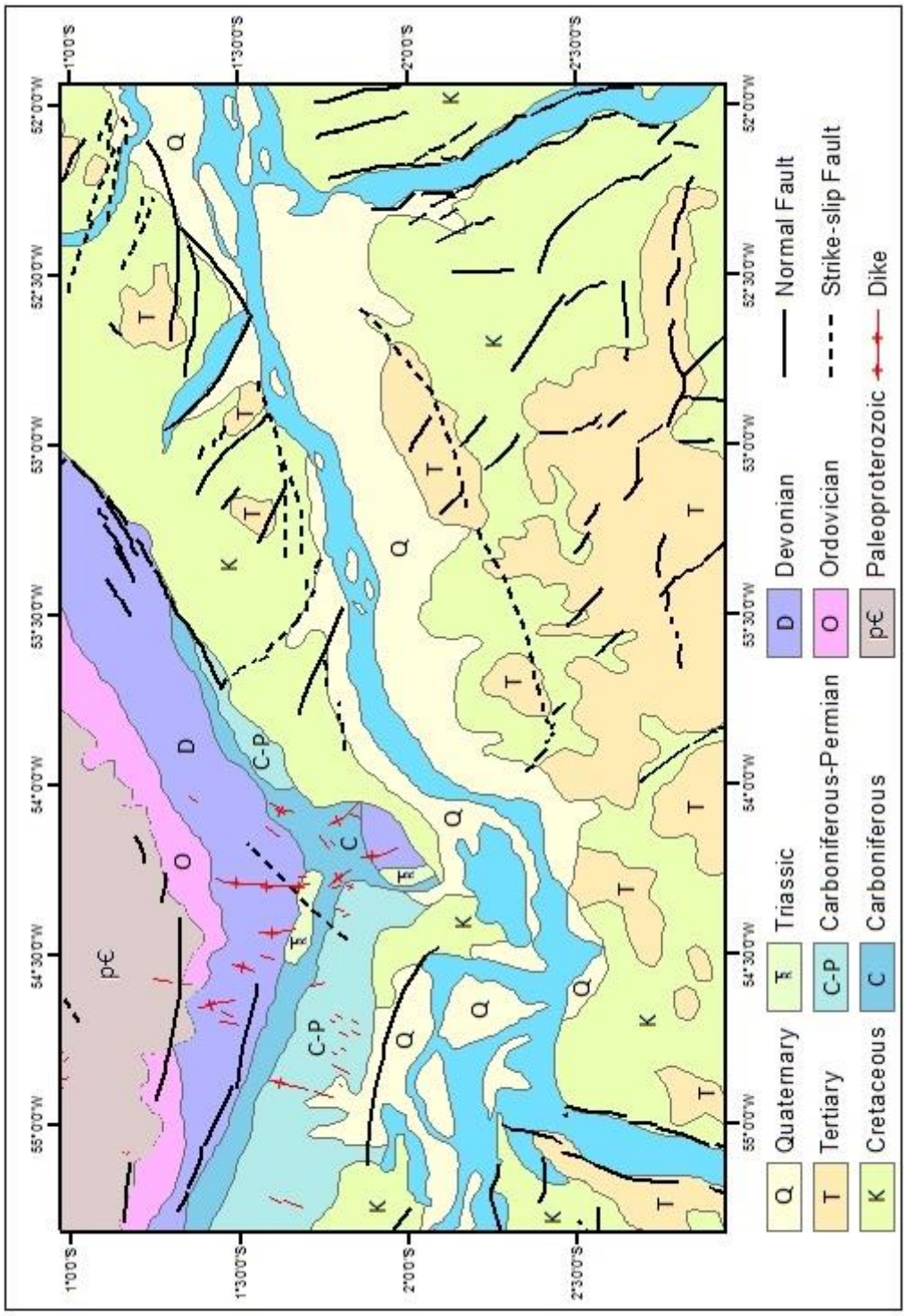

Figure 2.4. Geologic map of the study area. Data from the Geological Survey of Brazil - Companhia de Pesquisa de Recursos Minerais (CPRM).

Guyana shield

The Precambrian basement rocks that flank the outer limits of the Amazon River Valley are part of the Amazon Craton, and crop out as part of the Guyana shield in the northern portion of the study area (Melo and Loboziak, 2003). The geology in this domain is very complex due to numerous geotectonic cycles that have led to compound metamorphic lithologies, numerous fractures and unconformities between levels of the crystalline shield as well as younger metasedimentary and igneous rocks (Cordani et al., 1973). Although the domain was once a tectonically active environment, it has been a relatively inactive area since the Neoproterozoic with the youngest reactivation taking place ~ 900 mya and lasting until about 500 mya (Almedia et al., 1976; Cordani and Sato, 1999). Within the study area, the Guyana Shield is characterized by a highly eroded surface, and relatively low relief with a elevation near 250 m above sea-level (asl), as a result of uplift during the Mesozoic (Almeida et al., 1981; Klammer, 1984).The domain is bordered by the Paleozoic Belt to the south, where it begins to dip gently towards center of the basin defining the northern edge of the syneclise (Almeida et al., 1981; Milani and Zalan, 1999).

Paleozoic Belt

The Paleozoic Belt is north of the Amazon River and borders the E-W trending edge of the Guyana shield. Units dip gently, on average 1° - 3° southward towards the center of the basin. Variations in elevation and appearance of the belt are associated with the breakup of Gondwana and consequent volcanic and tectonic activity (Kroemmelbein, 1967). As a result of variations present in the rocks and unconformities, the belt is

commonly divided into three lithostratigraphic units (Melo and Loboziak, 2003), the Late Ordovician-Early Devonian Trombetas Group, Early Devonian-Early Carboniferous Urupadi and Curua Groups and the late Carboniferous-Permian Tapajos group (Figure 2.5).

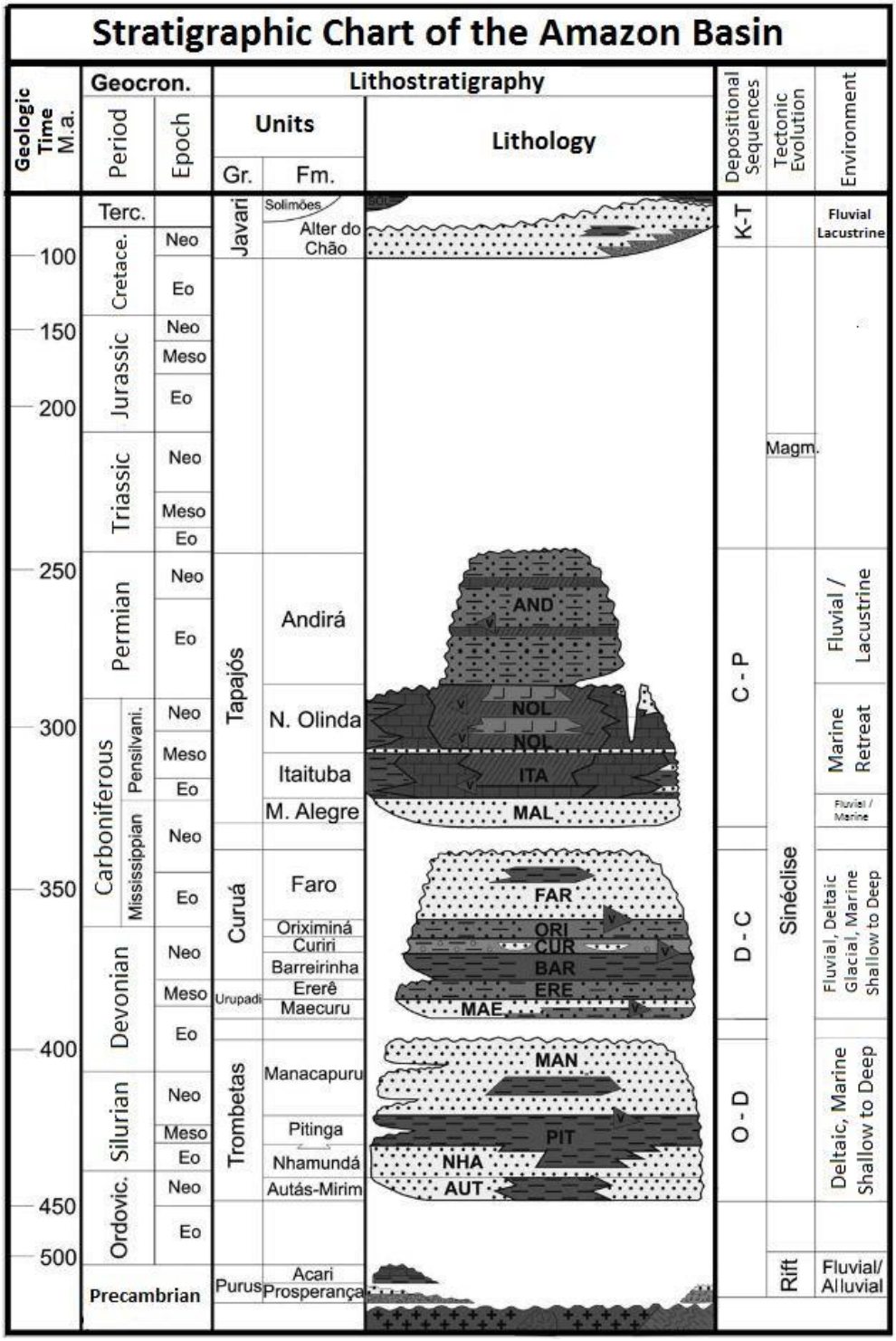

Figure 2.5. Amazon Sedimentary Basin stratigraphy (modified from Mendes et al., 2012).

The Trombetas Group was deposited pre-Gondwana rifting and is expressed on the southern edge of the Guyana Shield (Milani and Zalan, 1999). The group contains a mixture of fluvial-deltaic and marine clastic sedimentary rocks that reach a thickness of nearly 800 m in the center of the basin. This group underlies the highest elevations in the study area, and is characterized by a terrain with steep ridges and dissected hills formed by deeply incised fluvial valleys.

The Urupadi and Curua Groups crop out with a thickness of 50 km near the city of Monte Alegre and can be found at depths up to 1,600 m in the center of the basin. The rocks near the base of this group are described as a mixture of deltaic and tidal-flat sandstones in the lower limits and marine shale near the top. In the study area, these formations crop out between elevations of 120 - 160 m and underlie an erosional surface that is interrupted by dissected hill complexes.

The Tapajós Group was deposited during the early stages of rifting associated with the Gondwana breakup, and is the upper limit to the Paleozoic sequences found in the belt. The unit contains a mixture of sandstones, carbonates and evaporates that can be reach thicknesses of 1,500 m (Mosmann et al., 1984). The Tapajós Group crops out at elevations much lower than others in the belt and is primarily located in the western half of the study area where it appears as dissected hills that appear to form a surface. The lithologies contained within the Paleozoic record illustrate the lacustrine and marine coastal environments associated with regressions and transgressions events associated

with base level changes and the early stages of Gondwana rifting (Almedia et al., 1981; Melo and Loboziak, 2003).

Meso-Cenozoic fill

The Meso-Cenozoic fill reaches a thicknesses of 550 m in the center of the basin (Mosmann et al., 1984), and is found on both sides of the EAV. The domain contains rocks that range from the Late Cretaceous to Quaternary and is primarily comprised of a body of sedimentary rocks commonly referred to as the Alter do Chao Formation. These rocks are characterized by fluvial clastic material that range from mudstones to sandstone (Mendes et al., 2012), and include sections that act as a hydrologic aquifer (Geologico, Servico, and D. O. Brasil–CPRM). Within the literature, there is general agreement that the lower limit of units contained in this domain are Late Cretaceous (Figure 2.6), however the specific age and number of units that comprise the fill is controversial and will be addressed later in this report. The Late Cretaceous age for the lower limit of this domain and its outcrop pattern indicates that a regional angular unconformity existed that is associated with uplift and the breakup of Gondwana (Mosmann et al., 1984). The nearly 550 m of sediment that was deposited on top of this unconformity once again highlights that this area was a center for deposition through Cretaceous time.

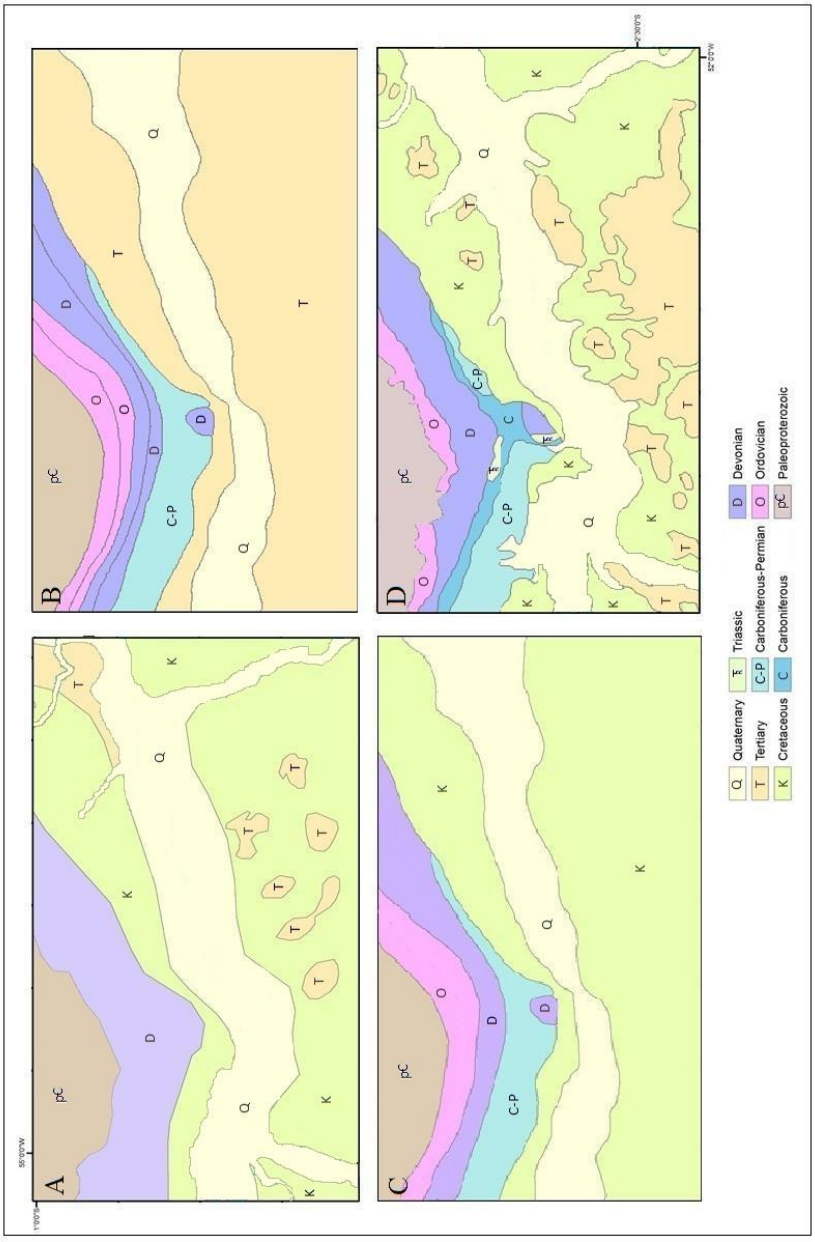

Figure 2.6. Geologic maps and interpretations of Meso-Cenozoic fill. Maps from four sources show a rather similar characterization of the Precambrian and Paleozoic rocks, but differ w.r.t. the distribution of Cretaceous and Tertiary units. (a) Brazilian Institute of Geography and Statistics (IBGE) (2006), (b) U.S. Geological Survey (2012), (c) Daemon & Contreiras (1971), (d) Geological Survey of Brazil (CPRM) (2011).

Within the literature the Meso-Cenozoic fill is commonly referred to as ‘terra firme’, a nomenclature used to describe land that does not flood (Sternberg, 1975). Even though the domain is relatively low-lying, it is morphologically complex. The most dominant feature is a plateau landscape that rises abruptly from the surrounding terrain (Figure 2.7). The plateaus are nearly flat topped, covered by a layer of ochre colored clays and dense rainforest vegetation (Irion, 1984). In the south, they appear as a nearly continuous surface except where intersected by fluvial valleys (Truckenbrodt et al., 1991). In the north, they maintain a butte or mesa type appearance and occur primarily in the eastern half of the study area. The lower elevations of the ‘terra firme’ landscape are characterized as a relatively well-drained undulating landscape (Soembroek, 2000).

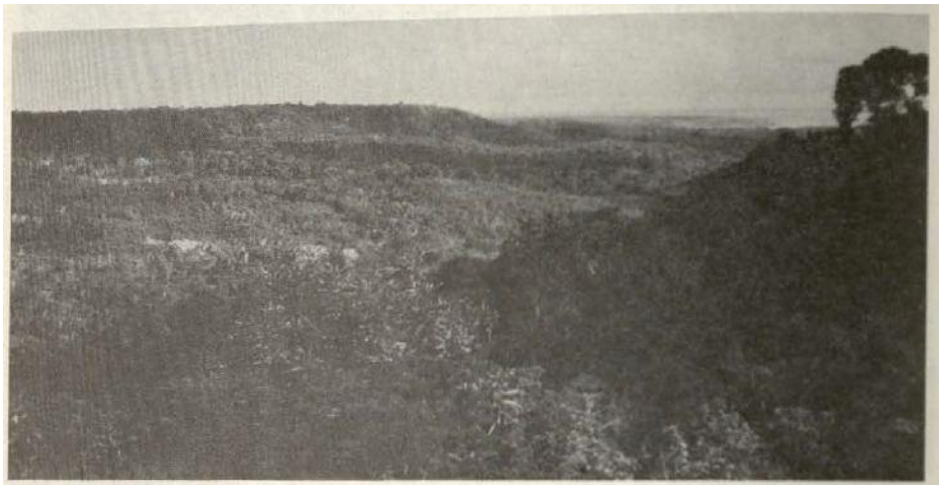

Figure 2.7. Historical picture taken by Sternberg (1975) a pioneer in the study of Amazon Geomorphology. Plateaus can be seen in the near right and distant left of the image, with ‘terra firme’ that maintains gentler relief between the two plateaus.

Holocene floodplain

The youngest domain in the study area is the Holocene floodplain. The domain is actively influenced by the Amazon River and its tributaries, and considered to be a remnant of Holocene climate change (Latrubesse, 2012). Measurements at Óbidos show that the river's average water discharge is 210,000 m^3/s, with an annual sediment flux between 600 and 1300 Mt yr^{-1} (Park and Latrubesse, 2014). Average sediment concentration is 176 mg/l, much lower than the upper reaches due to sediment poor waters draining from the Amazon depression and being farther away from the Andean zone, a key sediment source (Martinelli et al., 1989). Although the waters in this area contain a low sediment concentration, the floodplain is currently experiencing net deposition (Vital and Stattegger, 2000), with much of the sediment arriving to the floodplain from tributaries and small channels branching from the Amazon (Mertes et al., 1996).

Within the literature, the floodplain is referred to as the 'varenzá', a term commonly used to describe low lying land subjected to inundation (Sternberg, 1975). The geomorphology is comprised of an assortment of levees, lakes and lateral channels that vary significantly in their distribution. In the western portion of the study area the floodplain is relatively saturated and contains a complex mosaic of landforms (Figure 2.8). These landforms are relatively constrained to the north bank of the river where the floodplain shows signs of being both an impeded and a scroll dominated feature. The complexity of this portion of the floodplain is a relic of the confluence with the Tapajós River and the abundance of blocked fluvial valleys (Latrubesse, 2012). Downstream, the

channel sinuosity straightens to near 1 and islands and lakes dramatically reduce in size and number. The floodplain is still a dynamic environment, however, it is relatively mature compared to its western counterpart. This section of the floodplain is affected by strike-slip faults that enhance the generation of isolated lakes, and primarily crop out along the southern shore until reaching the Xingu River (Costa et al., 2001). East of the Xingu River confluence the floodplain shifts towards the northern shore and the size of islands begin to increase once again as the environment transitions towards a delta dominated depositional system (Vital et al., 1998).

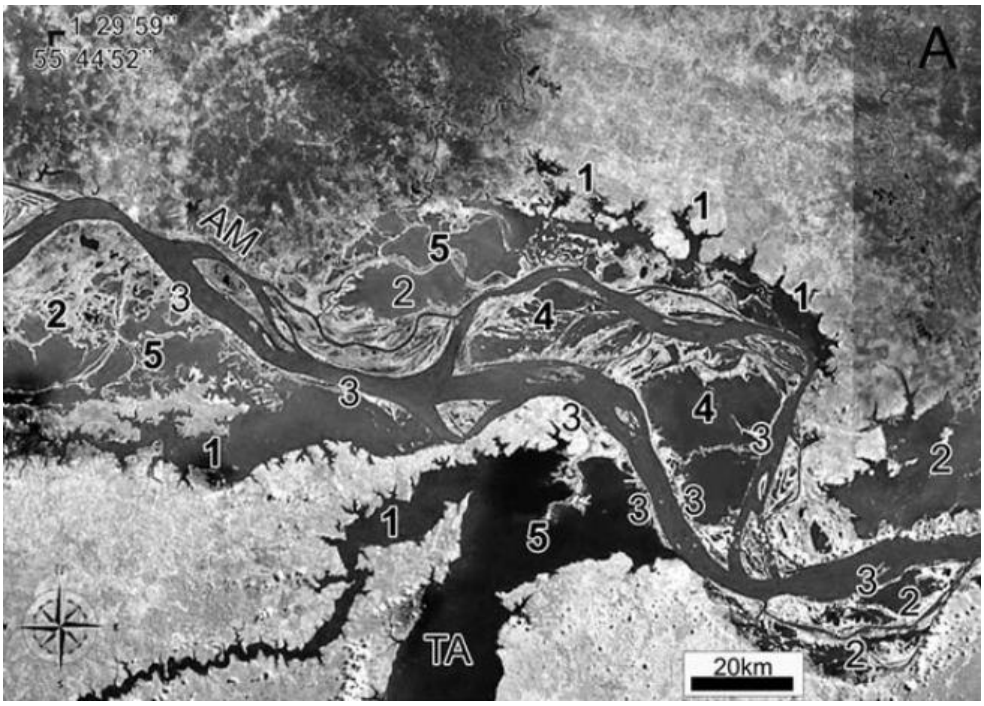

Figure 2.8. The western floodplain displays a complex mosaic of landforms within the 'varenzá' in the western limit of the study area (Latrubesse, 2012). Distinct features are numbered 1=blocked valleys 2=rounded lakes 3= levees 4= large islands and island lakes 5=delta system (Source: Latrubesse, 2012).

Neotectonics

The Amazon region contains several neotectonic structures that uniquely relate to transpressive and transtensive areas or a combination of both (Costa et al., 2001). Although the uplift of the Andean cordillera in Late Miocene triggered many types of movement in the Amazon basin, the controlling factor of South American neotectonics is primarily related to intraplate tectonics and the rotation of the South American plate to the west (Costa et al., 1996; Costa et al., 2001). Neotectonic events are known to have a profound impact on the development of waterways, to act as a control on sediment deposition patterns and to affect the development of landforms throughout the Cenozoic (Costa et al., 2001). The primary neotectonic features in the EAV are associated with the Monte Alegre, Lower Tapajós and Macapa Fault systems, all of which are believed to be presently active (Figure 2.9).

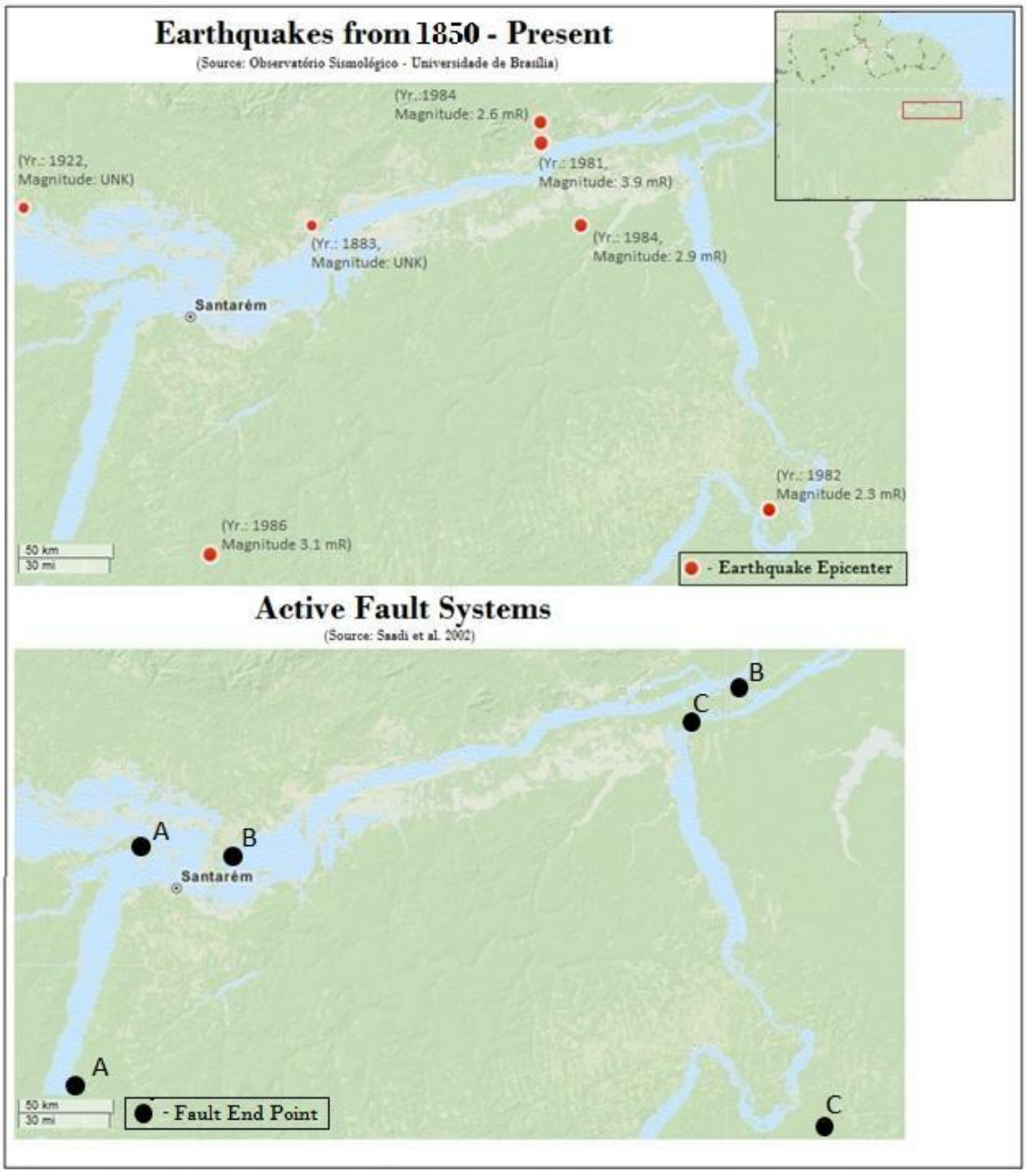

Figure 2.9. Neotectonic activity in the EAV. The two maps show a correlation between earthquake activity and fault systems. Earthquake epicenters indicate the year and magnitude of event in parentheses near point. Endpoint A = Lower Tapajós Fault System, Endpoint B = Monte Alegre Fault System, Endpoint C = Lower Xingu Fault System.

According to Costa et al. (2001) two major periods of neotectonic activity are responsible for variations in relief and drainage patterns in the EAV. Costa et al. (2001) suggests that the first neotectonic events occurred during the Late Tertiary and are responsible for NE-SW, ENE-WSW trending folds and reverse faults along the Tapajós River near the city of Santarem (Figure 2.10). In addition, dextral strike-slip faulting and normal faulting along the Amazon River near the Mouth of the Xingu River remained active until the Late Tertiary (Figure 2.11). These faults are responsible displacements along the northern shore and act as a control on drainage patterns in this area (Costa et al., 2001).

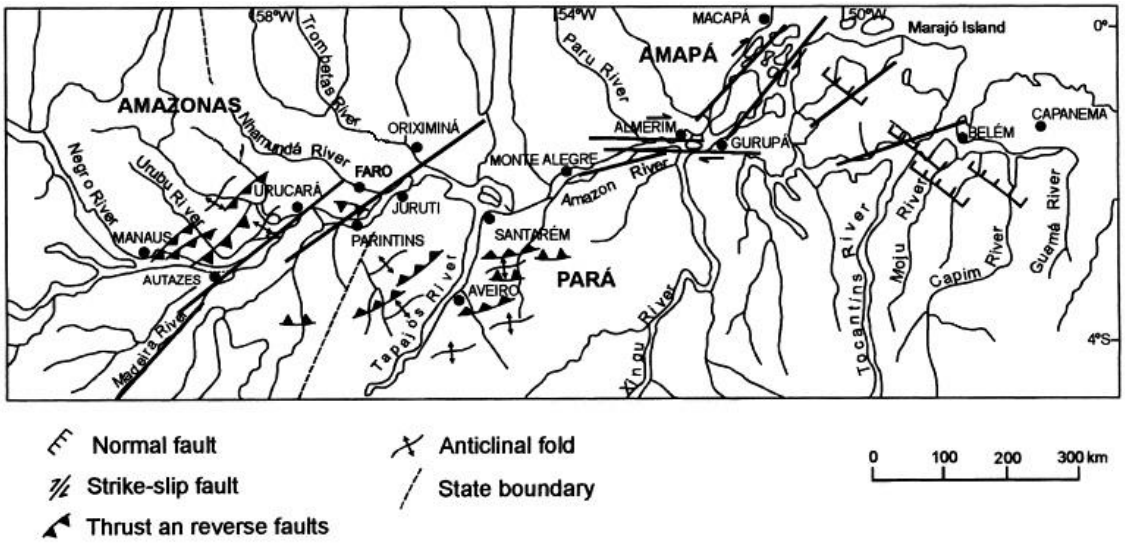

Figure 2.10. Late Tertiary neotectonic features of importance are located between Tapajós and Xingu Rivers (modified from Costa et al., 2001).

The second period of neotectonic activity began in the Late Pleistocene and remains active. It is marked by ENE-WSW strike-slip faults in between the Tapajós and the Xingu Rivers, NNW-SSE normal faults along the Xingu River and NE-SW normal

faults that along the Tapajós River (Figure 2.11). Neotectonic activity in this area is believed to be responsible for many anomalies within the terrain, with the most obvious being related to normal and strike-slip faults along the nearly straight segments of the Lower Tapajós and Lower Amazon Rivers. The strike-slip faults are also responsible for the blocked mouths of the Tapajós and Xingu Rivers, a floodplain that reaches 80 km in width and large isolated lakes (Costa et al., 2001).

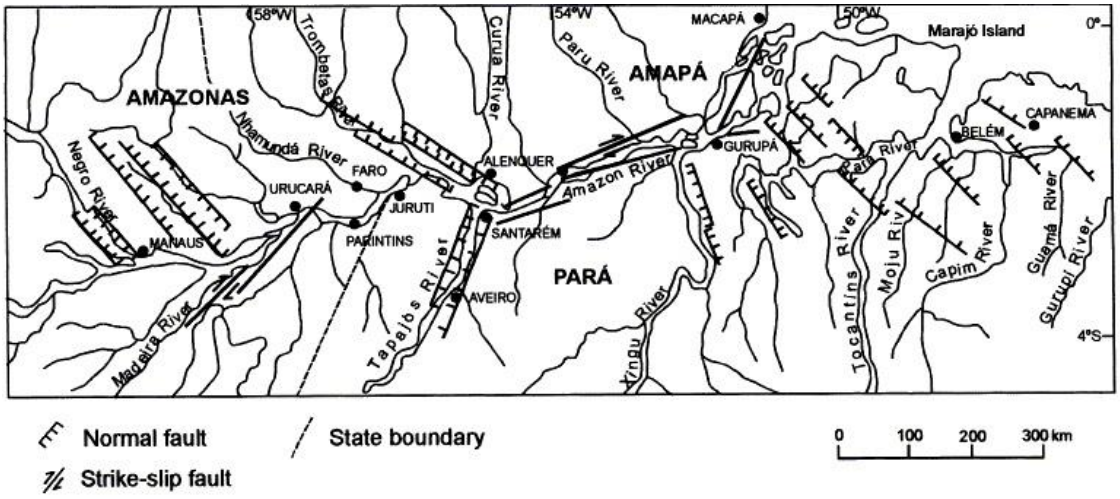

Figure 2.11. Late Pleistocene neotectonic features of importance are located between Tapajós and Xingu Rivers (modified from Costa et al., 2001).

Chapter 3: Methods and Data

Introduction

This report employs an integrated method that combines data found in the literature with terrain information derived from a digital elevation model (DEM), a common tool used in geomorphologic studies (Carvalho and Latrubesse, 2010; Latrubesse and Restrepo, 2014). This method is somewhat underutilized in tropical regions due to dense vegetative cover that can magnify errors in elevation values (Baugh et al., 2013), however, error correction techniques can be applied to minimize this effect (Wilson et al., 2007). The aim of this method was to develop a comprehensive understanding of the physical environment in the EAV that would aid in the development of a geomorphologic map while simultaneously identifying where problematic areas in the literature may exist. This method provides the necessary data needed to better understand the study area and previous observations. The interpretation of DEM data is unique to this study. A Geographic Information System (GIS) allowed for assessment of the data in a geographic setting, provided an interface that allows for the juxtaposition of datasets and supplied tools that assisted in the creation of a geomorphologic map. This chapter begins by presenting the working procedure connected to the methodology, and the workflow used to create the geomorphologic map included in this report. In addition, this chapter identifies data that contributed to this report, and closes with an overview of the products and techniques used to identify geomorphologic landforms.

Methodology

The working procedure that this report follows is organized into four steps; data acquisition, data processing, identification and interpretation and presentation of the data. The section below provides a general overview of each step (see Figure 3.1).

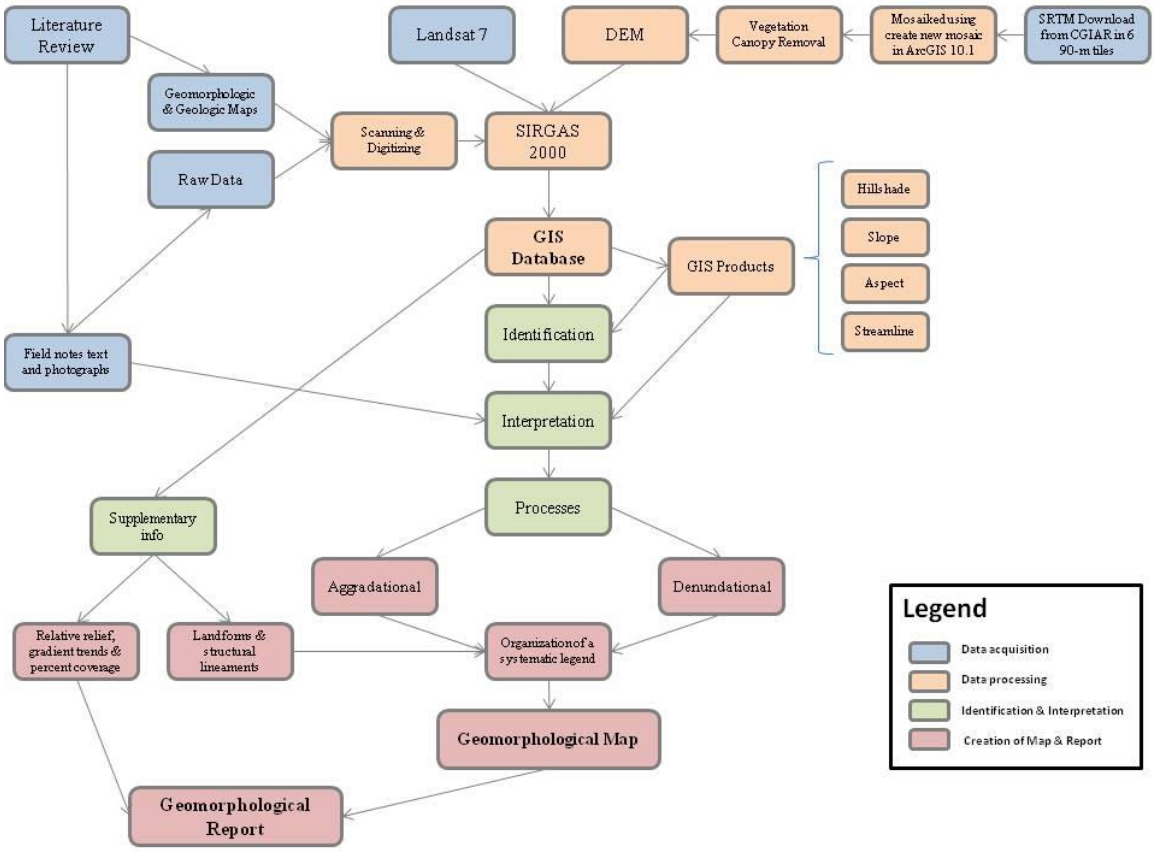

Figure 3.1. Methodology flowchart, color coded to correspond with main steps in working procedure.

Data Acquisition: Geospatial datasets relevant to this study were obtained through a number of agencies. The data included a DEM, aerial imagery and geologic shapefiles. In addition to these spatial datasets a comprehensive literature review was conducted to search for additional data that could contribute to this report. Data obtained

during this process included photographs, geomorphologic and geologic maps, field notes and sedimentological data.

Data Processing: To attain a working GIS environment all data included in this report underwent pre-processing to ensure that it could be readily compared. This included scanning and georeferencing of data found in the literature, mosaicking of DEM tiles, vegetation canopy removal and ensuring that all data were displayed with a uniform projection. Data were projected to SIRGAS 2000, a variant of an Albers equal area conic projection. This projection provides minimal distortion of areas, and has horizontal units in meters. In addition to pre-processing, digital terrain modeling (DTM) products were created to model surface parameters useful for interpreting the earth's surface.

Identification and Interpretation: This analysis assumes that geomorphologic units have unique patterns that can be detected with remote sensing and DTM techniques. These patterns are recognizable because of differences in tone, texture and shape (Walstra et al., 2011). When viewed over a continuous surface these patterns can aid in the delineation of landform boundaries, which can lead to process identification (Pike, 2000). Working under this assumption, a comprehensive analysis of digital terrain images was undertaken to identify where similar units and boundaries in the landscape may exist. In addition to visual interpretation, topographic profiles were generated to differentiate between landforms with similar appearances. To provide further insight into units identified with the previous techniques, supplementary information was created with tools available in the GIS. This included information on relative relief, gradient trends and percent coverage charts. In addition to identifying and characterizing

landforms the techniques listed above were also used to survey data presented in the literature. Each unit was then categorized as an erosional or aggradational unit by incorporating interpretations found in the literature.

Creation of a Geomorphologic Map: This report follows the general concept that landscapes contain a set of genetically interconnected landforms that can record the development of a system (Latrubesse, 2006; De Graaff et al., 1987). To gain a better understanding of these relationships in the EAV, units were mapped and incorporated into a genetic classification system that discriminates between aggradational and erosional landforms. This classification scheme specifically aided in recognizing the morphogenesis and morpho-arrangement of landforms in the study area; both attributes critical to developing an improved understanding of the landscape.

(i) Map Procedure: Previous steps lay the foundation for a geographic database that integrates numerous datasets and parameters useful for the creation of a geomorphologic map. To delineate the units identified in the previous step the report uses shapefiles that allow for the creation of layers tied to a geographic location. The first step in the mapping process was to delineate features with sharply defined contacts. This included water bodies, floodplains, hill complexes and plateaus. These units where used as reference markers because they appear as abrupt changes on nearly every DTM product. The next and more difficult step was the delineation of units with similar appearance, but that occur in different elevation ranges. This required combining both elevation transects and hypsometric maps to map boundaries that divide the surface of a

unit from the scarp or debris slope. In addition to the newly created shapefiles, structural lineaments and drainage networks found in the literature were included in the map.

(ii) Map design: The map included in this report was designed with the intention of creating a product that could be useful for understanding changes that lead to development of the present day EAV. The map uses both polylines and polygons to identify units in the landscape. Polylines were useful for displaying linear elements such as escarpments and faults, whereas polygons were used to delineate the area that a specific unit occupies. In order to accommodate the number of units included in the map both color and patterns were used to enhance differences between geomorphologic units. Units with similar characteristics or origin were mapped with similar colors, and patterns were used to help further subdivide the unit and enhance readability. The genetic classification system used in this mapping project classifies a unit to currently be acting as a depositional or erosional landform. Because of these divisions the legend is arranged in three parts. The first part is features and includes structural lineaments and other landforms that may lead to anomalies in the landscape. The second division separates erosional landforms and includes plantation surfaces, hill complexes and sloping debris and/or cliffs. The final division in the legend includes aggradational landforms, which in the study area is the buildup of colluvium and depositional floodplains.

Data and Tools

Primary and secondary datasets are used to carry out the methodology described in the previous section. Primary datasets are considered to be geospatial products that directly aided in the creation of the geomorphologic map. These include the DEM, and

Landsat 7 imagery. Primary datasets were incorporated into either ArcGIS 10.1 or Global Mapper 15, two geographic info software packages that together provide a wide range of functions useful for interpreting and manipulating geographic data. Secondary datasets are those that assisted in the interpretation of landforms, and helped to develop a better understanding of the landscape. The secondary datasets were critical to this research since field work was not feasible.

The basemap utilized in this report was Landsat 7 imagery. Landsat imagery is multi spectral, however for the purpose of this project only the natural color bandwidth combination was utilized. Landsat imagery provided a ground control useful for georeferencing figures (Walstra et al., 2011) and provided a check on units identified by DTM products. Although the basemap provided meaningful information, the DEM was the most valuable dataset. It not only provided elevation values, but was also manipulated to provide additional visualization and DTM products. The specific DEM utilized in this report is a derivative of the finished-grade 90-m Shuttle Radar Topography Mission (SRTM) data downloaded from http://srtm.csi.cgiar.org/Index.asp on November 8th, 2012. The elevation values contained in this dataset have global relevance as they are referenced to the sea level datum of the Earth Gravitational Model 1996. This dataset is finished in the sense that it has been edited to remove large sinks and spikes, provide more flattened water bodies and provide better transitions to areas with high slopes. A detailed description of the interpolation techniques used to create the DEM can be found at srtm.csi.cgiar.org/SRTMdataprocessingmethodology.asp.

SRTM vertical accuracy in a tropical region is hindered by dense vegetative cover. In tropical rainforest the error has been shown to be on average 22.35 m over a smooth surface (Carabajal and Harding, 2006), compared to the normal average of less than 7m (Rodriquez et al., 2007). To correct this error and relate the values obtained from the DEM to actual bare earth measurements, SRTM vegetation removal techniques were applied following a method developed by Baugh et al., (2013) for the floodplain region and Carabajal and Harding, (2006) and Wilson et al., (2007) for the 'terra firme'. These methods follow the premise that a relatively uniform spatial error exists between areas with similar vegetation and canopy cover.

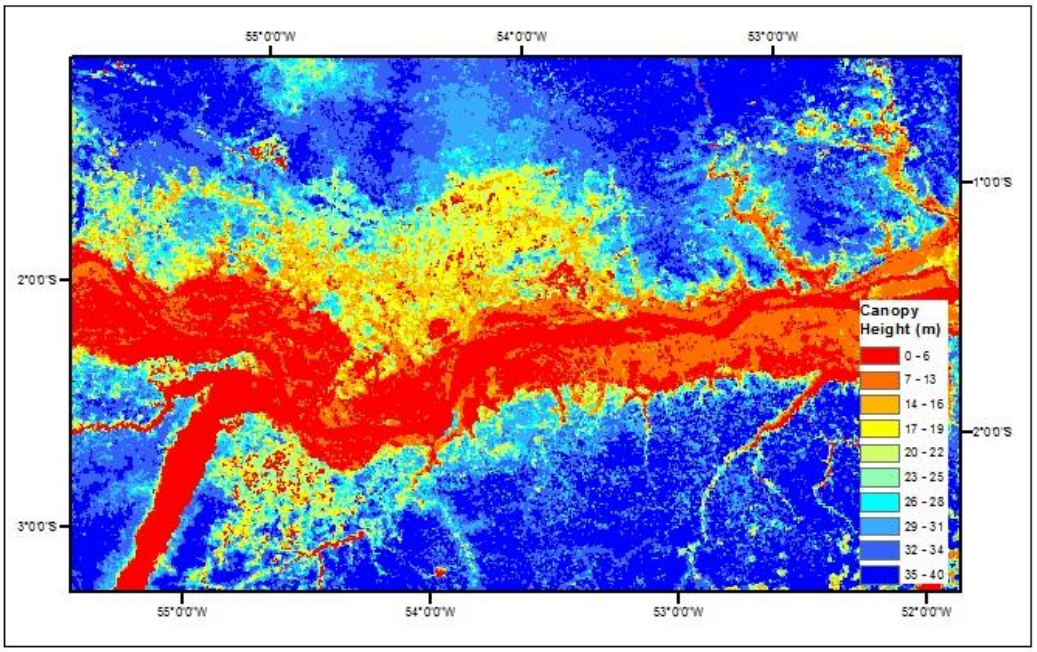

Figure 3.2. Vegetation height grid with 1 km resolution, obtained from Simard et al. (2011).

Vegetation heights for the study area came from the global vegetative cover dataset of Simard et al. (2011) (Figure 3.2). The dataset has a 1 km resolution. Following the methods discussed previously, geoprocessing tools were used in combination with the raster calculator tool in ArcGIS 10.1 to separate elevation values between the floodplain, water features and other land (Figure 3.3). Using these subsets a 50% decrease in canopy heights was applied to the vegetation values within the floodplain and a 60% decrease in canopy heights was applied to the vegetation values located in the 'terra firme' region. These new vegetation heights were then subtracted from the SRTM dataset to obtain elevation values that more accurately resemble the Earth's surface.

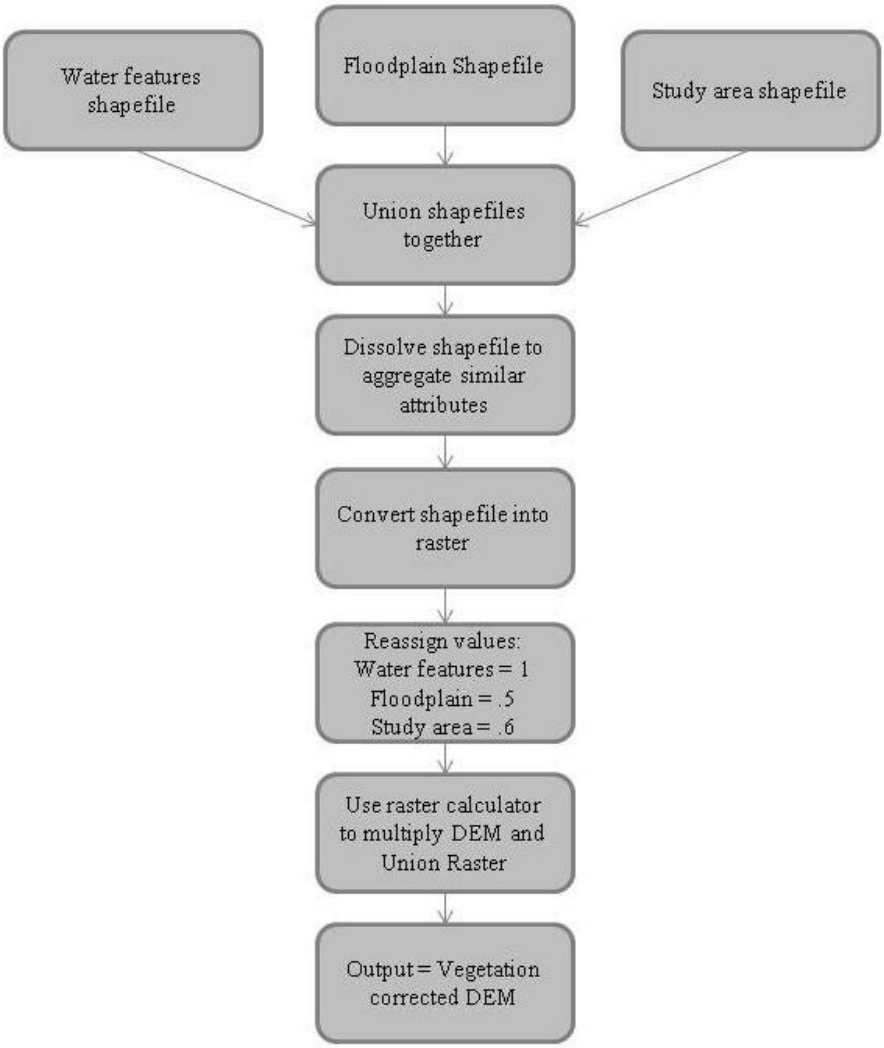

Figure 3.3. Vegetation canopy removal flowchart.

DEM: Derivatives and Derived products

DEM visualization products and terrain derivatives were used to identify and characterize geomorphologic units. Visualization products aided in developing a sense of relief and the magnitude of certain features, while the DTM products provided an additional layer of topographic information and/or highlighted statistical differences between cells. These tools helped to identify patterns and attributes related to specific

processes, and aided in the delineation of boundaries over large spatial extents. The GIS not only incorporates these tools and products into a database but also allows for different types of data to be integrated with one another through the process of layering, a fundamental advantage of a GIS system.

Hillshade

A hillshade model was created for the study area in both ArcGIS 10.1 and Global Mapper 15 to visualize the shaded relief of features in the landscape. By using both the azimuth and altitude of an artificial light source above the horizon the GIS provided an intensity value for each cell based on the angle that the source intersects the cell. The GIS then interprets these intensity values and outputs a surface that highlights the sun's shadowing effect on the landscape. The hillshade image provides what appears as a bare earth image that illuminates variations in relief (Figure 3.4). This product was a fundamental tool in understanding the spatial distribution and variation in geomorphic landforms with high amounts of relative relief across the study area.

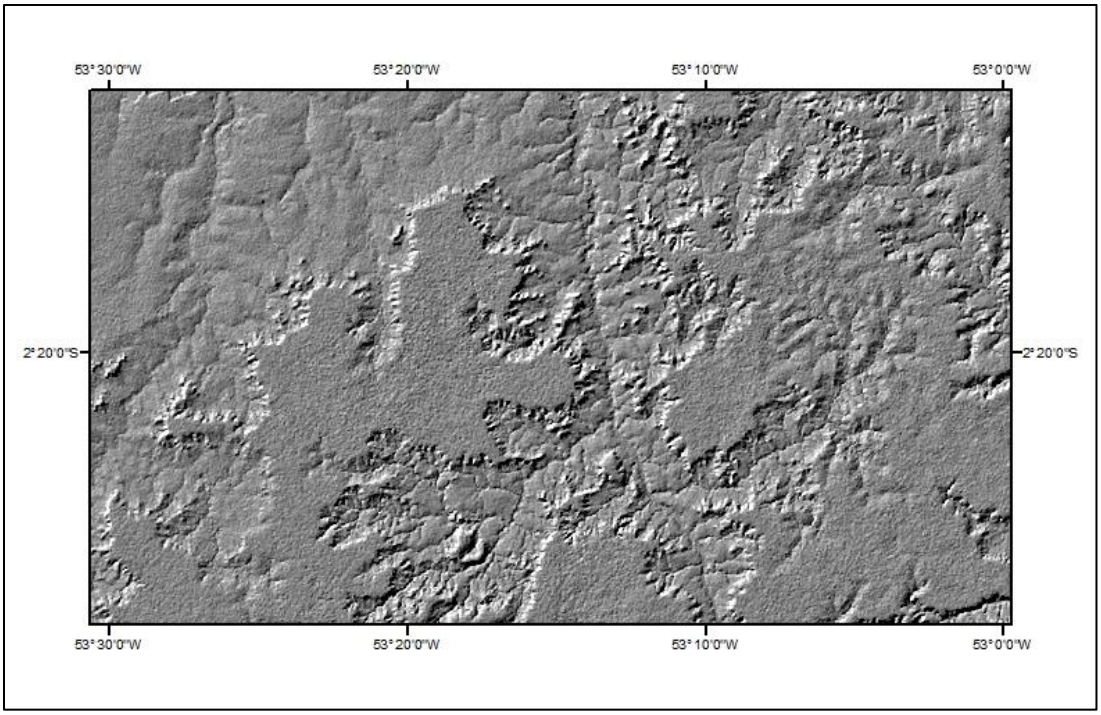

Figure 3.4. Hillshade image illuminates plateaus in the southern half of the study area by using an azimuth of 315 and elevation of 45.

Slope

Slope, the 1st order terrain derivative, was calculated in ArcGIS 10.1 through use of the HORN algorithm in the Spatial Analyst toolbox. Each cell within the raster is viewed in a 3 x 3 cell window and assigned a value based on its relationship to its eight surrounding cells. This value is the maximum rate of change between the cell and its neighbors. Slopes were used to identify and assess the magnitude of breaks in the landscape, and identify where units of relatively similar relief may exist. It was especially helpful when delineating escarpments, floodplains and visualizing where subtle surfaces may exist (Figure 3.5).

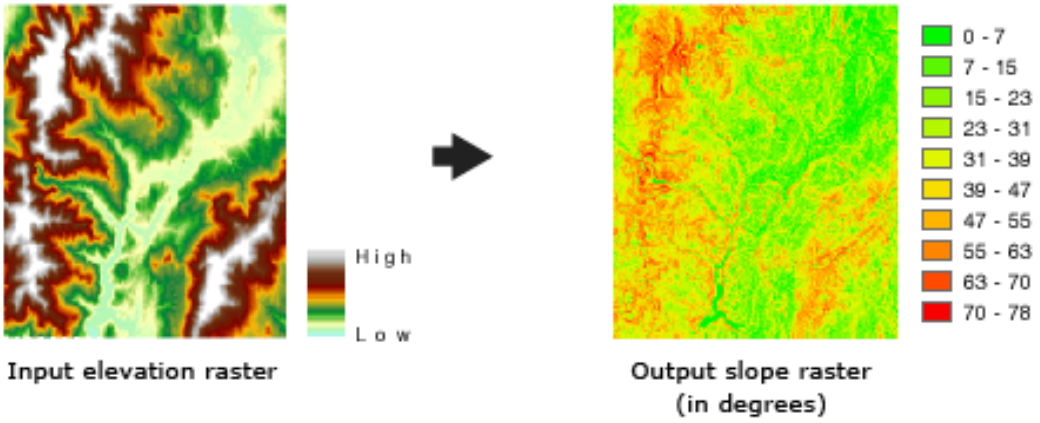

Figure 3.5. Slope modeling with a hypsometric DEM image (left) and a slope raster (right).

Aspect

Aspect, another 1st order terrain derivative was created in ArcGIS 10.1 with the Spatial Analyst tool box. It illuminates trends in the orientation of cells within the DEM. This provided an additional visualization element that specifically aided in the identification of flat surfaces. Although similar to the hillshade model in appearance, a benefit of this model is that it helped highlight level surfaces in lower lying areas. A limitation is that it does not provide a sense of relative relief. In figure 3.6 the red outlines highlight several areas where the terrain remains relatively horizontal. The units transition from lower elevation in the north to a higher elevation unit in the south, a trend that would be hard to recognize with this image alone. The normal ArcGIS aspect output is a coded grid in relation to cardinal directions, however, a stretched color ramp based on the directional degree provided a more useful output for this report.

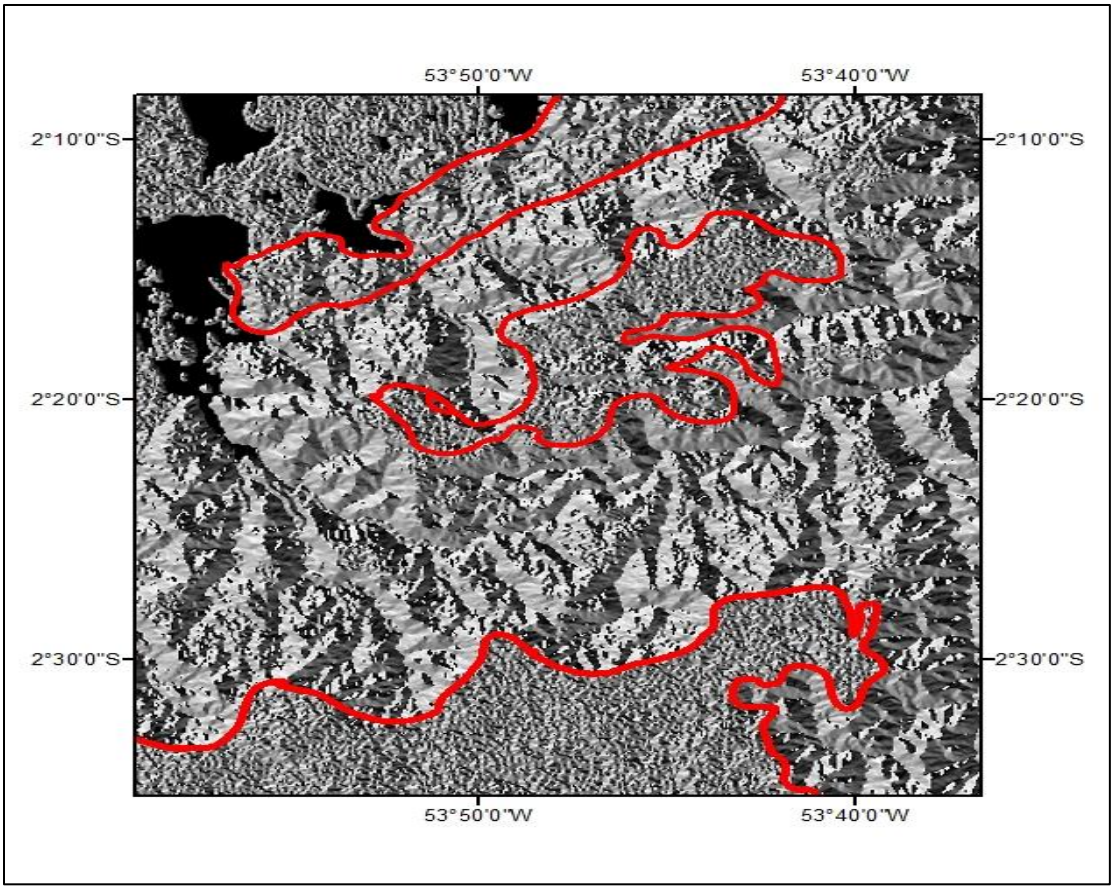

Figure 3.6. - Aspect image of the southern half of the study area. The red outlines highlight areas of different elevation that maintain relatively smooth surfaces.

Transects and Profiles

Transects and profiles were created in ArcGIS 10.1 using the 3D Analysis toolbox which provides a series of tools that can be used to extrapolate values from a raster through digitized points, lines and polygons. When using this function on a DEM the extracted values correspond to the elevation value stored in the corresponding cell. For this report the extraction of elevation values along a transect line was the most useful function of this toolbox. This function allows for the creation of both topographic and longitudinal profiles. Profile graphs were used to detect knick points between geomorphic

landforms, measure relative relief, and to help visualize stratigraphic relationships between units. A limitation of the GIS software is that it does not provide information on vertical exaggeration of the standard topographic profile output. To correct for this and measure the vertical exaggeration the data was exported to Adobe Illustrator which allows for scaling of the x and y axis.

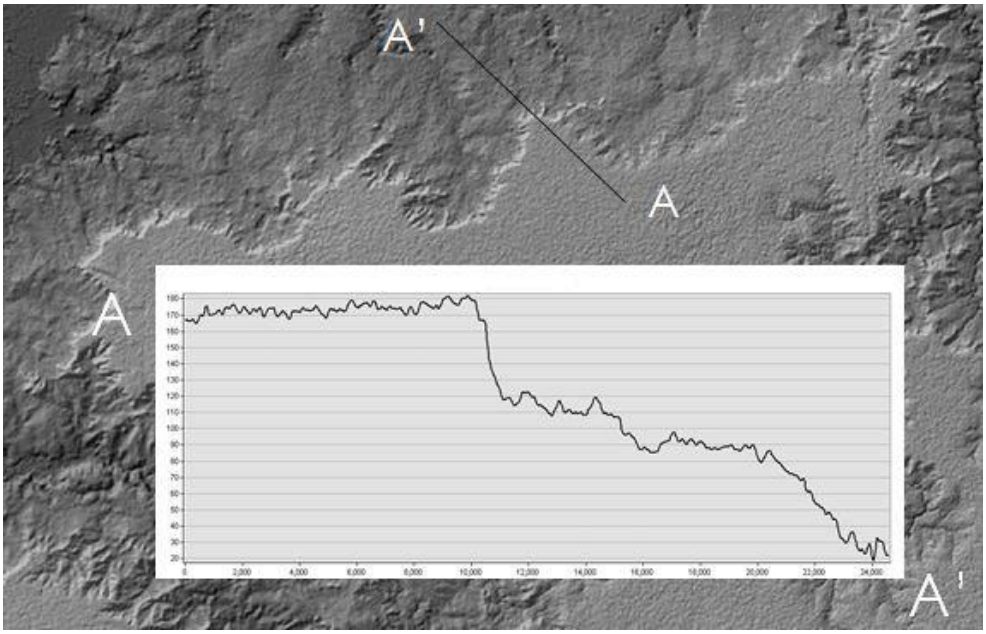

Figure 3.7. Transect output illustrates the relationships between the hillshade model and the DEM. The vertical exaggeration is unstated but significant.

Chapter 4 - Results and Analysis

Introduction

This chapter provides an inventory of geomorphologic units identified with a GIS and related products in the EAV. By using a pattern to landform identification technique and the genetic classification scheme discussed in Chapter 3 the GIS allowed for the delineation and characterization of seven distinct surfaces, and numerous erosional environments which are displayed in Figure 4.1.

To better understand the relationships between units, the following section highlights characteristics unique to each. Although many of these units are spatially autonomous by sharp variations in shape and form, an emphasis is placed on the units elevations to better understand relationships between different parts of the study area. Thus transects are used generously throughout to identify knick points and general trends and fluctuations in elevation. The units identified in this chapter provide the data needed to better understand both the plateau and terraces landscape.

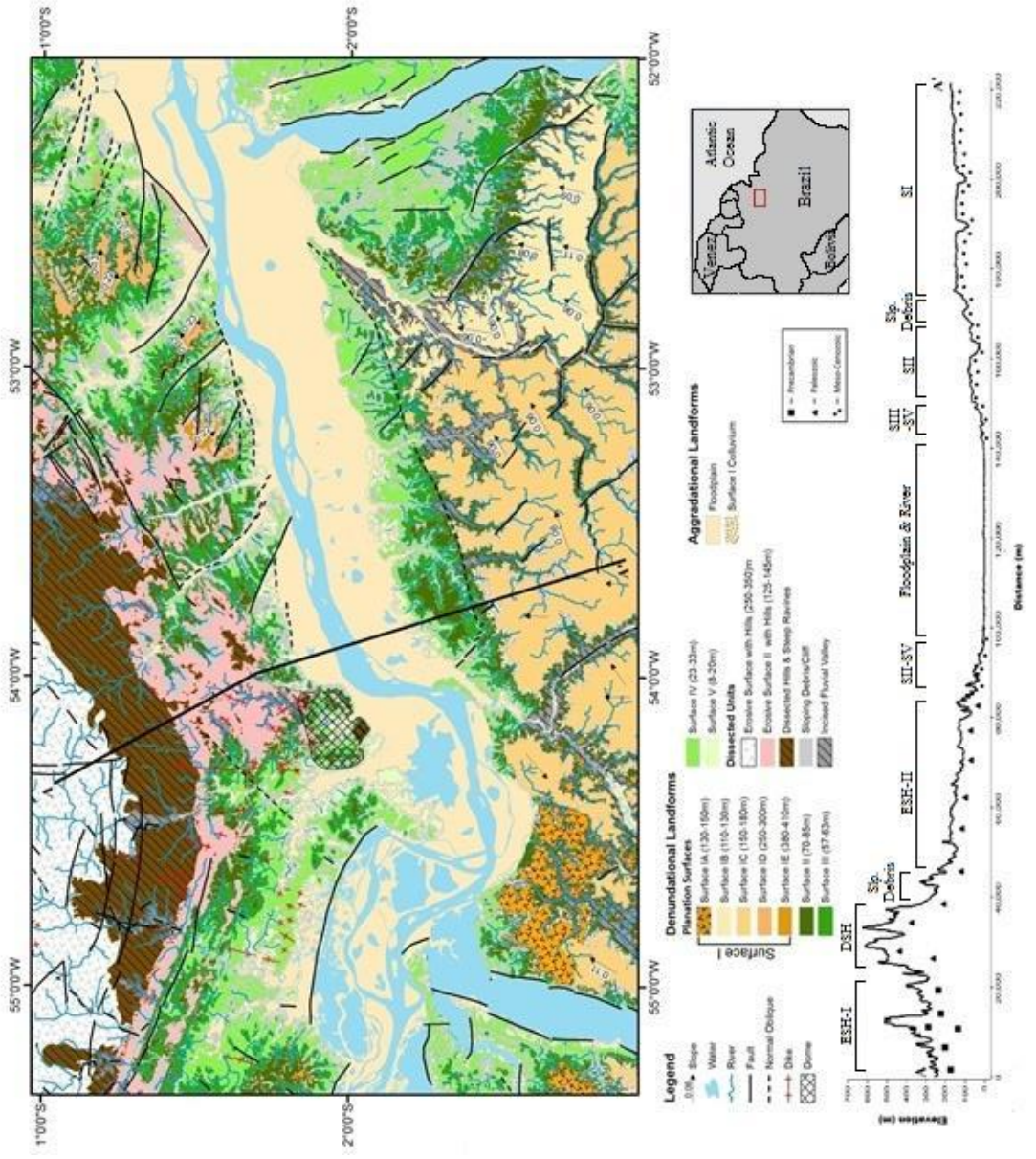

Figure 4.1. Geomorphologic Map of the study area .The units in this figure were identified with the analysis conducted in this report except for water features and tectonic lineaments, these shapefiles were obtained from CPRM.

Geomorphologic Units

Erosive Surface with Hills (ESH-I)

The erosive surface with hills occurs nearly exclusively within the Guyana Shield in the northwest portion of the study area. The surface is characterized by an undulating topography that predominantly maintains elevations between 200 - 250 m (Figure 4.2). Higher elevations occur where the surface is interrupted by ~20 m hills, and occasionally larger hill complexes that reach upwards of 450 m. The surface appears to be relatively well drained by dendritic/pinnate drainage patterns that drain towards the Amazon valley axis. Near the Paleozoic Belt to the south, the surface is interrupted by E-W trending normal faults that are responsible for offsets that ranges from 10 - 30 m. There is no apparent correlation between their location and hill complex occurrences.

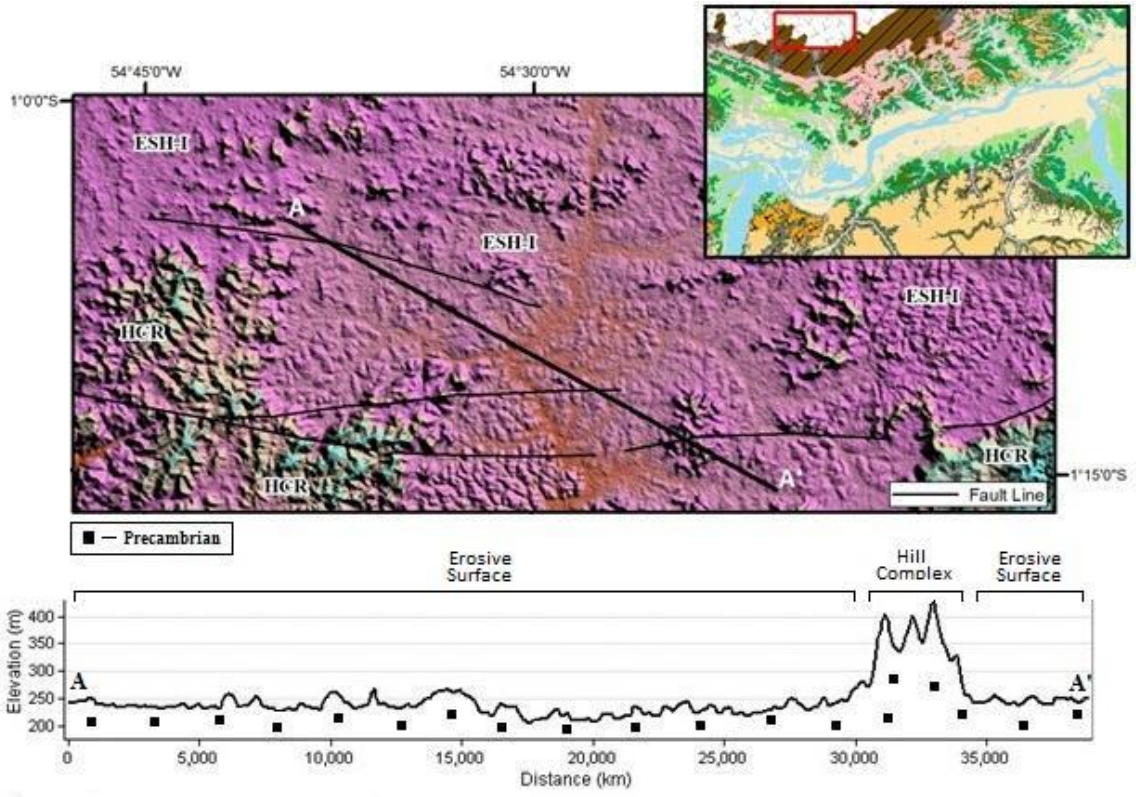

Figure 4.2. Erosive surface with hills (EHS – I). Transect A-A' demonstrates the gently undulating surface and provides an example of the relative relief associated with the larger hill complexes. The southern extent of the image is bordered by the Hill complex and Ravines unit (HCR), and is bordered by E-W faults. For this and all following hillshade models colors correspond to different elevations, see transects for elevation values.

Hill Complexes and Ravines (HCR)

The hill complexes and ravines unit is considered to be a collection of denudational landforms that have been shaped by erosive and fluvial processes. Its occurrence is nearly exclusive to Paleozoic Belt domain, where it occurs as a continuous, belt-like landform along the Guyana Shield and isolated hill complexes towards the center of the basin. Although the relief and type of the landforms contained in the unit vary considerably, they appear to be representative of a single unit that has been impacted

by similar denudational processes. The highest elevations in the study area are also contained in this unit, reaching 800 m between 54° and 53° 45’ W, where the surface has been deeply incised (Figure 4.3). Elsewhere, it primarily appears as alternating hills and ravines with many orientations. The ravines commonly incise 150 m of rock and in the most extreme cases incise nearly 300 m. In addition, these larger ravines are situated along NW-SE trending faults and associated fractures. The unit tapers out westward, where relative relief diminishes.

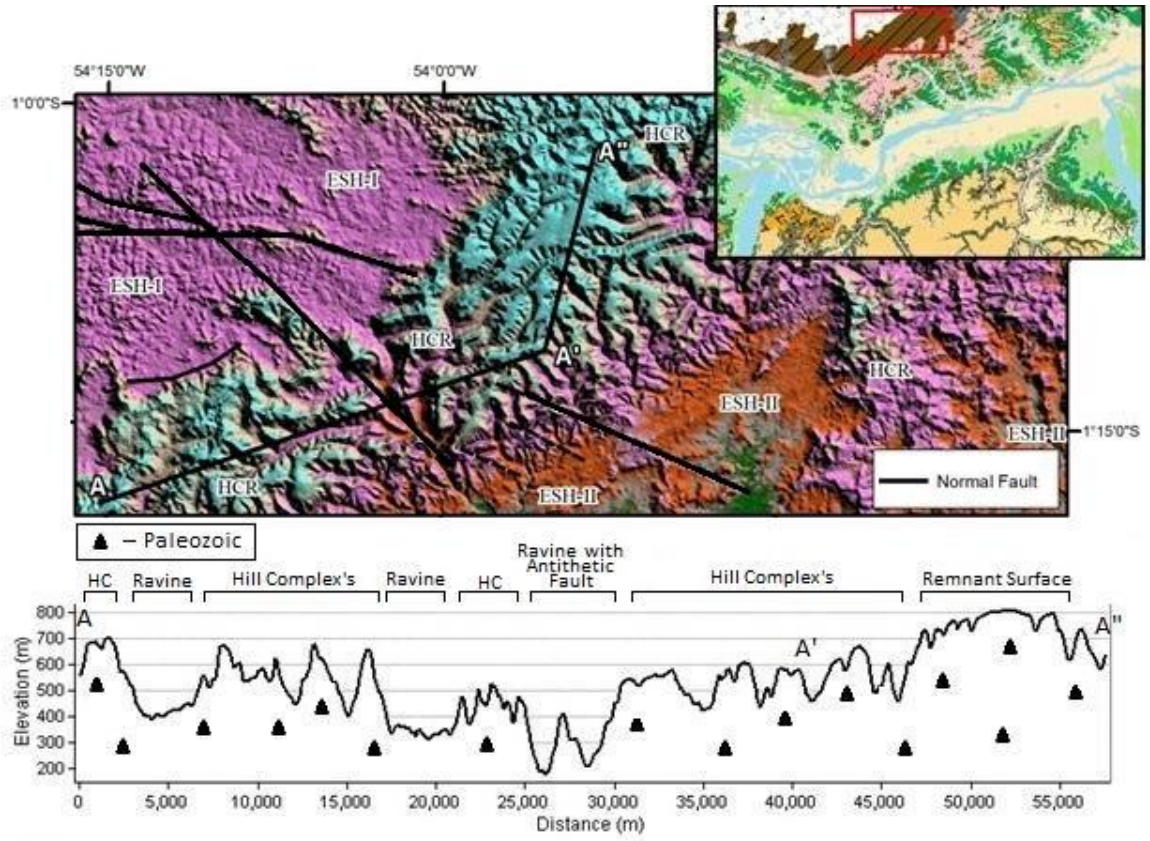

Figure 4.3. Hill complexes and ravines (HCR). Transect A-A' demonstrates the variability of elevation values within the hill complexes and ravines (HCR) unit. Higher values are associated with ridges and Hills and lower values represent valleys. The deepest valley recorded in Transect A-A' corresponds with a NW-SE subsidiary fault. The HCR is in a unique position between the eroded surface with hills I (ESH – I) unit to the north and eroded surface with hills II (ESH – II) unit to the south.

Planation Surface I (SI)

Surface I occurs north and south of the Amazon River, but is dissimilar on either side. There is also noticeable variation in the surface from east to west across the landscape (Figure 4.4). In the southern half of the valley the surface spans the study area with elevations ranging from 110 - 180 m asl with lower elevations located just west of both the Tapajós and Xingu Rivers. In the northern half of the valley the surface

primarily occurs east of 53° 30’ W and ranges from approximately 120 - 400 m in elevation with a regional tilt that diminishes from 0.22° to 0.06° toward the Atlantic.

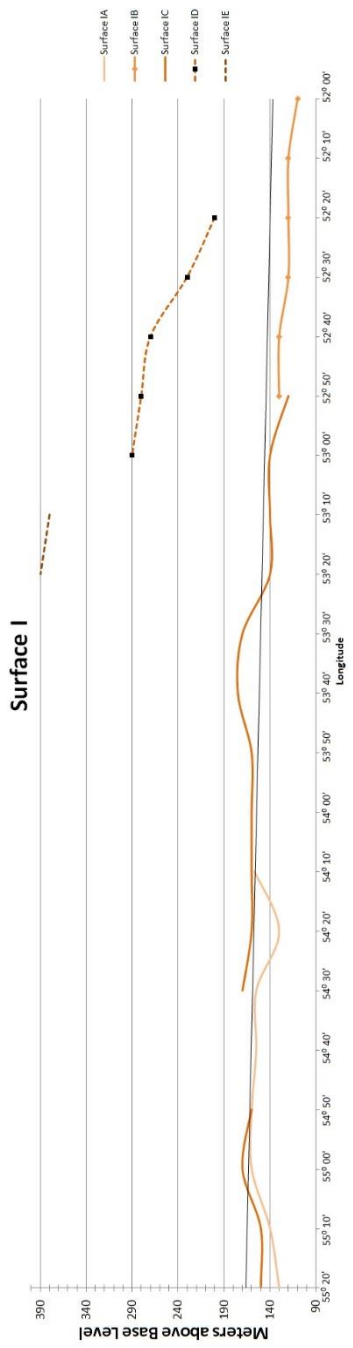

Figure 4.4. Surface I elevation trends from west to east in study area.

Variations in elevation, slope and relative relief between different portions of the plateau allow distinction of 5 subunits here denoted as Surface IA, IB, IC, ID and IE (Table 4.1).

Subunits	Side of Valley	Bounding Longitudes	Elevation Range (m)	Slope	Relative Relief	Area (Km^2)
Surface IA	N & S	54° 10’ W & 55° 30’ W	130-150	N/A	20-40	1,184
Surface IB	N & S	52° W & 53° W	100-140	0.06° - 0.11°	20-60	2,365
Surface IC	N & S	52° 10’ W & 55° 30’ W	150-180	0.06° - 0.11°	40-80	7,458
Surface ID	N	52° 20’ W & 53° 05’ W	220-270	0.11° - 0.23°	150	517
Surface IE	N	53° W & 53° 20’ W	370-410	0.22°	200	70

Table 4.1. Identification of Subunits and characteristics unique to each.

Planation Surface I subunits (SIA-SIE)

Surface IA (SIA) occurs exclusively in the western half of the study area, where it is a mixture of a plateau-like landscape with gently undulating surfaces. Although different in appearance, it retains a similar elevation to the surrounding Surface I, ranging in elevation from 130 - 150 m, with lower elevations occurring upstream of 55° W (Figure 4.5). The surface is highly segmented by fluvial valleys that have lower amounts of vertical incision compared to the surrounding Surface IC subunit. This subunit of Surface I is exclusively underlain by Meso-Cenozoic fill.

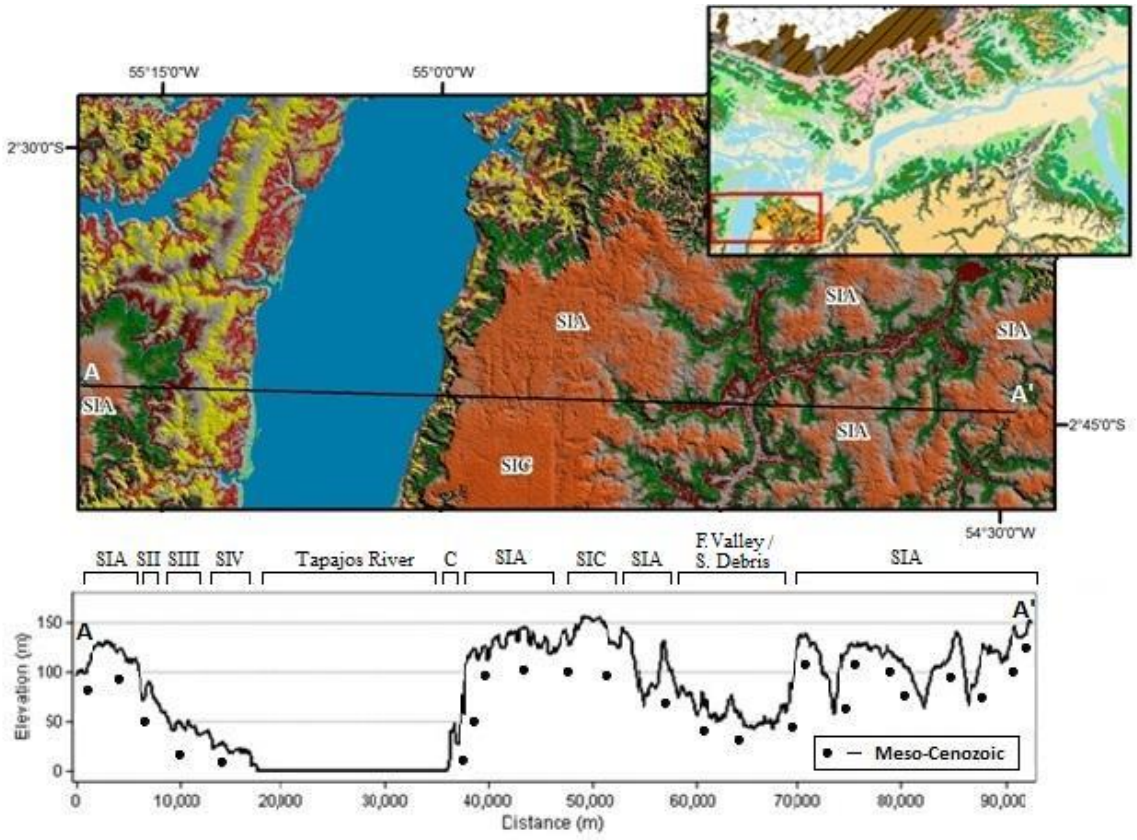

Figure 4.5. Surface IA (SIA) transect A-A' illustrates the relatively uniform elevation and structure of SIA. A small portion of transect A captures elevations and the structure of Surface IC (SIC). Transect A-A' provides a useful comparison between SIA, SIC, Surface II (SII), Surface III (SIII), Surface IV (SIV) and Cliff/Escarpment (C).

Surface IB (SIB) appears entirely downstream of 53° W and ranges from 100 - 140 m in elevation. The surface differs from the higher Surface IC by a lower elevation and increased slope of 0.06° (Figure 4.6). Associated normal faults produce ~10 m of offset and appear to have generated a tilted block structure. Associated with the uniform slope is a parallel drainage network that has shaped the surface into a dissected plateau with elongated branches that extend E and NE. Although the surface is relatively smooth

and displays a plateau-like appearance, the relative relief and escarpments associated with this unit are fairly low and decrease in magnitude towards the center of the basin. According to geologic maps, the subunit lies over the Meso-Cenozoic fill.

Surface IC (SIC) is the most aerially extensive subunit of the Surface I series, and ranges in elevation from 130 - 180 m with escarpment heights of 40 - 80 m (Figure 4.6). The subunit primarily appears in the southern half of the study area, where it is characterized by broad surfaces that measure 10s of km in width with the largest slightly over 100 km 53° W and 54° W. The highest elevations attained by the subunit are in the upstream portions of the study area and away from the center of the valley. Trends in elevation define a NE dip that appears downstream of 54° W, where the unit is segmented by normal faults (Figure 4.6). These faults have offsets of 5 - 20 m and are accompanied by deeply incised valleys with little to no floodplain. The unit corresponds exclusively to the Meso-Cenozoic fill.

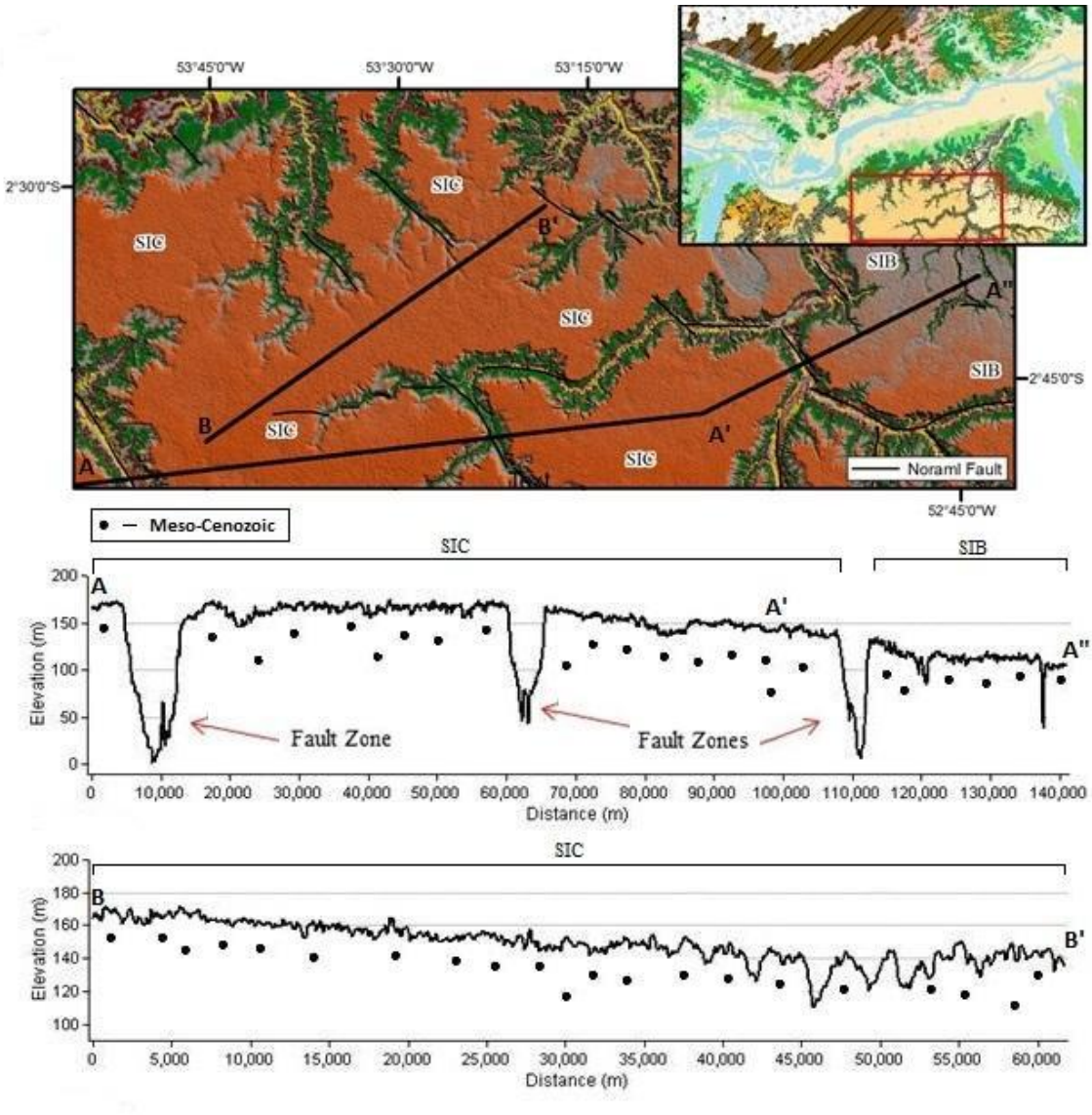

Figure 4.6. Surface IB (SIB) & IC (SIC) in relation to faults in the area. Transect A-A' maintains a relatively uniform elevation until crossing a normal fault zone where the gradient increases and the unit transitions into Surface IB (SIB). Transect B-B' illustrates the gentle slope that develops on SIC as you move east.

Surface ID (SID) occurs north of the Amazon River, where it ranges in elevation from 220 - 270 m while spanning an area nearly 100 km wide. Plateaus that comprise this

subunit rise abruptly and have escarpments with heights of 100 - 200 m (Figure 4.7). Near the Amazon River the subunit defines elongated NW-SE plateaus that transition to an E-W orientation toward the Paleozoic Belt. These changes in orientation and the dissection of this surface correspond to fractures and faults with offsets of 40 - 70 m. Like other subunits, this one dips in the downstream direction. The larger plateaus of this are composed of Meso-Cenozoic fill, while the smaller show some overlap with Paleozoic rocks.

Surface IE (SIE) has the smallest area of the series and is localized to a single plateau that has an elevation of 380 - 410 m, and an east tilt of 0.22°. The escarpments associated with this subunit are the most dramatic, with a height of 200 m, and are accompanied by sloping materials that extend up to 1 km from the plateau (Figure 4.7). The subunit has several east-elongated sections that radiate from the main plateau connected to the main plateau by narrow ridges. These ridges appear to have developed between normal faults with 20 - 30 m of offset. The subunit lies entirely over Meso-Cenozoic fill.

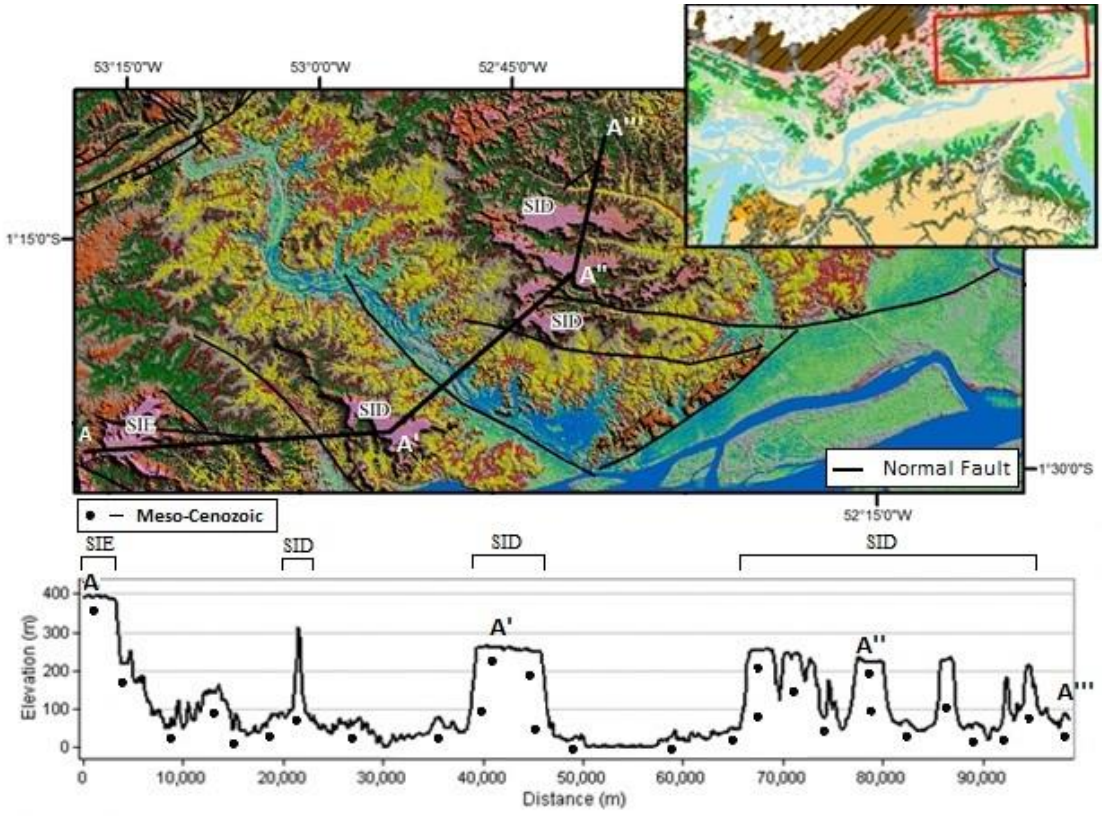

Figure 4.7. Surface ID (SID) & IE (SIE) illustrated by hillshade model and transect A-A'.

Erosive surface with hills II (ESH-II)

The erosive surface with hills II surface only appears in the northern half of the study area where it occupies elevations of 120 – 150 m asl, with the lower elevations occurring downstream of 53° W. The surface is best developed in the center of the study area, where it outcrops entirely over Carboniferous rocks as an erosive surface with scattered hills and fluvial valleys (Figure 4.8). West of this central surface the unit it forms cuestas as it primarily outcrops over Devonian rocks as a belt along the dissected hills and ravines unit. In the eastern half of the study area the surface appears as both a belt along the higher elevations similarly to the western portion, and a highly fragmented

and eroded surface with intermittent cuestas. This fragmentation corresponds to larger fluvial valleys, and primarily covers the Meso-Cenozoic fill.

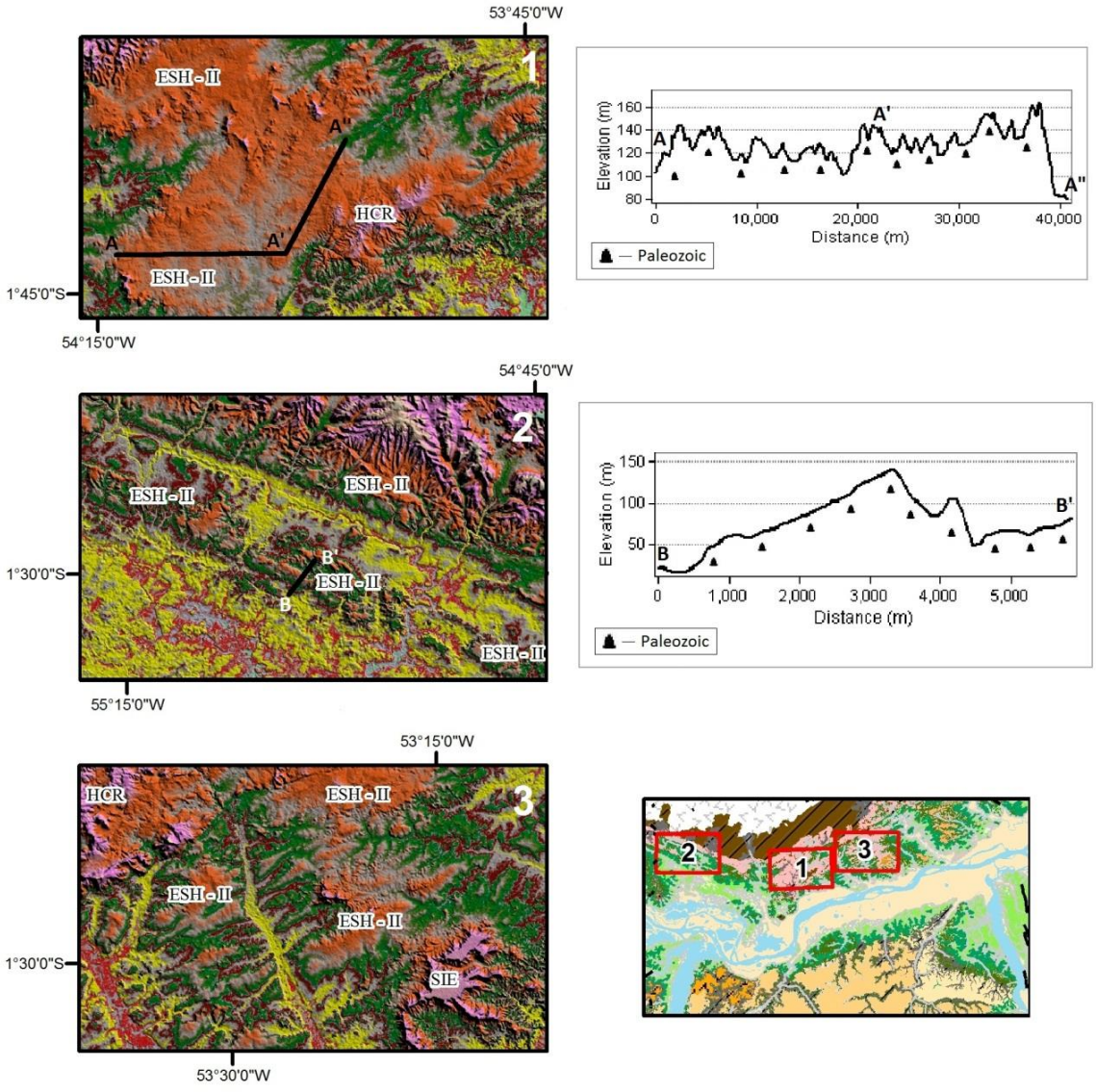

Figure 4.8. Erosive surface with hills II crops out in image 1 as a large erosive surface that occupies the center of the study area on the north shore. Image 2 shows an area in the western portion of the study area where the unit forms a cuesta. Image 3 is a section of the unit in the eastern half of the study area where it displays a much more eroded and dissected appearance.

Surface I Colluvium (D-SIC)

Surface I colluvium only appears south of the river, where it outcrops as a narrow strip usually 1 - 3 km's wide and approximately 95 - 110 m asl. The unit has a close relationship with Surface I, appearing only where Surface I has heights above 150 m, experiences similar fluctuations in elevation and is separated by a escarpment and narrow strip of sloping debris. Based on its form and close proximity to Surface I, this unit is depositional and most likely formed by the retreat of Surface I. In addition the unit is present within several of the highly dissected fluvial valleys.

Planation Surface II (SII)

Surface II has heights of 70 - 80 m in elevation south of the Amazon River and 65 - 90 m to the north (Figure 4.9). Both regions show a similar pattern between changes in elevation, with a general trend of decreasing elevation downstream.

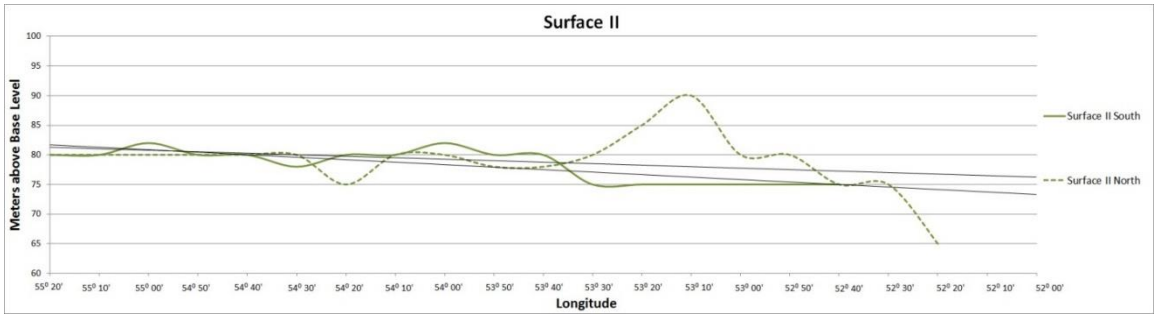

Figure 4.9. Elevation of Surface II remains relatively constant until downstream of 53° 30' where a slope 0.06° develops on the southern shore and a spike in elevation occurs on the northern shore.

In the southern portion of the study area the surface resides west of the Tapajós River, comprised of isolated platforms near the Amazon River and extensions from areas of higher relief. Throughout the rest of the southern half of the valley the surface is

primarily an extension of higher units, and maintains a relatively level elevation until moving downstream of 54° W where it slopes 0.06°. This increase in slope corresponds to a series of NW-SE normal faults that have offsets of ~5 - 20 m. At 54° W the surface comprises large, level surfaces with scarp heights of nearly 30 m but quickly diminish in occurrence downstream (Figure 4.10). The surface is also found between many of the fluvial valleys that dissect the higher Belterra landscape (Figure 4.11). All of the southern portion of the surface rests upon Meso-Cenozoic fill.

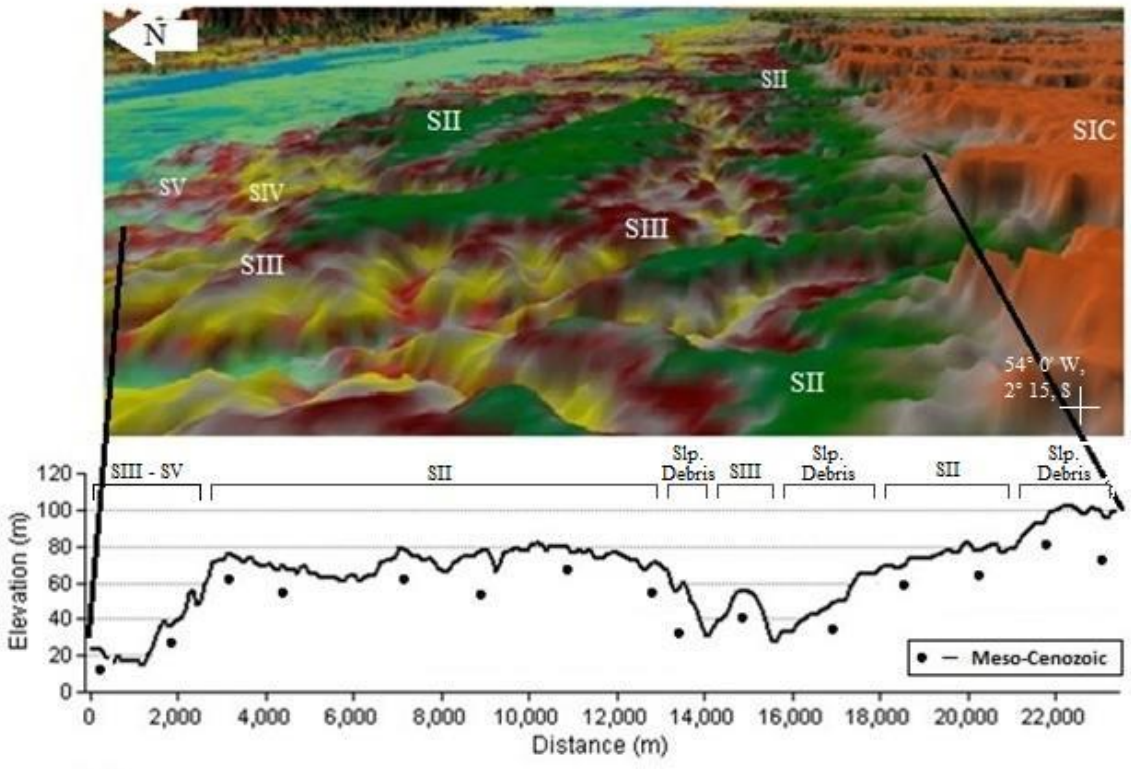

Figure 4.10. Surface II (SII) image is taken at 54° W and looks downstream. The image provides an oblique view of SII and the surrounding units. In this location SII outcrops as a large planation surface that displays a gentle slope downriver.

In the northern half of the study area Surface II attains its highest elevations and is most prominent in the far western portion of the study area where it covers the Meso-Cenozoic fill close to the Amazon River and Paleozoic rocks closer to the shield. In this area the surface appears as a long linear surface that extends from the Erosive Surface with Hills II towards the Amazon River and transitions to a narrower surface towards the Atlantic. Downstream of 53° W it is primarily underlain by Meso-Cenozoic fill and experiences a spike in elevation that is followed by a gentle decrease in slope towards the Atlantic Ocean, similar to the southern portion of the surface.

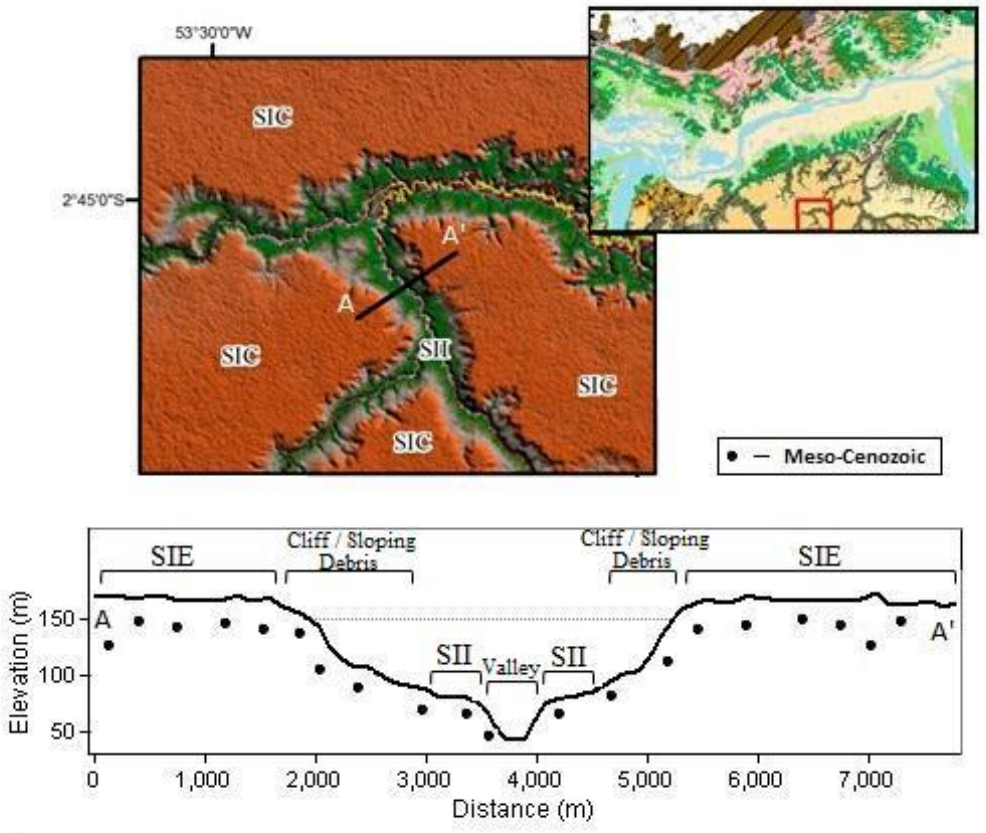

Figure 4.11. Surface II (SII) crops out in many of the fluvial valleys in the south half of the valley.

Planation Surface III (SIII)

Surface III typically resides between 44 - 63 m in elevation in the southern half of the valley, and at 45 - 60 m in the north (Figure 4.12). South of the Amazon River and west of the Tapajós River the surface comprises hills near the Amazon River, and inland as extensions from areas of higher relief. In the downstream direction the surface is relatively limited in extent until east of 54° W, it begins to occur as surfaces that stretch nearly 10 km in length that cover Meso-Cenozoic fill (Figure 4.13). It is in this area the

surface reaches its highest elevations before beginning to gently slope in the downstream direction.

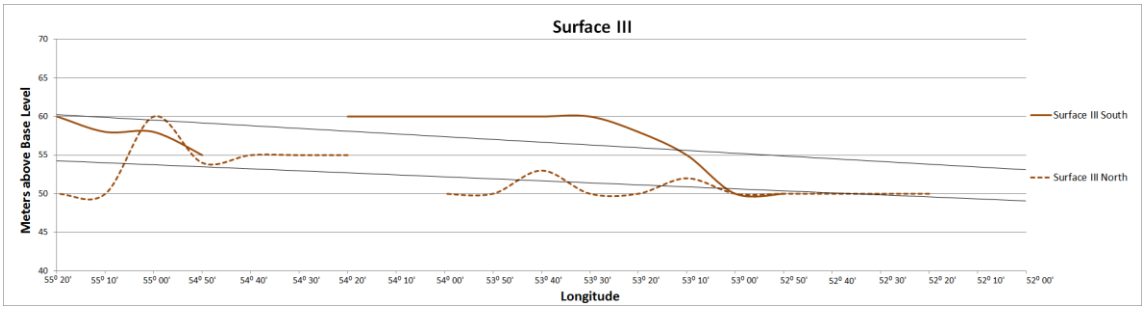

Figure 4.12. Elevation of surface III (SIII) through the study area. Both north and south sections of the unit have a tendency to decrease in elevation as you move downriver.

Upstream of 54° W and north of the river Surface III occurs as broad surfaces extending from higher elevations as well as isolated features that cover the Meso-Cenozoic fill near the Amazon River and Paleozoic rocks elsewhere. Downstream of this area it becomes much narrower and/or nonexistent, especially where there are Paleozoic rocks. Where the unit does appear it is primarily underlain by the Meso-Cenozoic Fill and away from the river. Surface III is somewhat limited in the north and decrease in elevation downstream.

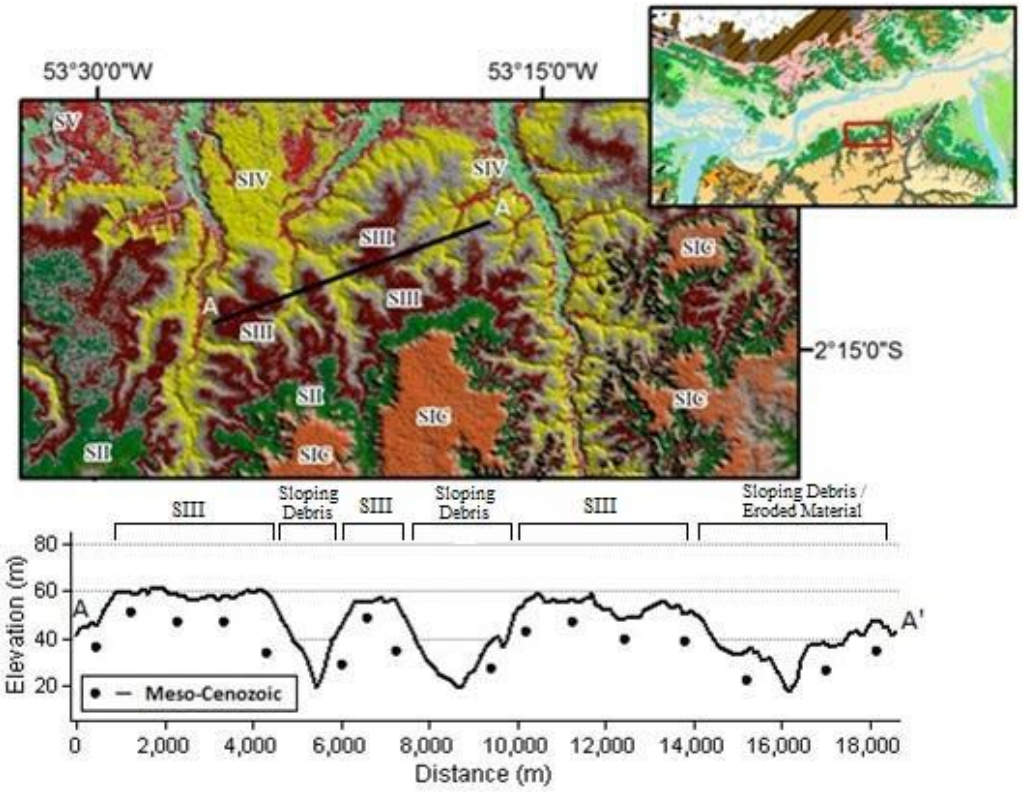

Figure 4.13. Surface III (SIII) in a portion of southern half of valley.

Planation Surface IV (SIV)

Surface IV is the second lowest surface of the study area, occurring at 25 - 33 m in elevation in the south and 27 - 30 m in elevation in the north (Figure 4.14). The surface maintains a near constant level of elevation through the study area.

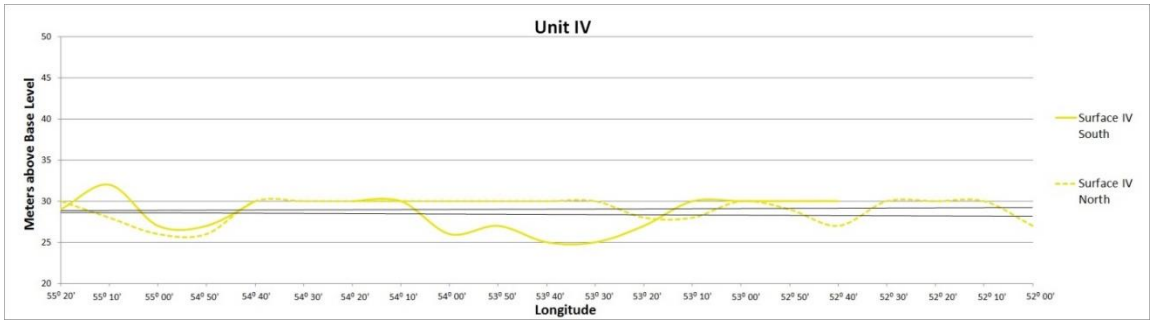

Figure 4.14. Elevation of Surface IV through the study area.

South of the river it occurs as both a continuous belt and as elongated platforms west of the Tapajós River. East of the Tapajós River occurrences are somewhat limited until moving downstream of 54° W, where it transitions from a continuous belt to surfaces nearly 20 km wide that extend from higher elevations towards the Amazon River. Downstream of 52° 30’ W there is a small jump in the elevation as the surface transitions into a broad area that exists on both sides of the Xingu River. The changes in elevation that occur downstream of 54° W appear to correspond to faults until reaching the Xingu River. In the southern half of the study area the surface is underlain exclusively by Meso-Cenozoic fill.

In the northern half of the study area the surface is most prominent between 55° 20’ and 54° 10’ W, where it occurs as a nearly level area that is interrupted by fluvial dissection and Surface III. This area is primarily underlain by Carboniferous rocks, and Cretaceous rocks closer to the Amazon River. Eastward, the surface primarily covers Meso-Cenozoic fill and appears similar to the southern portion, comprising narrow strips that show a tendency to increase in width downstream. Unlike the southern portion, its elevation remains nearly constant throughout the entire northern reach of the study area.

Planation Surface V (SV)

Surface V is the lowest of the surfaces. It is relatively fragmented because of dissection from fluvial valleys and/or interruption from the floodplain, and diminishes in the downstream portions of the study area. It is typically found between 12 - 17 m in elevation but ranges from 8 - 21 m in elevation, with the highest elevations primarily occurring on the northern bank (Figure 4.15). Both north and south portions of the surface follow a similar trend in fluctuations of elevation downstream, especially between 54° and 53° W.

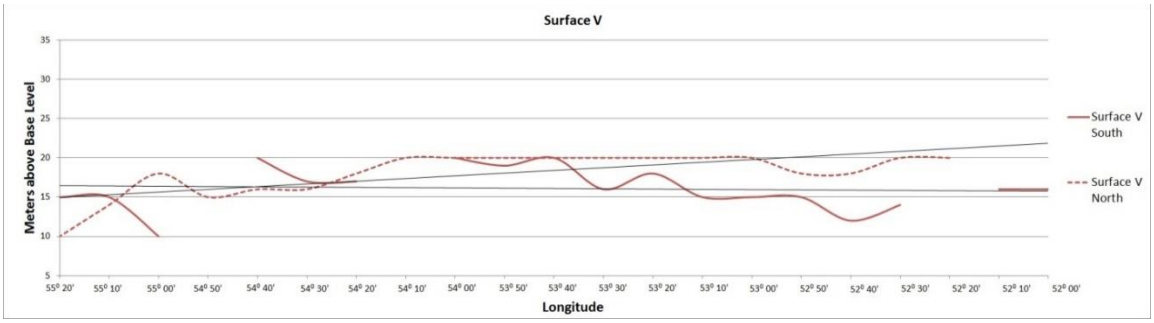

Figure 4.15. Elevation of Surface V through the study area.

South of the river Surface V occurs as relatively narrow strips of land never exceeding 5 km wide, that primarily cover the Meso-Cenozoic fill except west of the Tapajós River, where the surface is coextensive with a mixture of Quaternary and Meso-Cenozoic fill. West of the Tapajós River the unit can be found along most borders of the ‘varenzá’ and ‘terra firme’ with the larger occurrences along the Tapajós River and at its confluence with the Amazon. On the Eastern bank of the Tapajós River the surface is either absent or is too small to map. The surface is largely absent downstream until reaching the high in elevation that occurs between 54° and 53° W. Here the surface

appears as multiple platforms interrupted by fluvial dissection from waters draining the 'terra firme' (Figure 4.16). Past this point it seemingly decreases in occurrence until east of the Xingu River, where it primarily occurs along the eastern bank in a fashion similar to the west bank of the Tapajós River.

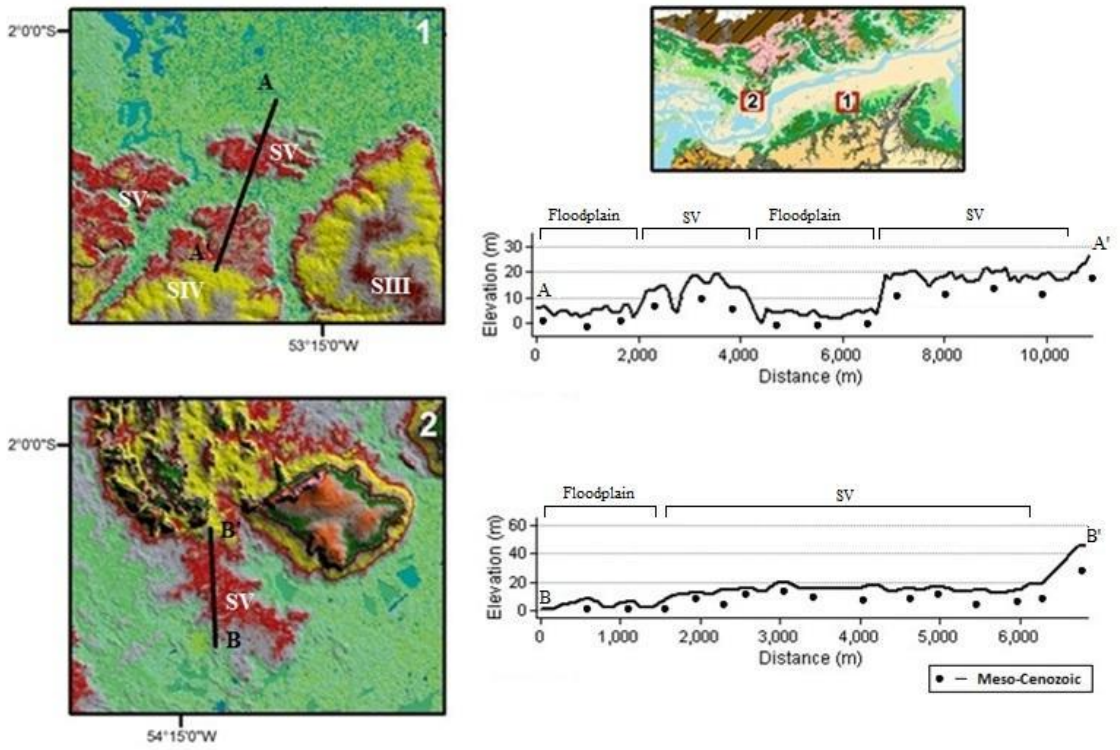

Figure 4.16. Surface V hillshade model and topographic profiles. Both sections of Surface V (SV) show a slight decrease in elevation as you move towards the center of the valley. Transect A-A' illustrates a section of the surface that is separated from the headland and surrounded by floodplain. Transect B-B' illustrates the break in topography between the floodplain and SV.

On the northern shore the most pronounced appearance of the surface is in the western half of the study area where it defines surfaces nearly 15 km in width. In this area

the surface primarily sits above Carboniferous, however downstream of the 54° 30’ W the surface rest almost entirely on the Meso-Cenozoic fill as it occurs adjacent to higher elevation units (Figure 4.16). Similar to the south bank, the surface experiences a high in elevation before becoming more limited in occurrence downstream (Figure 4.15).

Chapter 5 – Plateaus

Introduction

Relief in the EAV varies between geomorphologic units, however in general maintains a relatively flat topographic gradient (Sakamoto, 1960). This relatively low lying topography in combination with the appearance of laterite has produced low rates of erosion (Grubb, 1979), thus creating a prime environment for the study of landform evolution. This preserves a plateau landscape (Grubb, 1979) commonly referred to as the Amazon Planalto (Sombroek, 1966), or Belterra Plateau (Sternberg, 1975), recognized as Planation Surface I in this report. These plateaus have long attracted attention due to their abrupt rise from the surrounding landscape (Truckenbrodt et al., 1991), and economic significance (Dennen and Norton, 1977; Grubb, 1979). Theories of their development are varied (Sternberg, 1975), with divergent ideas about their age and origin.

To understand changes in the EAV through the Cenozoic requires a better understanding of its geomorphological units. Such an understanding can help address long-standing questions:

1) Were plateaus once part of a single surface? If so, what can be learned from dissection that has since ensued?

2) How did plateaus develop level surfaces? The processes by which this occurs has both regional and local significance.

3) What are the ages of the underlying substrate? Current interpretations give ages of deposition that range from the Late Mesozoic to Late Cenozoic, a difference of nearly 65 my.

This chapter begins with a review of current ideas about plateau ages and development. It finishes with a discussion that examines contradictions and similarities among different theories. Incorporation of data obtained from this study provides a regional-scale analysis of the spatial distribution of the plateau landscape, something lacking in published works. This new constraint contributes to a better understanding of EAV landscape evolution

Plateau Description

Descriptions of plateau geology differ as a consequence of differences in dates for the Meso-Cenozoic sedimentary fill (Caputo, 2011). A plateau may be viewed as containing one Formation or two, with the latter distinguishing a younger clay rich cap covering much older sandstone.

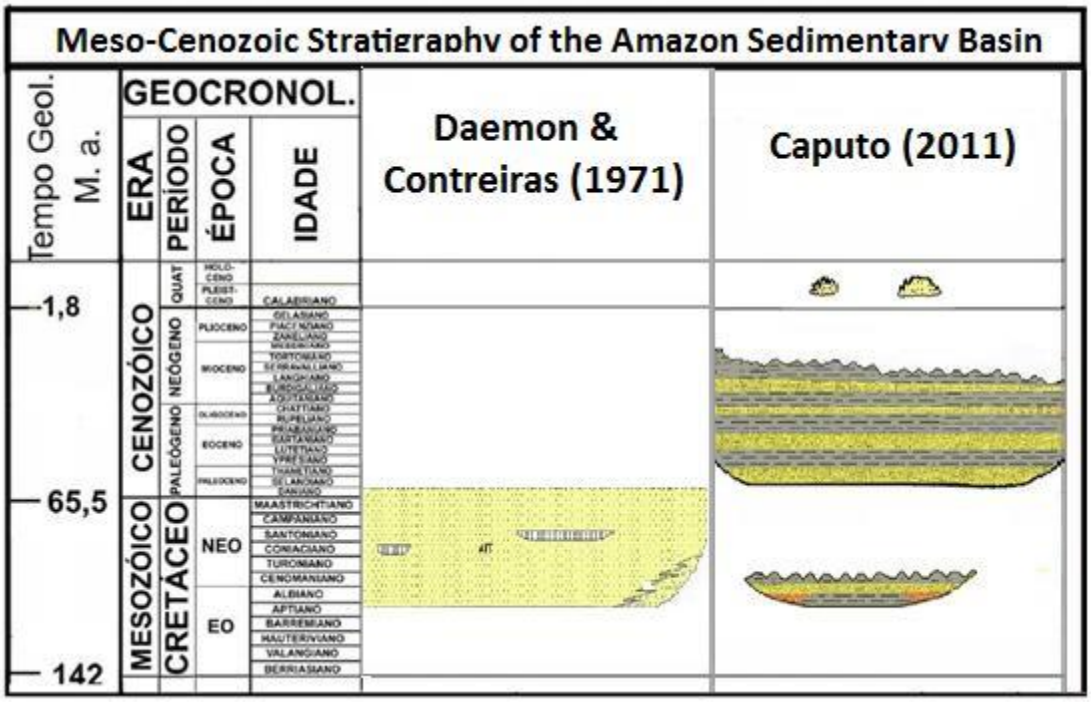

Figure 5.1. Meso-Cenozoic geologic interpretations illustrating the divergence in geologic interpretations of the Meso-Cenozoic fill. The interpretation of Daemon & Contreiras (1971) indicates a single, thick clastic sequence nearly entirely Late Cretaceous. The interpretation by Caputo (2011) recognized two separate deposition units, one that is Cretaceous another that is exclusively Cenozoic (modified from Caputo, 2011).

One of the earliest and most frequently reproduced interpretations is that of Daemon and Contreiras (1971), who identified the sedimentary fill as a single unit associated with the Alter do Chao Formation (Figure 5.1). This interpretation was developed from samples obtained 40 km SW of Santarem, at Petrobas well site AC-1-PA, where Late Cretaceous palynomorphs were identified at 502 m depth. This date was applied to the entire column, giving a Late Cretaceous age to the Formation.

An alternative interpretation was proposed by Sombroek (1966), who believed that the clays in the upper portions of the plateaus were unrelated to the lower strata. The

two are believed to be separated by n erosional unconformity that ranges in depth between ~20 - 60 m, with Tertiary clays resting on Cretaceous sandstones. Sombroek (1966) identified the Tertiary deposit as being a near uniform mixture of clay and silt with horizons of laterite, whereas the underlying unit was believed to be a Cretaceous clastic material. This theory is based on the belief that an intercontinental seaway or estuary-like body of water deposited the clays when sea-level was 180 m higher than the present.

A third interpretation of the geology is offered by Caputo (2011), who identified the Meso-Cenozoic fill as primarily Tertiary, and overlying a thinner sequence of Late Cretaceous rock (Figure 5.1). Caputo (2011) separates the two units, keeping the Alter do Chao name for the younger unit and giving the name Jazida da Fazendinha to the older unit. This interpretation is based upon unpublished palynology research by Eglemar Conde Lima that shows Paleocene and Eocene fossils at 425 m depth (Figure 5.2). This analysis was conducted on the same core data that Daemon and Contreiras (1971) used. On the basis of this information and seismic data, Caputo (2011) argues that the Late Cretaceous rock identified by Damon and Contreiras (1971) at 502 m depth are relatively thin and buried by a thicker sequence of Tertiary rocks that are Paleocene-Eocene near their base in the subsurface and Oligocene-Miocene on plateaus.

Material	K_1	K_2	Paleo	Eo	Olig	Mio.	Plio.	Pleist.	Terc.Indet	Holoc.
Equisetum L.		X	X	X	X	X	X	X		X
Coccoloba L.			X	X					X	X
Minispermites Lesq.	X	X		X						
Capparis L.				X		X				
Rhamnus L		X		X	X					
Gerviopsis Sap.		X	X	X						

Figure 5.2. Palynomorphs used by Caputo (2011) for age control. At 425 m the youngest fossils in the core provide an Eocene age (Source: Caputo, 2011).

Studies of plateau stratigraphy provide relatively consistent results (Fig. 5.5). The clay layer on top of plateaus is 5 - 15 m thick and sits above of a thin layer of iron laterite. The iron laterite is occasionally contains bauxites (Grubb, 1979). Beneath the laterite is a 5 - 20 m weathering zone that comprised of a mixture of gibbsite and mottled clays (Dennen and Norton, 1977; Truckenbrodt et al., 1991), both of which are known to be products of the lateritization process. This layer sits above a thick layer of kaolinite clays occasionally interrupted by iron oxide and sandy horizons, and is succeeded downward by a thin transitional clay zone approximately 5 m thick that covers a cross bedded, poorly consolidated sandstone (Hartt, 1874).

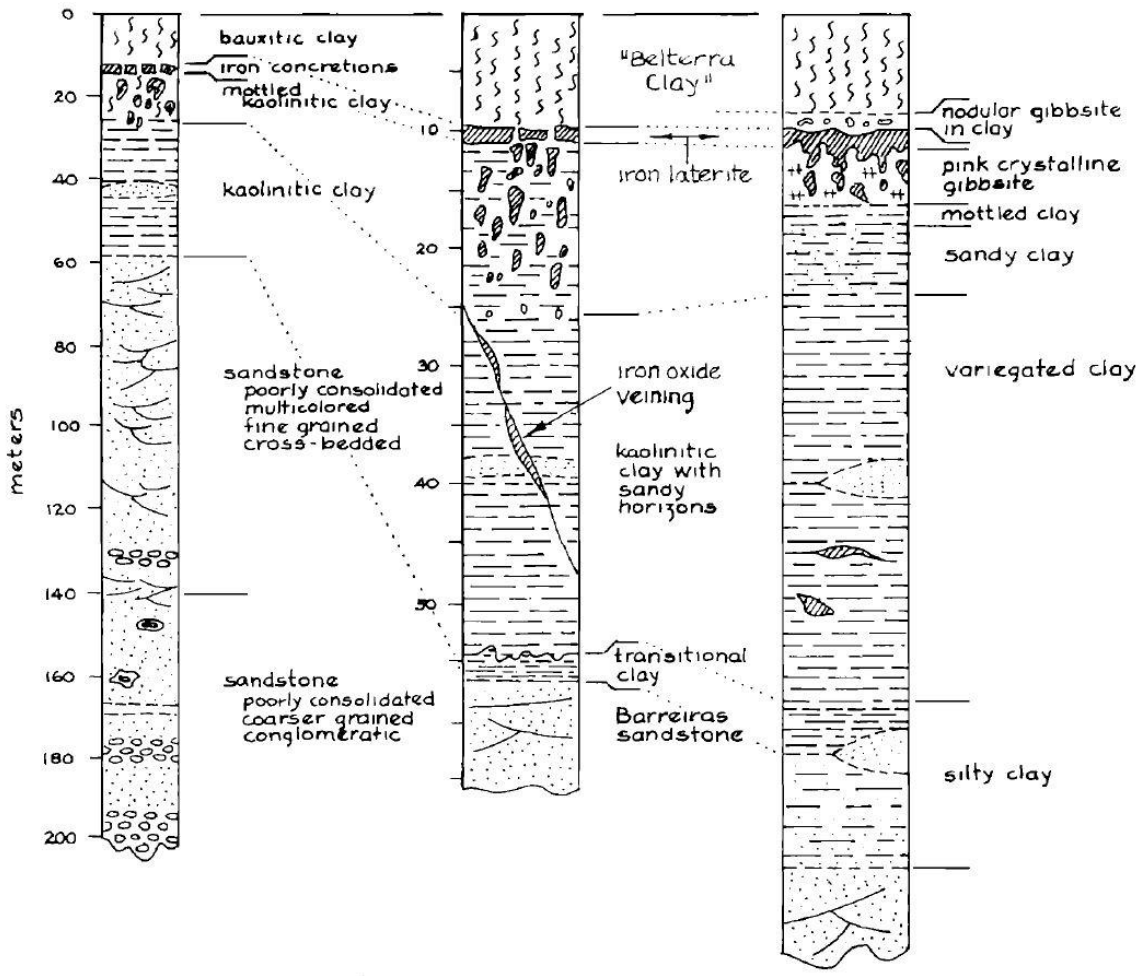

Figure 5.3. Stratigraphic sections of plateaus in the EAV. Section on the left is from Hartt (1874), middle section from Klammer (1971) and right from Dennen and Norton (1977) (Source: Dennen and Norton, 1977).

Soil descriptions of the Belterra Clay horizon commonly describe an unstratified, ochre-colored clay (Irion, 1984; Sternberg, 1975) that is comprised of a mixture of kaolinite, illite, goethite, aluminum-chloride, rectorite and montmorillonite (Irion, 1984). Near Santarem, the soil profile contains 64% Clay, 16% silt, 20% sand and gravel 2 m below the surface and 41% clay and 59% silt at 8 m below the surface (Table 5.1). Soil horizons vary in thickness across the landscape, with thicker profiles over more

permeable rocks (Irion, 1984). It has also been noted that there are slight variations in soil composition between different localities (Trukenbrodt et al., 1991).

Depth (m)	Description	Grain Size (%)			Minerals
		Clay	Silt	Sand/Gravel	
1	Beige	64	16	20	Kaolinite, Illite, Goethite
2	Red with pisolithe				Quartz, Kaolinite, Illite, Aluminium-Chloride, Goethite
4	Grey to red				Quartz, Kaolinite, Illite, Rectorite, Montmorillonite
6	Strongly weathered shales	59	41	-	Quartz, Kaolinite, Illite, Rectorite, Montmorillonite
8	Moderately weathered shales	41	59	-	Quartz, Kaolinite, Illite traces, Montmorillonite

Table 5.1. Soil components of plateaus from a sample obtained 40 km SW of Santarem (Source: Irion, 1984).

Plateau Development

The clay-rich caps of the relatively flat top plateaus have been interpreted as both allochthonous and autochthonous, leading to different interpretations of plateau origins. (Truckenbrodt et al., 1991). The following discussion looks at three models. The models, are referred to as ‘Belterra Clay’, ‘Mechanical Morphogenesis’ and ‘In-Situ Weathering’. The Belterra Clay model (Sombroek, 1966; Klammer, 1978) relates the relatively unstratified and uniform structure of the clays in the upper 20 - 60 m of plateaus to a low energy depositional system (Figure 5.5). The large flux of fine-grained sediment needed

to cover the EAV in this model is provided by sediment from the Andes via an intercontinental sea-way or estuary-like body of water during the Plio-Pleistocene, when sea level was sufficiently high to flood the eastern half of the continent (Figure 5.6). Coarser particles would have been deposited near the Andes; more distal fine-grained clay would have blanketed the eastern half of the continent. Belterra Clay found at lower elevations is assumed to be eroded material that was reworked and deposited as sea-level fell during the Pleistocene. Erosion during this time removed Belterra Clay west of Óbidos.

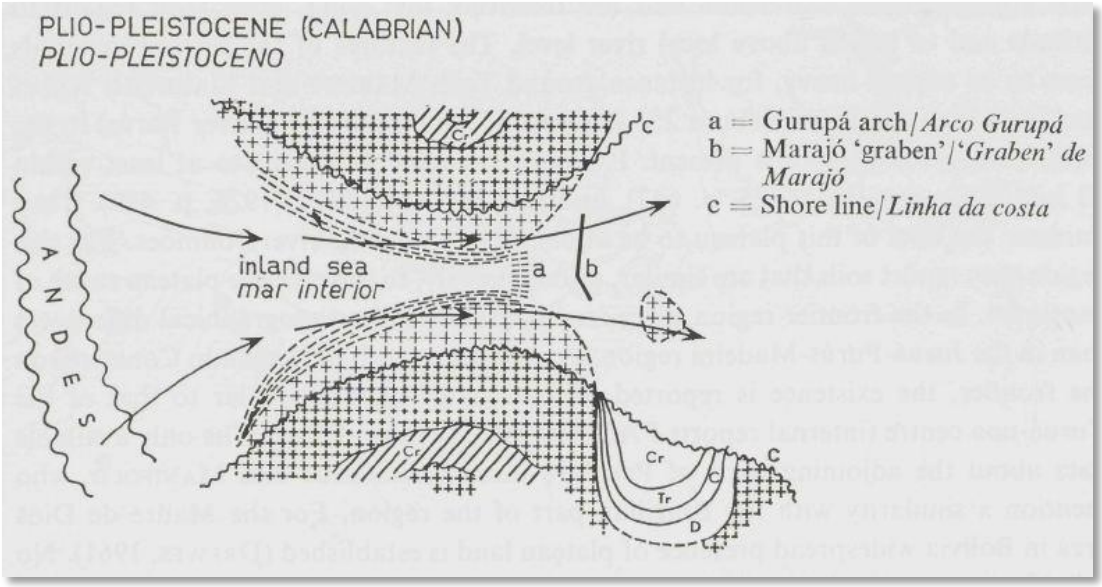

Figure 5.4. Intercontinental sea-way proposed by Sombroek (1966). Sediment was sourced from the Andes, heavy minerals were deposited near the Andes and lighter clays and silts were transported towards the eastern half of the South American Continent (Source: Sombroek, 1966).

The Mechanical Geomorphogenesis (Radambrasil, 1977) model posits that smooth plateau surface were formed through pedimentation. It is assumed that

mechanical breakdown of material was active through the Cenozoic due to drier climatic conditions and terminated sometime during the Plio-Pleistocene, when cooler and wetter climates prevailed. This model cites horizons of stone lines as indicative of a semiarid/arid climate (Figure 5.7). Climatic oscillations from a humid to dry were presumed to trigger a mechanical breakdown of underlying formations which, in combination with deflation and pediment formation, had a smoothing effect on the terrain, removing any relief that once existed in the landscape (Radambrasil, 1976).

Figure 5.5. Stone Line in an outcrop near road PA -254, interpreted as desert pavement by Radambrasil (1977) (Source: Radambrasil, 1977).

The In-Situ Weathering model, adopted by several authors, argues that the smooth top plateau surfaces formed by chemical weathering during the last 10 - 35 mya (Costa, 1991; Irion, 1995; Truckenbrodt et al., 1991). The model relies upon breakdown of sand and larger sediment into the silts and clays by chemical weathering in a humid

environment over an extended period (Irion 1984). Observations cited in support of a dominant role for chemical weathering are thick clay profiles, similarities in chemical compositions of the clay and underlying strata and the presence of laterite (Truckenbrodt, 1991; Irion, 1995). Though there is no consensus on the timing and duration of intense weathering (Late Eocene to the Miocene ages are suggested), all agree on the upper levels are produced from the underlying strata.

Analysis and Discussion

Current geologic age and process model discrepancies result in markedly divergent interpretations of landscape evolution in the EAV. Discrepant age interpretations result in differences in the age of plateau sediment deposition that range from ~65 to 2.5 my. These inconsistencies bear directly upon understanding the development of clay-rich surfaces, incision of the plateau and neotectonic activity. Daemon and Contreiras (1971) use well data 502 m below the surface to extrapolate an age for surface exposures. Klammer (1984) uses paleo sea-levels to determine when, since the Cretaceous, sea-levels and the average elevation of the Belterra Plateau were equal. Caputo (2011), using fossil pollen ages, extrapolates an age trend observed at 550 m to 100 m below the surface to the elevation of the plateau. Lacking new age data or a means of independently verifying earlier result, an indirect approach that examines the development and connection of the plateaus to their surrounding landscape is developed below.

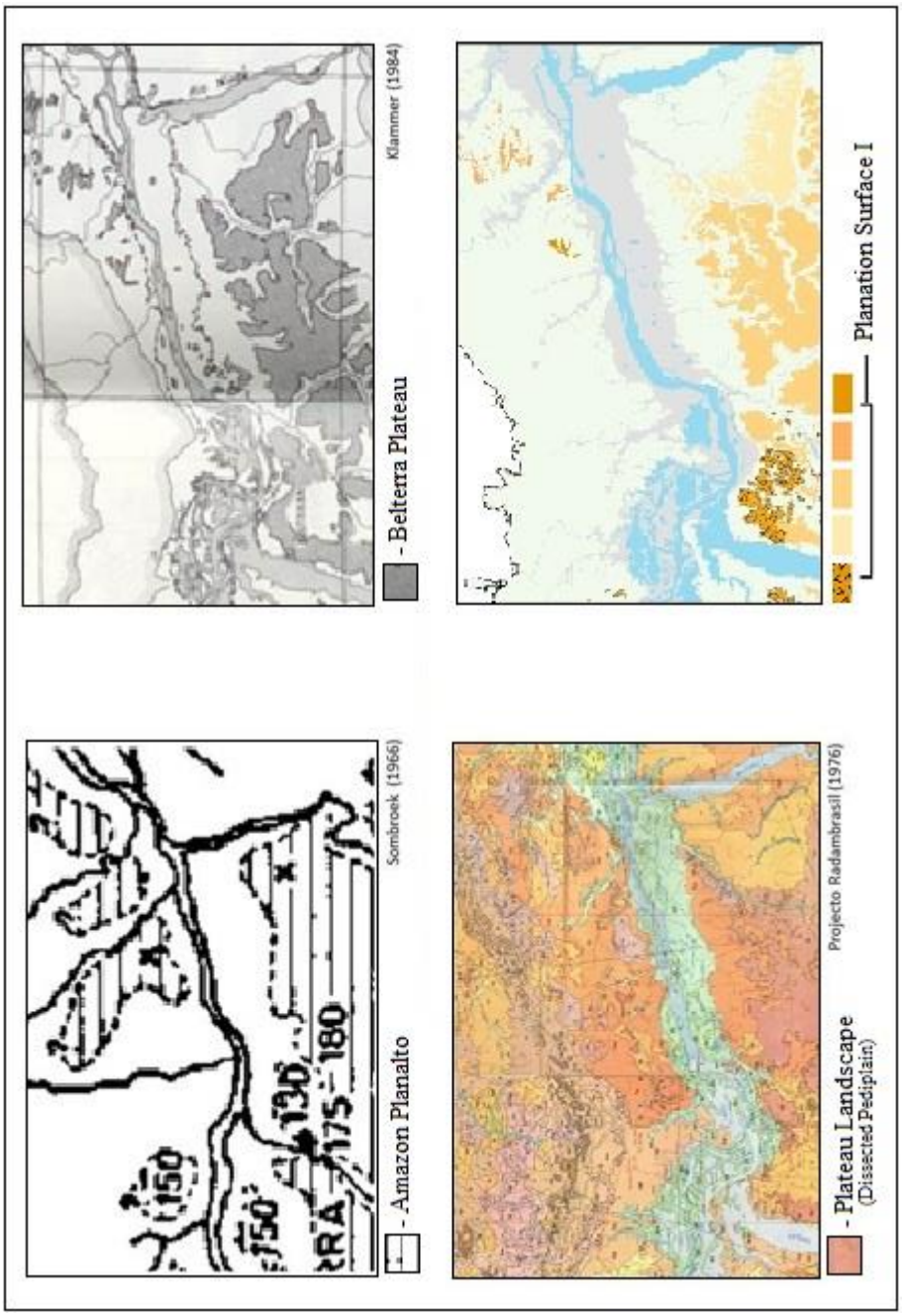

Figure 5.6. Comparisons of Surface I identified in this study and previously published plateau landscapes. Larger images of the geologic maps included in Figure 5.6 are located in the appendix.

Previous studies of the plateau landscape have assumed a prior connection between isolated plateau segments on the basis of similar form and composition of the upper layers but do not rigorously compare elevations. There is also presently no agreement on the area comprising the plateau (see Fig. 5.6). From the geomorphologic analysis conducted here, Surface I most closely corresponds to areas previously identified as the plateau landscape (Figure 5.6). By rigorously evaluating elevation differences and the morpho-arrangement of the surfaces, it includes areas not previously identified as being part of the same surface (e.g. Surface IA and IB) (Fig. 5.6)

In the western portion of the study area Surfaces IC and IA appear related and similar, differing only slightly in elevation but showing differences in dissection and denudation. Figure 5.7 shows that although the IA surface is lower than the nearby IC surface, differences in elevation are minimal, with both extending similarly from the lower 'terra firme'. In addition this unit underlies a neotectonically active area (Costa et al., 1991) (Figure 2.8), possibly resulting in greater dissection and erosion than Surface IC.

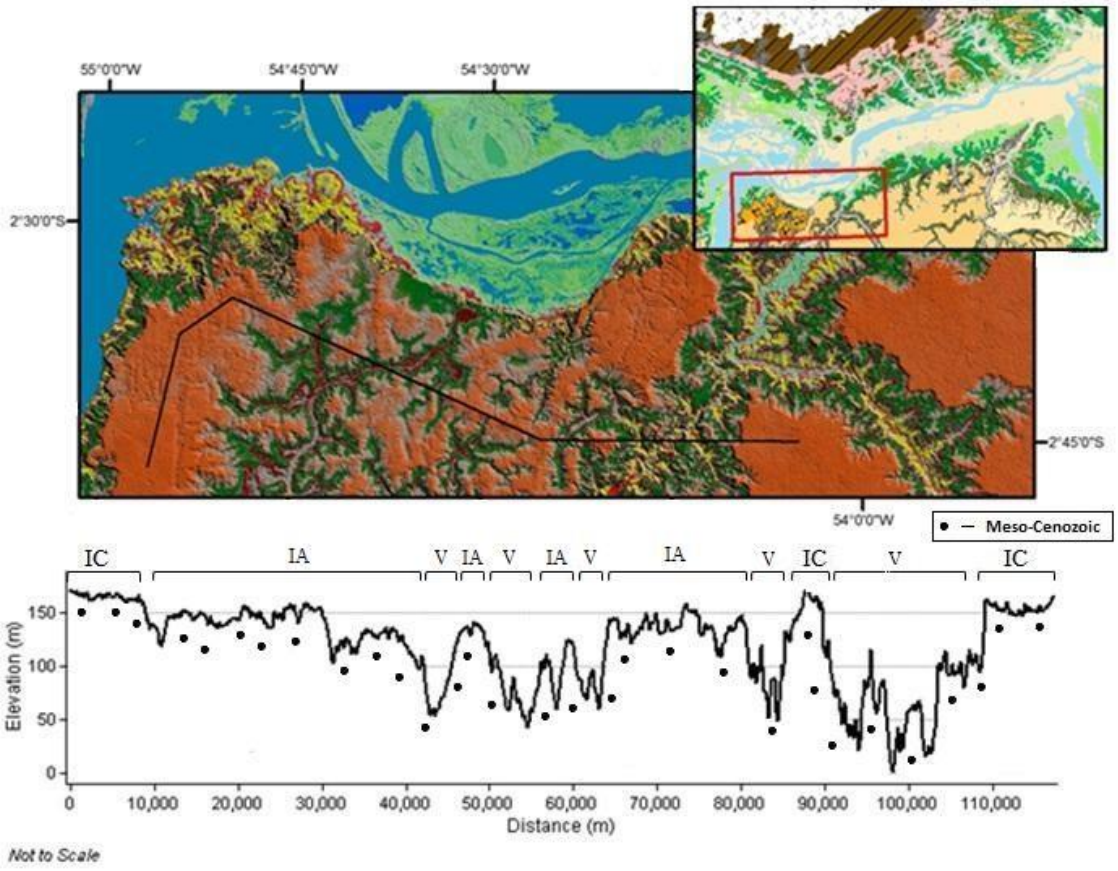

Figure 5.7. Proposed connections of Surface IA (SIA) & IC (SIC). SIA is much more dissected, however is only slightly lower than SIC. SIA is segmented by numerous fluvial valleys (V).

Downstream of 54° W Surface IC has a low gradient slope that appears coextensive with Surface IB (Figure 5.8). Higher slopes and lower elevations of Surface IB, are directly associated with fault zones and/or tectonic lineaments. Near 100 m elevation Surface IB appears to have been removed by erosion. Surface IB and IA are thus related to Surface IC, but appear dissimilar because of erosion associated with recent tectonic activity. When subunits IA, IB and IC are recognized as part of the same surface

it is apparent that nearly the entire southern half of the study area was once covered by the same surface, here referred to as Surface I.

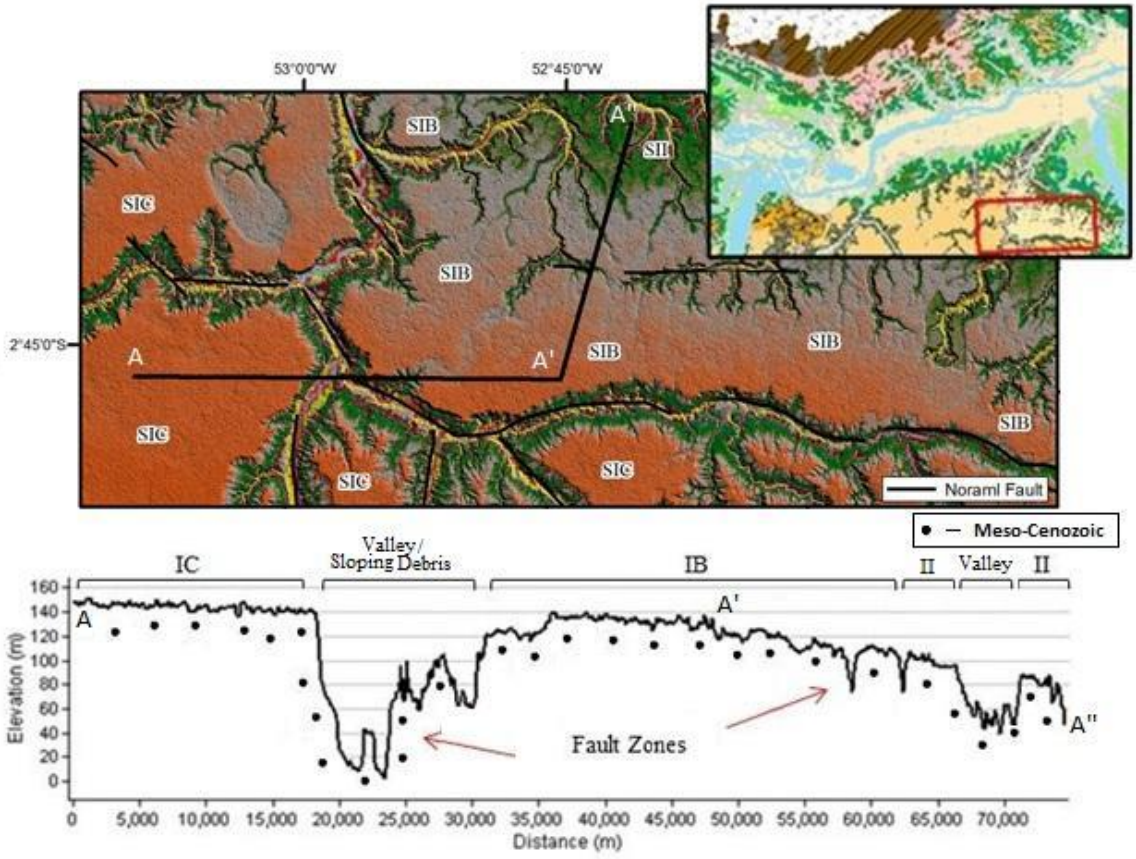

Figure 5.8. Relationship between Surface IB (SIB) & IC (SIC). Transect A-A' highlights a gradient increase in relation to fault zones. A gentle transition from SIB to Surface II (SII) is near 110 m elevation along transect A-A'.

In the northern half of the valley Surface I corresponds well with plateaus identified by others (see Fig. 5.6) but, unlike the southern half of the valley, the connection between subunits is not as easily discerned. The low gradient slope between Surface ID and IE makes correlation appear probable (Figure 5.9). If original the regional tilt that may have existed would have only had a diminutive influence on depositional

processes. Differences in slope may also be associated with mapped faults/tectonic lineaments that separate IE, and ID Surfaces (see Fig. 5.9).

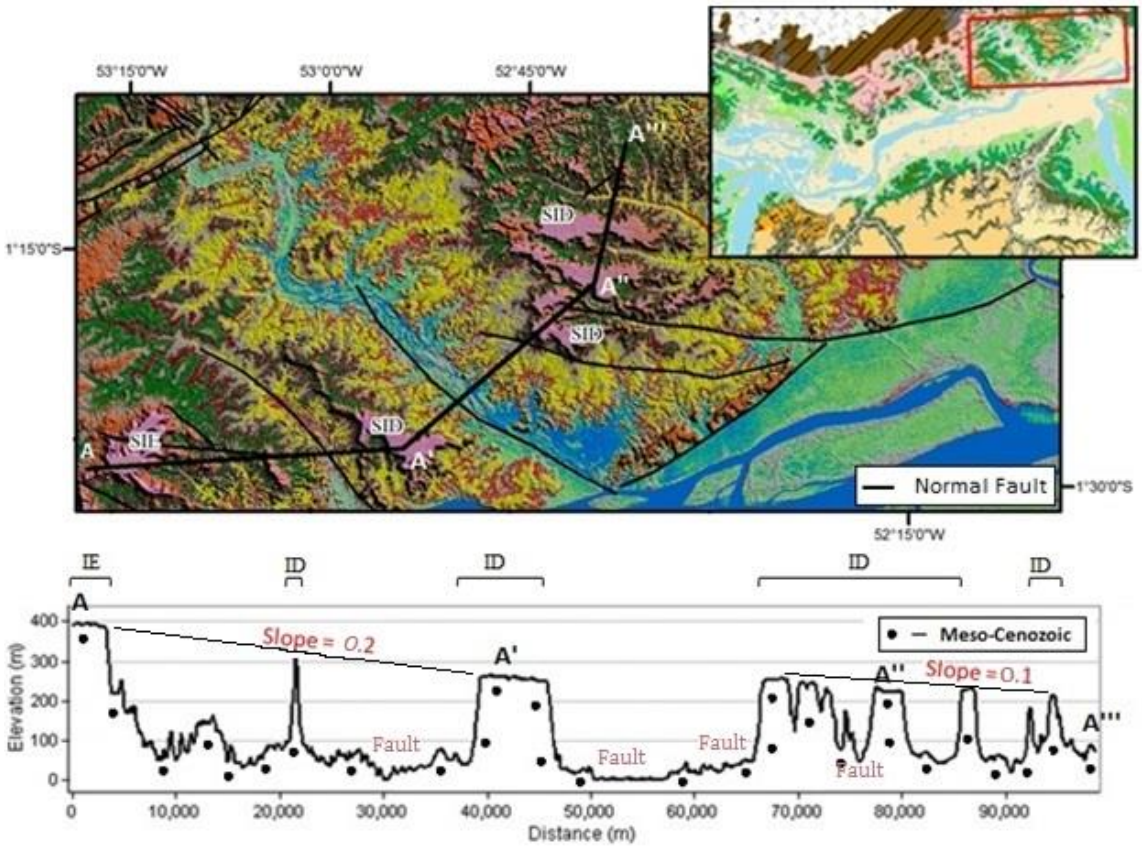

Figure 5.9. Proposed connections of Surface ID (SID) and IE (SIE). Transect A-A' links the plateau landscape in the NE portion of the study area by very low gradient slopes.

General trends and fluctuations in elevation can be used to relate plateaus in the northern and southern halves of the study area. At the western most extent of the study area, Surface IA occurs on both sides of the valley at similar elevations (Figure 5.10 Transect A). Connection of Subunit IE and IC, on the north and south sides of the river, respectively, requires only a low gradient slope (Figure 5.10, Transect B). As suggested

by these correlations, a single, continuous plateau surface on both sides of the river is most easily accommodated by a plateau forming process(es), experienced at the same time throughout the region. It is difficult to envision such a process were the Amazon River present when it occurred.

Although it appears through this analysis that differences in elevation and slope of plateau subunits are unrelated to the presence of the Amazon, it remains to be determined whether a plateau (Surface I) covered all of the northern study area or developed just within regions underlain by Meso-Cenozoic rocks. When comparing the elevation of Surface IC, underlain by Meso-Cenozoic rocks in the southern part of the study area, with the Erosive Surface with Hills II unit, underlain by Paleozoic rocks north of the river, a similar height in elevation can be observed (Figure 10 Transect C). On the basis of the different underlying geology of each unit and their similar elevation, this connection indicates that a substantial thickness of Meso-Cenozoic fill did not cover the Paleozoic rocks that make up the erosive surface with hills II unit.

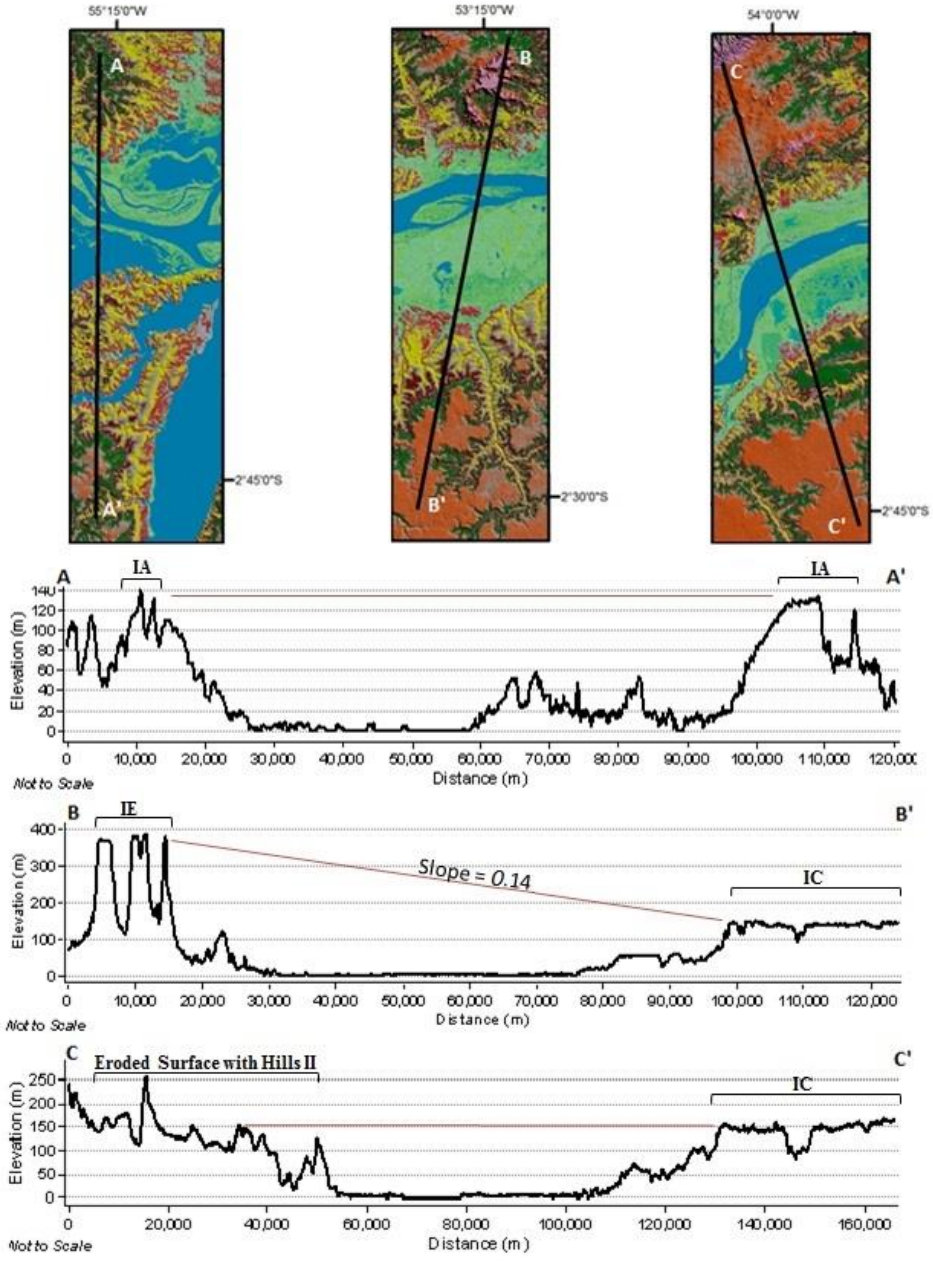

Figure 5.10. Potential connections of north and south units and surfaces. Transect A-A' illustrates the potential connection of Surface IA (IA) between north and south sections of study area. Transect B-B' illustrates low slope that separates Surface IE (IE) from Surface IC (IC). Transect C-C' illustrates the potential connection between the eroded surface with hills II and IC.

Another part of the landscape that displays a similar relationship between areas of differing underlying rocks occurs in the northern part of the study area. Here Surface IE is developed upon Meso-Cenozoic rocks and the dissected hills and ravines unit that is comprised of Paleozoic rock (Figure 5.11). The similarity in elevation of these units provides additional evidence for a widespread erosional event that affected most, if not all, substrates throughout the study area.

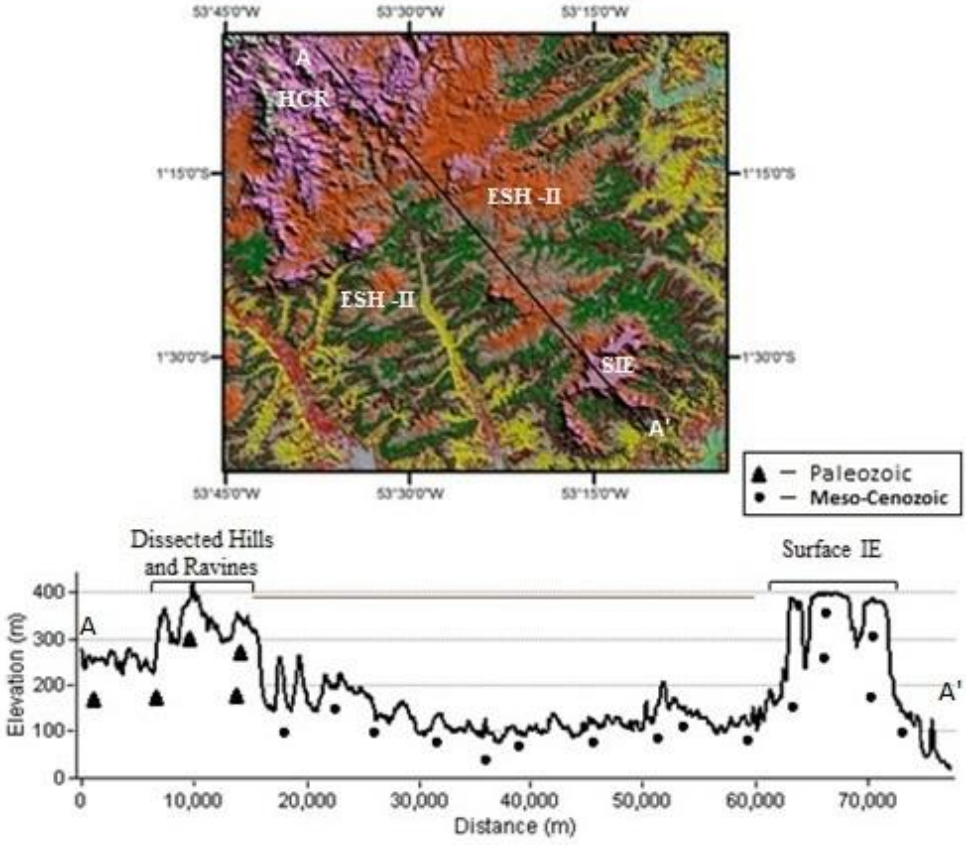

Figure 5.11. Proposed connection of dissected hills and ravines unit with Surface IE.

The development of a single contemporaneous plateau surface, Surface I, requires a process-based explanation that is not completely accounted for in published models. The Belterra Clay model sees the clay surface as a depositional unit related to a low energy environment. This model relies on the geologic interpretation of Sombroek (1966) that allows for an unconformity within the upper portions of the plateau. For this model to be sustainable sea level must have been at a height of 180 m above the present base level sometime after the Cretaceous period. Current research (Krantz, 1991; Miller et al. 2005) shows this was unlikely to have occurred. Furthermore the sand and gravel found in upper parts of plateaus (Fig. 5.3), and lack of uniformity between lithologic samples noted by Truckenbrodt et al. (1991) are both observations that are at odds with deposition by an estuary-like or deep body of water.

Mechanical Geomorphogenesis and In-Situ Weathering models both posit that the plateau surface is a derivative of the underlying geology. Analysis by Truckenbrodt et al. (1991) also supports this theory due to the close similarity in chemical composition of kaolinite and underlying strata, however the conditions that would have facilitated weathering in each model are very different. The Mechanical Geomorphogenesis model relies on dry climatic conditions while the In-Situ Weathering model relies on seasonality and fluctuations in the water table. The models are also dependent on which geologic constraints are imposed. If using the interpretation proposed by Damon and Contreiras (1971) one of these two processes acted on the landscape over a 65 my span. In contrast, Caputo's (2011) suggests that one of the processes was limited to the last 25 my.

Comparison of extant theories with the morphology of Surface I reveals certain aspects in common. The idea that the smooth plateau surface was once part of a regional pediplain is consistent with the plateau's gentle concave slope (Figure 4.1). When pediments coalesce they develop a concave shape. This observation does not explain the clay-rich composition of the plateau surface. This can, however, be accounted for by In-Situ Weathering model. Chemical weathering alone as a topographic smoothing agent is insufficient, in as much as it will not reduce surfaces at disparate elevations to a common datum.

Etchplanation processes, which have previously not been examined in the context of this plateau, may be relevant. A transition zone between weathered and unweathered material, a relatively homogenized soil profile, the appearance of laterite and thick zone of saprolite material may all provide support for the existence of a double planation surface as described to Büdel (1977). If etchplanation is considered, then a smoothing of the landscape through double planation processes is permissive. By this process. Surface I could have acted as the wash surface and Surface II (~80 m surface) as the basal surface on the basis of the thickness of clay material indicated in the soil profiles of Figure 5.5. Additional support for Surface I behaving as an etchplain is the stone lines identified by Radambrasil (1976). Thomas (1994) identified similar occurrences of stone lines in the Kodi etchplain but provided evidence that these occurrences were indicative of wash depressions that follow Büdel's (1977) etchplanation. Etchplanation processes in combination with divergent weathering can also be used to explain the development of laterite and relief generation in the valley (Figure 5.12). As noted in a previous section,

the Amazon Basin is a highly fractured zone; these fractures could have facilitated an accelerated lowering of the basin as demonstrated in intermontane environments (Figure 5.12). This interaction could have also facilitated subaquenous basal sapping (Thomas, 1994) that can help explain the gentle concave slope observed in Figure 4.1.

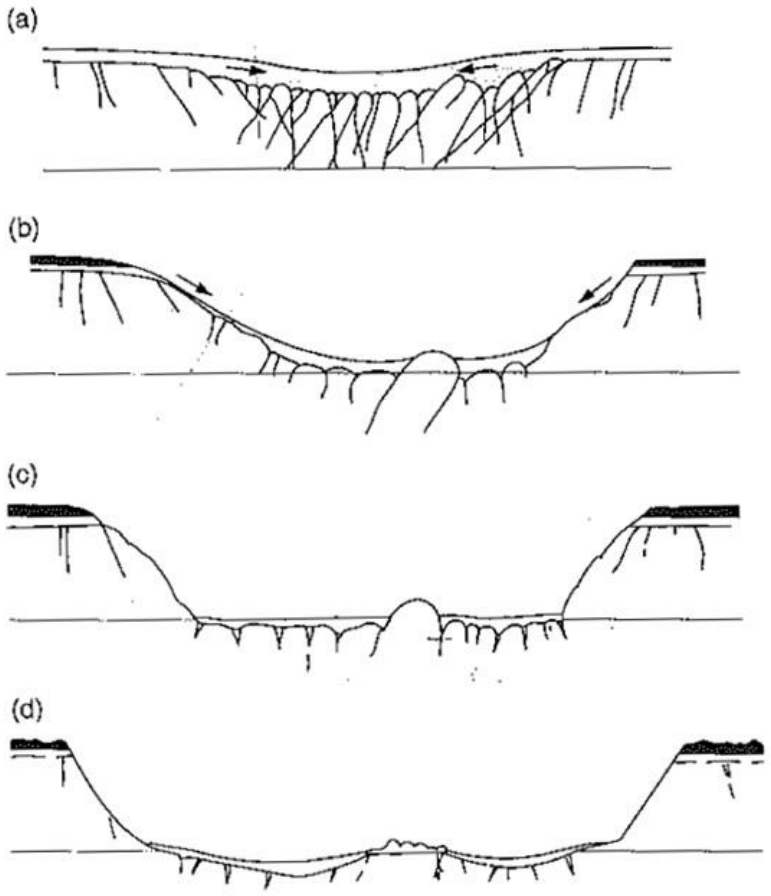

Figure 5.12. Divergent Weathering and etchplanation acting on a well jointed landscape. (a) jointing leads to inward water flow (b) continued lowering and duricrusts (in black) forma as water table falls (c) Steeping of piedmont and accumulation of soils in basin (d) Repetition of events. (Source: Thomas, 1977).

Chapter 6 - Terraces

Introduction

The existence of multiple topographic levels in the EAV is widely recognized, but poorly understood (Sternberg, 1975). Early reports on this landscape (e.g. (Katzer, 1903)) simply described these levels as dissected uplands with no relevant discussion of their age or origin. As more detailed analyses were conducted throughout the Amazon, these levels were recognized as smooth plains with a bench-like appearance without allusion to their origin (Marbut and Manifold, 1925). Gourou (1949) was one of the first to propose that some of these levels were terraces, but did so only for units between 20-30 m above the Tapajós River; he considered higher elevation benches eroded plains and remnant hills. Ab'Saber (1967) held a similar view and added that the units were most likely formed by pedimentation processes triggered by abrupt climatic change to arid and semi-arid conditions.

In the second half of the last century glacial eustatic models where used to explain the generation of relief in this area. One of the earliest interpretations was that of Sakamoto (1960), who thought that the lower levels (below 50 m) were quartz sand terraces that developed in interglacial times. Higher levels were thought to be erosional landforms formed by entrenchment and channeling in glacial periods. Since Sakamoto's (1961) interpretation no one has considered the plains to be erosional features. Instead, they have been characterized as constructional terraces associated with glacial eustatic changes in the Amazon region (Irion, 1984; Klammer, 1984; Soembroek, 1966). The most comprehensive model, that of Klammer (1984), identified numerous terraces

throughout the EAV and developed a qualitative eustatic model that conformed to the observations. Although this analysis was comprehensive, the methods and techniques are now viewed as primitive and ripe for revision (e.g. Mertes and Dunne, 2008).

The objective of this chapter is to compare terraces in the EAV with those identified by Klammer (1984). Comparable results warrant explanations that accommodate a more recent understanding of Late Cenozoic conditions. Alternatively, differences require a substitute explanations for terrace development in the EAV. This chapter begins with a review of Klammer's (1984) analysis, followed by a section that examines his glacial eustatic model. The chapter ends with a comparison to current literature as it pertains to the results of this work.

Gerald Klammer (1984)

Early terrace observations in the EAV ranged from identifying a single terrace (Katzer, 1903) to multiple terraces that bear little relationship to one another (Klammer, 1978). Inconsistencies were likely caused by inconsistent choices for terrace measurement, and use of varying river water levels for reference base level (Klammer, 1978). To rectify these discrepancies Klammer (1977) conducted a general study of 13 sites in the Jari-Paru River area, and shortly thereafter a comprehensive study that measured 158 slope profiles along the Trombetas River, a tributary to the Amazon (Klammer, 1971, 1975, 1978, 1979, 1984) (Figure 6.1).

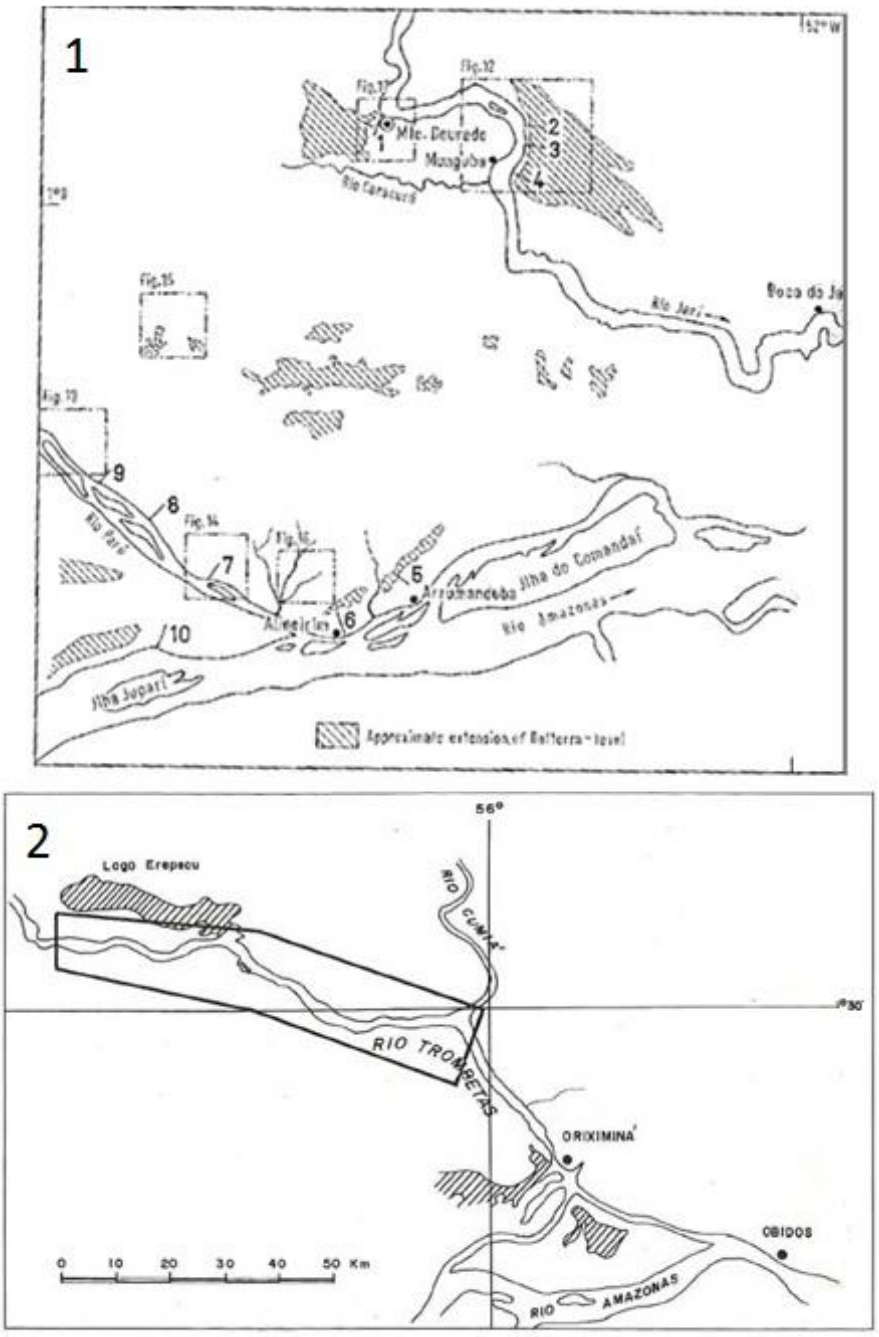

Figure 6.1. Gerald Klammer study sites from early and more comprehensive studies. Image on the left shows where transects and analyses of Klammer (1975-78). Image on the right highlights section of Trombetas River where a comprehensive survey was conducted (Klammer, 1984).

Klammer's early research primarily used transects and sedimentological data from sites along the Jari, Paru, Tapajós and Amazon Rivers. From these transects he identified terraces as level surfaces between 50 - 300 m in width (Klammer, 1977). Sedimentological data from these transects were used to demonstrate the dissimilarity between these lower elevation levels and the Plateau landscape. The samples also showed that although variation exists between terraces levels, they are all primarily comprised of poorly stratified coarse sands that is variably iron cemented (Figure 6.3).

River	Terrace Observation (m)
Tapajós River	9-10 x 2 8-11 ---------- 20-22 20-21 ---------- 68-69
Jarí River	9-10 10-11 ---------- 18-23 20-22 ---------- 28-31 30-31 ---------- 68-74
Parú River	23 20-27 ---------- 94-101
Amazon River	19-22 ---------- 28-31 ---------- 41-43 ---------- 88-92

Figure 6.2. Terraces proposed by Klammer (1977). Break (----) in graphic indicates a terraces grouping according to Klammer (1977) (modified from Klammer, 1977).

Based on these observations Klammer viewed his results as indicating the existence of 6 - 8 terraces levels in the EAV. He viewed this early analysis as insufficient (Klammer, 1977) because of the limited sample size and inconsistencies in terrace occurrence between study sites. Klammer (1977) assumes these variations in measurements where due to interruptions in slope profiles created by erosion.

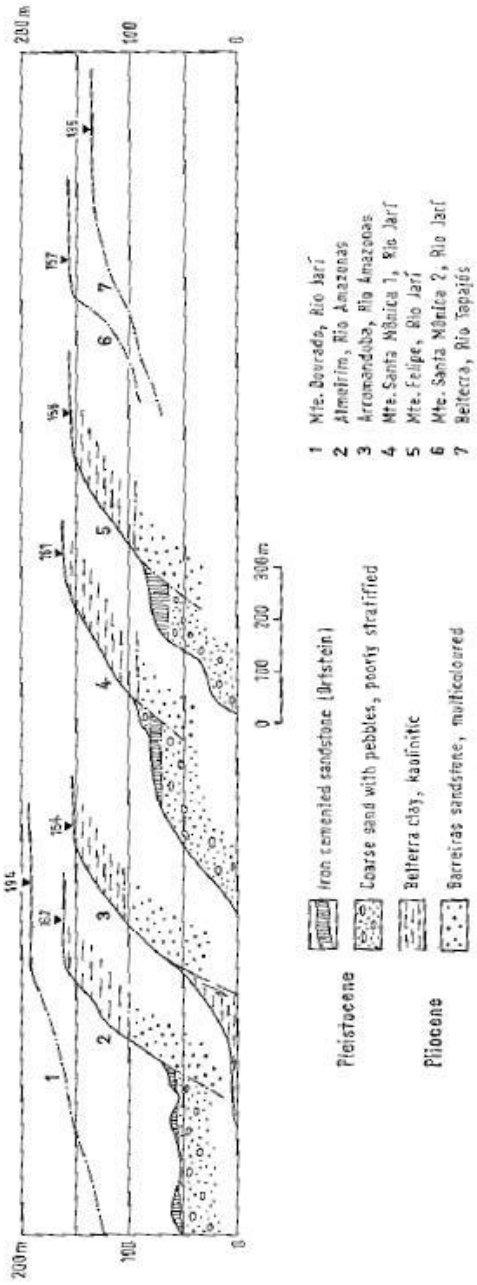

Figure 6.3. Transects with soil profiles recorded by Klammer (1977). Transects include a reference to soil properties. Lower levels with poorly stratified material are identified as terraces. Upper level of transects is identified as Belterra Clay. Belterra Clay found at lower levels is believed to be reworked material (Source: Klammer, 1977).

The inconsistencies present in earlier publications and Klammer's own research led him to a study site along the Trombetas River where it maintains a relatively straight course for 150 km. It was believed that this area was relatively uninterrupted by erosional processes, and since it is a tributary to the Amazon should have been affected by the same factors that affected the surrounding Amazon Region. This analysis uses the Trombetas River as base level and identifies the Belterra Plateau at ~160m, the post-Belterra relief at ~80m (the post-Belterra relief corresponds to Surface II in this report) and 9 or so terraces by measuring transects along the south bank of the Trombetas River (Figure 6.4). The Belterra Plateau was identified as having a nearly level slope that contains a nearly uniform distribution of materials less than and greater than 0.250 mm between locations. Post-Belterra erosional relief was identified with slopes having a concave shape and that ranged from 1° - 3°.

Of his 158 measurements, the most common terraces recorded by Klammer (1984) were at 10 m asl (18 occurrences), 33/29 m asl (17 occurences), 50 m asl (15 occurrences) and 66 m asl (15 occurrences). He also identified terraces at 6 m asl, 24/20 m asl, 44/40 m asl and 60 m asl, all of which were observed ten or less times. The flight of terraces between 66 m elevation and sea-level ranged in slope from 1° to 24° toward the river, however the mean slope of each terrace group was between 3 ½° and 5 ½°. Outliers that contained the higher slopes occurred at the lower 6, 10 and 20 m terraces and displayed a convex shape compared to the upper levels that were relatively concave. Additionally, sedimentological analysis showed dissimilarity between terrace sites, with sediment concentrations that ranged from a 30%/70% split between fine and course

grained material to an 80%/20% split. The terraces were also noted as containing up to 10 times more heavy minerals than the Belterra Plateau.

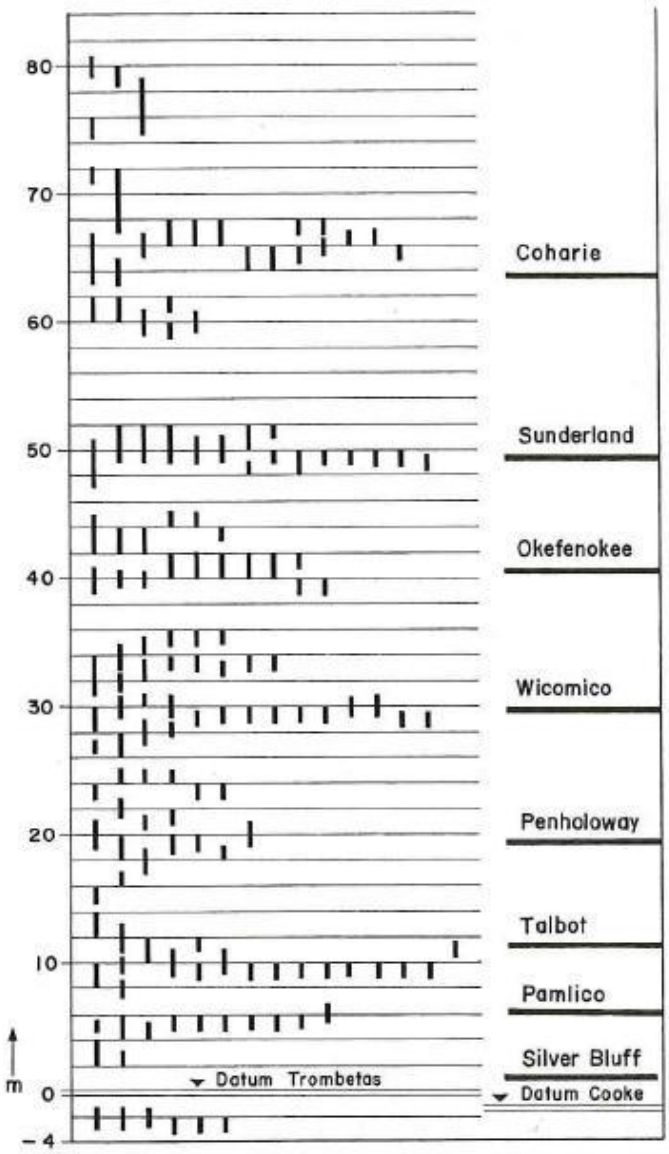

Figure 6.4. Klammer (1984) terrace observations along the Trombetas River. Terrace observations (left) are correlated to terraces in SE US (right) (Source: Klammer, 1984).

The flat gradient of the Post-Belterra surface is interpreted by Klammer (1984) as pointing to a slow decline in base level, whereas the higher gradient slopes on surfaces of the lower levels were interpreted as indicating quicker drops in base level. The spike in the slope of terrace surfaces at 20 m and lower is interpreted as being a product of partial flooding which would have left the higher end of each unit above water and absent of erosional and/or depositional processes. The fluctuations in concavity were interpreted similar to slope, with the concave shape thought to correspond to slower drops in base level and convex shapes to quicker drops. This interpretation would indicate that the higher elevation terraces with a concave shape were impacted less by rapid fluctuations compared to the lower elevation terraces that maintain a concave shape. Additionally Klammer (1984) interprets the disparity seen between the sediment concentration samples as proof that the plateaus and terraces were deposited under different circumstances. The relative uniformity of the plateau sediment samples is viewed as a depositional event that occurred over a long period of time with stable conditions. Whereas the variation and lack of stratification seen in the terrace sediments is viewed as result of deposition occurring at different times and at different speeds.

EAV Glacial-Eustatic Model

Glacial-eustatic models for the EAV are predicated on the assumption that eustatic fluctuations triggered by glacial and interglacial periods will lead to the formation of terraces in any fluvial valley experiencing these changes. These models follow the theory of a graded river in the belief that a fluvial system will readjust its gradient as sea-level fluctuates in response to changes in the volume of continental ice to

maintain a state of equilibrium (Mackin, 1948). Holding all other variables constant, these models believe that if base level falls the system responds by down cutting, which can promote formation of cut terraces (Leopold and Bull, 1979). If base level rises then aggradation occurs to slow the velocity, which can lead to development of fill terraces (Fisk, 1944). By recording the elevation and occurrence of terraces in the EAV these models reconstruct a qualitative history of ancient sea-level rise and fall.

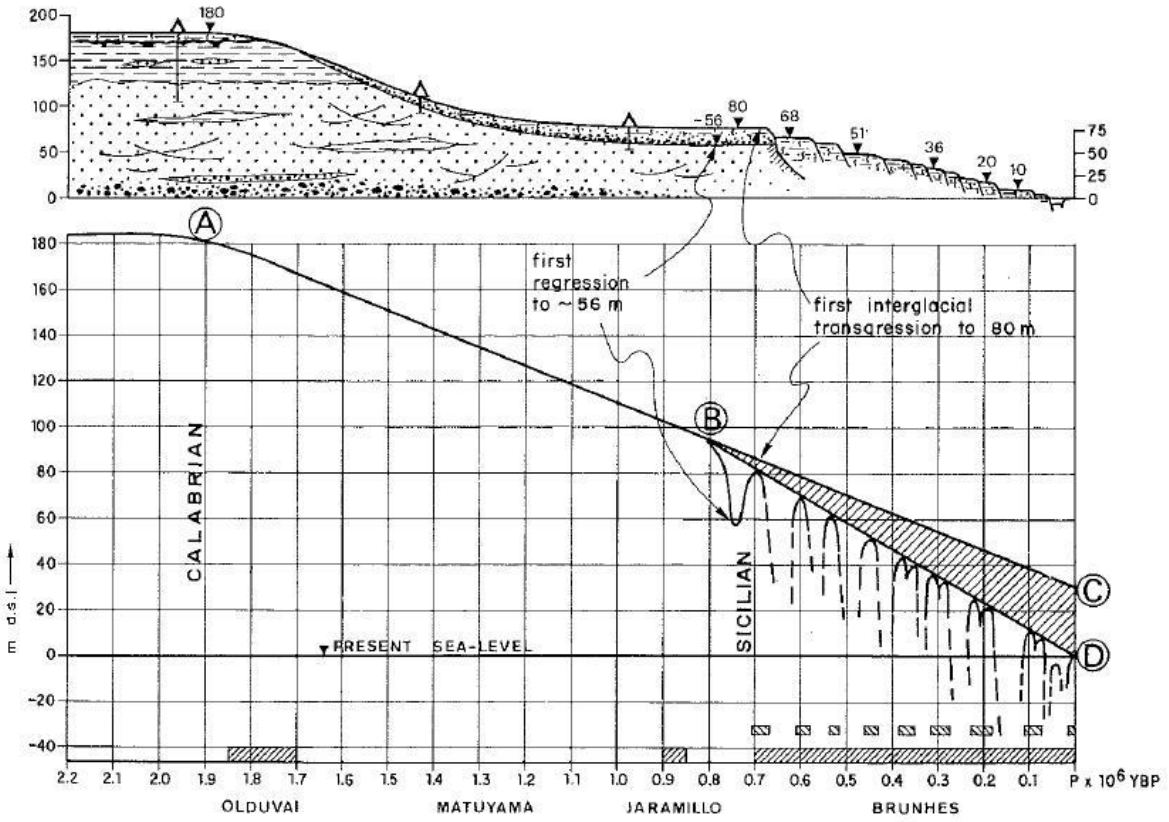

Figure 6.5. Klammer's eustatic model throughout the Pleistocene. During the Calabrian sea-level was thought to be ~180 m, then slowly declining until ~90 m where it took on a near rhythmic pattern until reaching its present level.

The most comprehensive and widely accepted eustaic model for the Amazon region was that of Klammer (1984), who used the variations observed in the slope, concavity and sediment distribution of terraces to model sea-level change through the Late Cenozoic (Figure 6.5). To integrate these theories into a eustatic model, Klammer (1984) hypothesizes that sea-level before and during the Calabrian stage (~0.781–1.9mya) was 180 m asl. Sea level would have slowly decreased to ~90 m asl into the Sicilian stage (~0.7mya). At this time sea-level is thought to have dropped more rapidly, before taking on a near rhythmic pattern of rise and fall until it reached its current level. To relate this theory to glacial cycles and date the early terrace observations, Klammer (1984) incorporated results from Fairbridge (1961) and Emiliani (1957) that suggest a relationship between sea temperatures and sea levels to support his theory of glacial-eustatic fluctuations in a sporadic downward trend through the Pleistocene to present. Klammer (1984) acknowledges that melt water from glaciers alone cannot explain the 180 m sea level high during the Calabrian (which is actually much higher if considering Subunit ID & IE), and expresses interest in hydrostatic fluctuations being a cause of this extreme height. Klammer (1984) also suggest that the pattern between terraces in the Lower Amazon is similar to ancient coastlines in Patagonia, the Southeastern United States and the Thames basin, consistent with a eustatic forcing.

Analysis & Discussion

Several concerns arise with Klammer's (1984) research. The first is the assumption that the Trombetas, Purus, and Jari Rivers can serve as proxies for the entire Amazon Region. Rivers are process response systems that respond at different rates, and

in different ways (Schumm and Brackenridge, 1987; Waters, 1985). Even though variations between the two systems can be small, when coupled with other factors unique to each system, they can be large enough to cause different responses (Castleden, 1980), making a direct connection nearly impossible. The fact that terraces exist along the Trombetas or any other tributary should not mean that the same can be said for the entire Amazon region without additional observations.

The analysis conducted in this report operated under the assumption that terraces should exist in the EAV, but an attempt to map them was unsuccessful. As indicated by the geomorphologic map (Figure 4.1), the 9 - 10 terraces identified along the Trombetas River were not found in the Amazon Region, nor were the 6 - 8 terraces identified in Klammer's early report. Instead, this analysis shows that erosional surfaces comprised the majority of the area. Even attempts at duplicating the observations of Klammer (1977) along his transect lines were unsuccessful for several of his locations. The only robust observation in Klammer's research that could be confirmed was the location of the Belterra plateau.

A second assertion worth revisiting is the role of glacial-eustasy (Klammer, 1984). The assumption that changes in base level during the Late Cenozoic are solely responsible for staircase-like terraces generally, and the EAV in particular, has been challenged by the more recent observation that the numbers of terraces in coastal environments is dissimilar globally (Bridgland and Westaway, 2008), and because they do not account for delay-effects (Vandenberghe 1995). Instead, current models recognize the role of uplift-coupled incision and aggradation in the formation of staircase terraces

(Bridgland and Westaway, 2008; Maddy and Bridgland, 2000). Examples of staircase terraces where these drivers have been invoked are in NW Europe (Antoine et al. 2000), Eastern Europe (Matoshko et al., 2004), NW United States (Merritts et al. 1994) and along the eastern coast of the United States (Westaway et al., 2007), an area that Klammer (1984) uses to confirm his results. If only base-level change is the driver, stacked terrace structures from alternating periods of incision and aggradation counter one another, and result in little change to the time-integrated base level record of the system (Bridgland and Westaway, 2008). Variations in the number of terraces recorded between fluvial systems can sometimes be better explained by different amounts of uplift (Bridgland and Westaway, 2008). To understand terraces in a coastal region, an examination of both eustatic and tectonic processes is required (Merritts et al., 1994). Models for the EAV currently ignore the later.

Further complications in the EAV eustatic terrace model arise when considering the effect of changes in base-level on aggradation and incision processes. Adjustments both in external (e.g. water in the system, variations in sediment inputs, eustatic fluctuations, and base level changes) and internal forces (e.g. events in other parts of the river) all impact landform development (Dawson and Gardiner, 1987). A model that operates relies solely on graded river theory overlooks the importance of changes in sediment and water supply (Vandenberghe, 1995). It has also been demonstrated that the effects of eustatically driven incision are much more dramatic along the continental shelf of passive margins than the upstream reaches of the river, where effects are negligible (Talling, 1998). In the Amazon River this holds true; the last glacial maxima only

increased river gradient to 5.5 cm/km compared to today's rate of 2 cm/km (Mertes and Dunne, 2007).

Finally sea-level curves for the Eastern United States, the area used by Klammer (1984) to calibrate and support his Amazon model, have undergone substantial revision and no longer support his model in detail. The maximum height above present base level during the Pliocene never exceeded 50 m (Figure 6.6), and during the Pleistocene was never higher than 15 m (Krantz, 1991). Klammer's (1984) eustatic model calls upon seal levels that reached nearly 180 m above present levels. Likewise, the slow decline in base level from the Belterra Plataeu to Post-Belterra relief is not plausible on the basis of current information. The earliest that sea-level could have been close to 180 m elevation is during the Early Eocene (Miller et al., 2005).

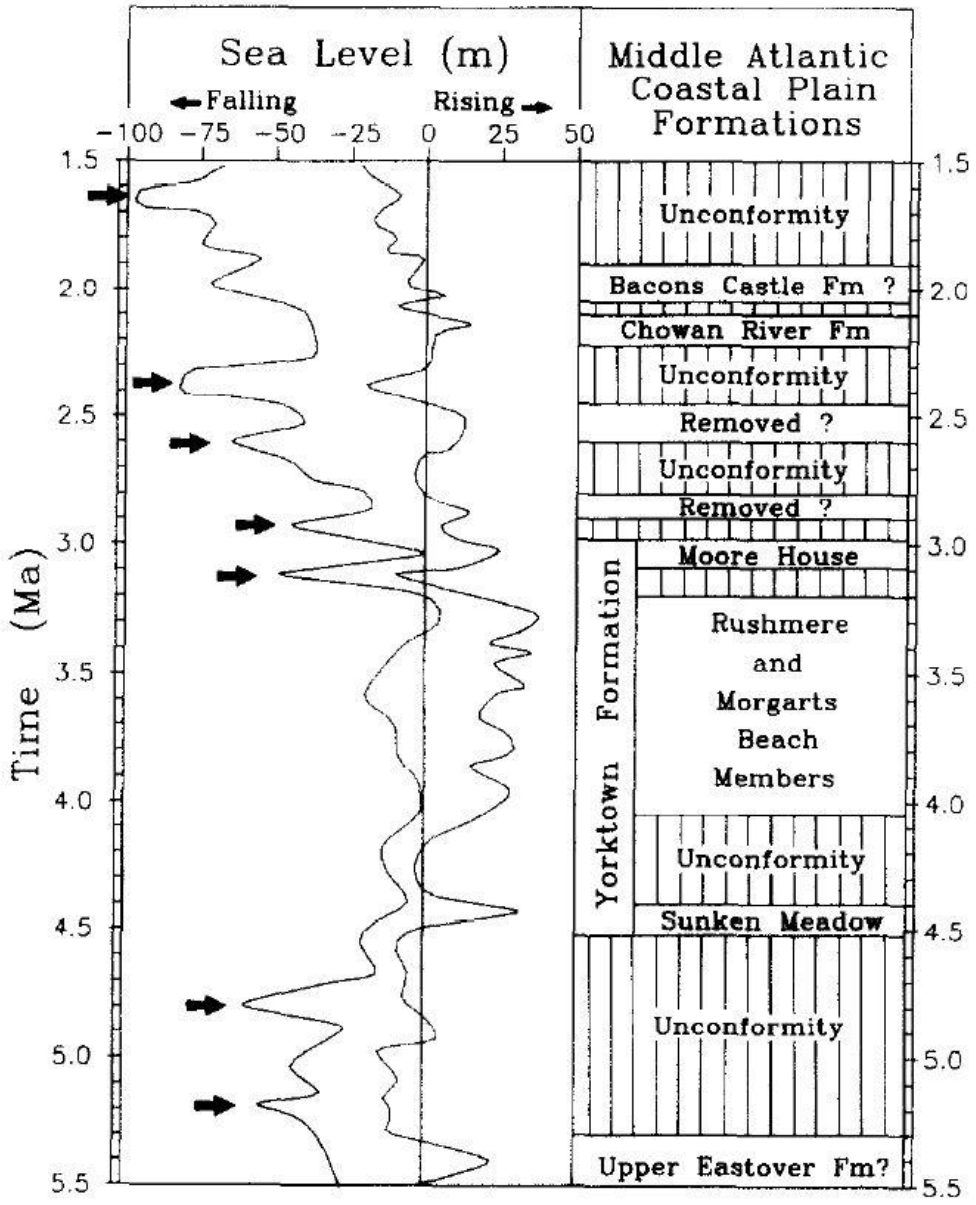

Figure 6.6. Sea-level for 5.5 - 1.5 mya curves for the SE US. Right line is from Krantz (1982) Left line indicates revised sea-levels according to Krantz (1991). Bold arrows highlight when regression events peaked. (Source: Krantz, 1991).

Several other studies are cited by Klammer (1984) as identifying terraces in the EAV, Some of these citations are without merit (i.e. Katzer, 1903 and Marbut and Maniforld, 1925 nowhere mention terraces) and some are too vague to properly evaluate (e.g. Gorou, 1949 and Day, 1959 mention terraces but with no direct reference to elevations).

This analysis, like that of Sakamoto (1961) and Ab'Saber (1967), supports an erosional origin for all surfaces in the EAV; evidence in support of terraces like those proposed by Klammer (1984) is lacking. Comparison of study area elevations and relative surface heights to those of Klammer (1977) (Fig. 6.7) nevertheless reveals certain gross similarities.

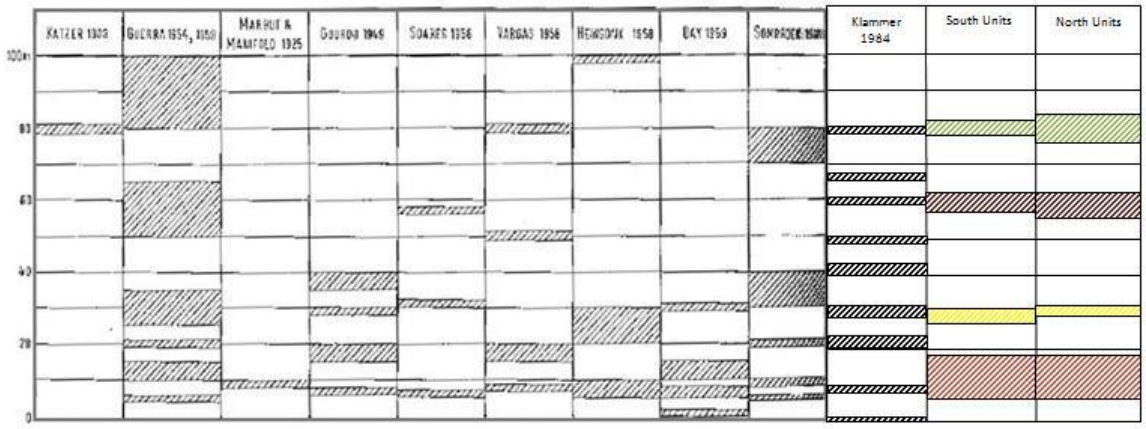

Figure 6.7. Comparison of elevation levels (y-axis) in the study area with terrace elevations from Klammer (1977). These units correspond relatively well with the erosive surfaces identified in this report. Colors correspond to hillshade model intervals. (modified from Klammer, 1977).

Each unit of this report corresponds to at least three units reported by earlier workers, with lower elevation surfaces overlapping most frequently. Surfaces noted by

Klammer (1984) also seem to generally correlate well. Variations may among data sets may be real or instead a consequence of methods used to measure surface heights (c.f. Klammer, 1976, EAV elevations do, in fact, vary both north to south and east to west (Figure 6.8). Figure 6.8 also illustrates how surface elevations can be site specific as well noted by the absence of surfaces along reaches of the Amazon Valley and fluctuations in the elevation of each surface.

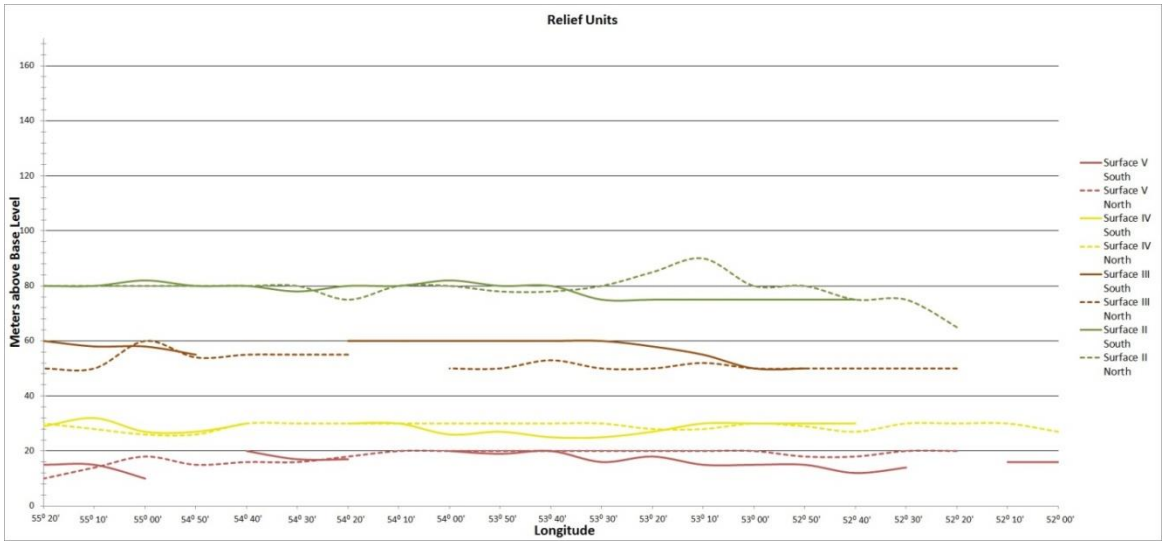

Figure 6.8. Elevation Trends of Surface II – V.

A final observation reported by Klammer that deserves discussion is his sedimentological analysis. Klammer‘s (1979) terraces are comprised of poorly sorted un-stratified materials that contain a mixture of clays, silt, coarse sands, and pebbles. This observation are at odds with current understanding of terrace formations. Terraces in lowland rivers are typically comprised of sediment ranging from silts to sand, with sediment accumulation influenced by processes that produce sorted deposits Meso-Cenozoic fill of the Alter do Chao Formation underlies the ‘terra firme’ in the landscape

and is primarily sandstone. Reworking/erosion of Alter do Chao Formation could produce sediment like that described by Klammer (1984) as terrace deposits, which might also include sources from higher elevations. Likewise, Klammer's (1984) average slope of less than 7° is consistent with an interpretation of such surfaces as pediments (Figure 6.9).

Chapter 7: Final Remarks

Careful GIS analysis of a vegetative corrected DEM provides new insights and a better understanding of the long term landscape evolution of the EAV. The most important findings are:

1) Erosional landforms make up the majority of the study area. These range from large planation surfaces to erosive surfaces littered with hill complexes. Results demonstrate that previous models of fluvial valley development for the EAV are likely invalid, illustrate correlations between different sections of the landscape, and provide new scenarios of development for the EAV.

2) Differences in geologic interpretations and theory hinder understanding of landscape development. The best geological constraint are likely those of Caputo (2011), whose comprehensive palynology age analysis of 450 m of core provides evidence of a Cretaceous-Tertiary unconformity. By developing a more precise age for the geologic units that comprise the plateaus, the subsequent weathering and incision of the plateau landscapes can be limited to the last 25 my.

3) The highest elevation plateaus in the EAV are likely part of a continuous erosional surface (Surface I) that has since been modified by neotectonic activity, and physical and chemical weathering. Evidence that supports a prior connection among the now isolated plateaus includes similar trends in elevation and slope physical weathering may have been the dominant process of the regional smoothing event that produced Surface I, as indicated by its relationships to underlying rock units. Deep chemical weathering indicated by laterite horizon and thick saprolite, was initiated after Surface I

developed. Other studies elsewhere in the Amazon basin (e.g. Balan et al. 2007) suggest that this event may have occurred during the Oligocene to Middle Miocene.

4) Lower levels of the 'terra firme' in the EAV are denudational landforms, not terraces as described by Klammer (1984). Several levels identified previously as terraces are coextensive with erosional surfaces of this analysis. Terraces which have no correlatives are thought to have misidentified erosional material imprecisely related to base level. Glacial-eustaic models used to support terrace development are not supported by present understanding of Late Cenozoic sea-levels, nor by recent advances in understanding how staircase-like terraces form.

5) Events that led to incision of the plateau landscape and development of sub-plateau erosional units are poorly constrained. Divergent weathering and etching processes may have been a contributor. Thick saprolite cover and fracture-enhanced permeability along valley axes are components of these processes. The ultimate driver of these and other erosional processes likely included both rock uplift and changes in base level. Once assumed to be tectonically stable because of proximal cratons, the area has been recently recognized as containing neotectonic faults and lineaments (Costa et al, 2001), that unequivocally demonstrate a potentially important role for tectonism and uplift in the evolution of this landscape. Due to its distance from the Andes the agent in this scenario would almost certainly have to relate to intraplate tectonics. Netotectonics in this area have been attributed to the rotation of South America (Costa et al. 2001), however recent research by Braun (2010) indicates that uplift and neotectonic activity in passive Atlantic coastlines can be related to rifting or dynamic mantle interactions. This

idea follows observations by Bridgland and Westaway (2008) who noted a global phenomenon of pulses of uplift in Pleistocene times in cratonic zones, and passive margins.

6) It is believed that previous studies of the EAV have fallen short on their analysis and provided inconsistent results because they conducted site or topic specific studies that not only ignored the surrounding landscape, but usually failed to relate their observations to other units in the area. Unlike previous studies that used a local study site and extrapolated the results to a larger area, this analysis studied the landscape in a regional context. The EAV is a landscape that has been dominated by erosive events throughout the Late Cenozoic. Because of this, a concern that still persists is the location of ancient fluvial systems during the planation event that developed Surface I.

Appendix 1 – Study Area Maps

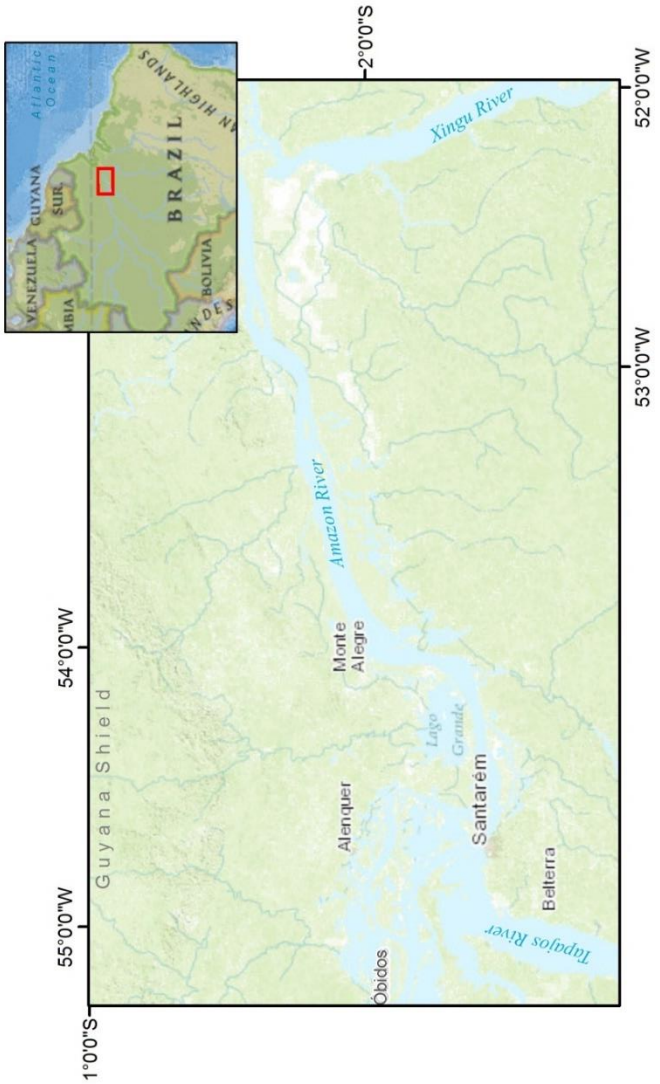

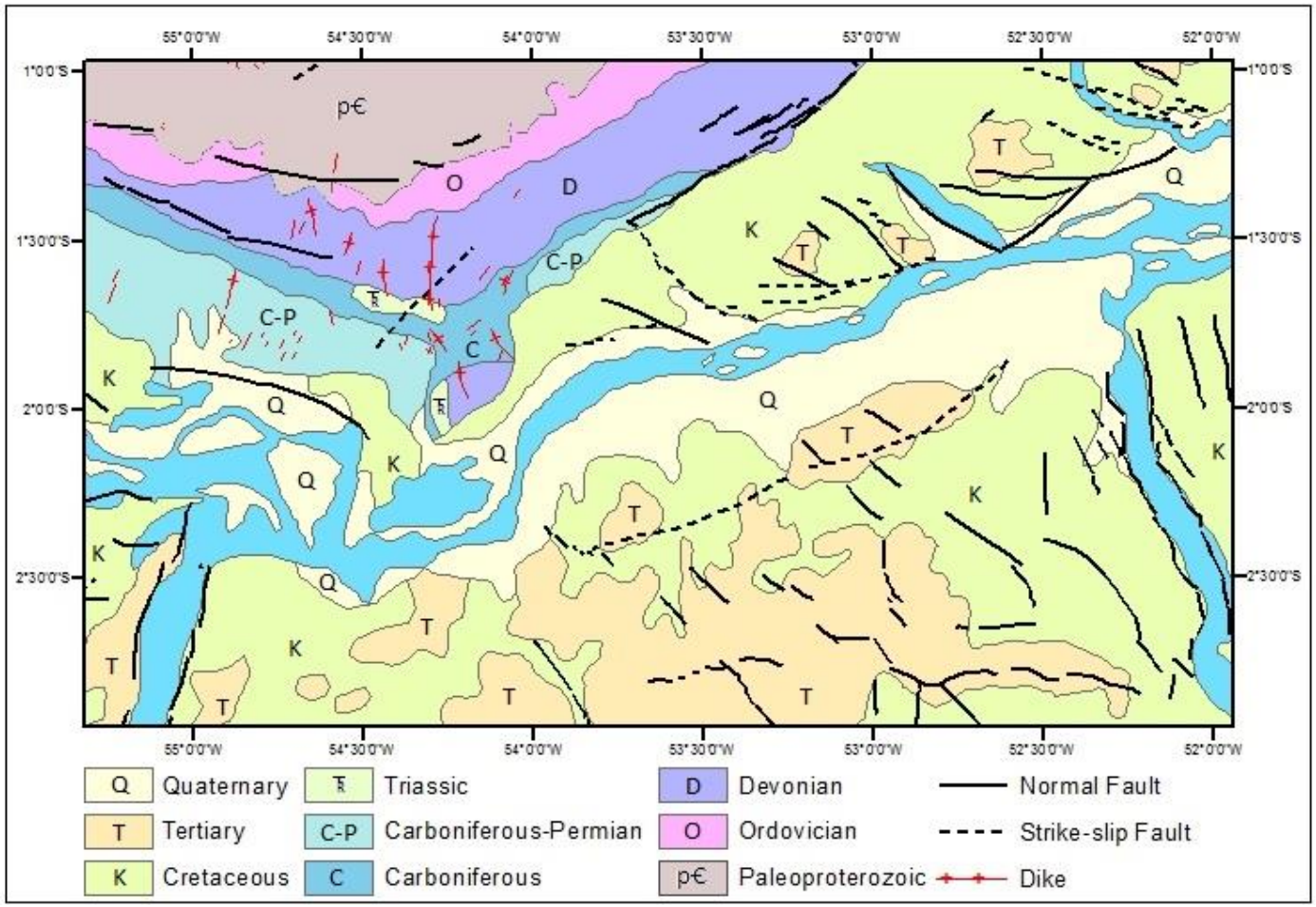
55°0'0"W
54°30'0"W
54°0'0"W
53°30'0"W
53°0'0"W
52°30'0"W
52°0'0"W
1°0'0"S
1°30'0"S
2°0'0"S
2°30'0"S
p€
O
D
C-P
C
K
Q
T
Q Quaternary
T Tertiary
K Cretaceous
Triassic
C-P Carboniferous-Permian
C Carboniferous
D Devonian
O Ordovician
p€ Paleoproterozoic
Normal Fault
Strike-slip Fault
Dike

1°0'0"S
2°0'0"S
55°0'0"W
54°0'0"W
53°0'0"W
52°0'0"W
Legend
Slope
Water
River
Fault
Normal Oblique
Dike
Dome
Denudational Landforms
Planation Surfaces
Surface IA (130-150m)
Surface IB (110-130m)
Surface IC (150-180m)
Surface ID (250-300m)
Surface IE (380-410m)
Surface II (70-85m)
Surface III (57-63m)
Surface I
Surface IV (23-33m)
Surface V (8-20m)
Dissected Units
Erosive Surface with Hills (250-350m)
Erosive Surface II with Hills (125-145m)
Dissected Hills & Steep Ravines
Sloping Debris/Cliff
Inclined Fluvial Valley
Aggradational Landforms
Floodplain
Surface I Colluvium
Precambrian
Paleozoic
Meso-Cenozoic
Atlantic Ocean
Brazil
Venez.
Bolivia
ESH-I
DSH
Slp. Debris
ESH-II
SII-SV
Floodplain & River
SIII -SV
SII
Slp. Debris
SI
A
A'
Elevation (m)
Distance (m)

Appendix 2 – Geologic Maps

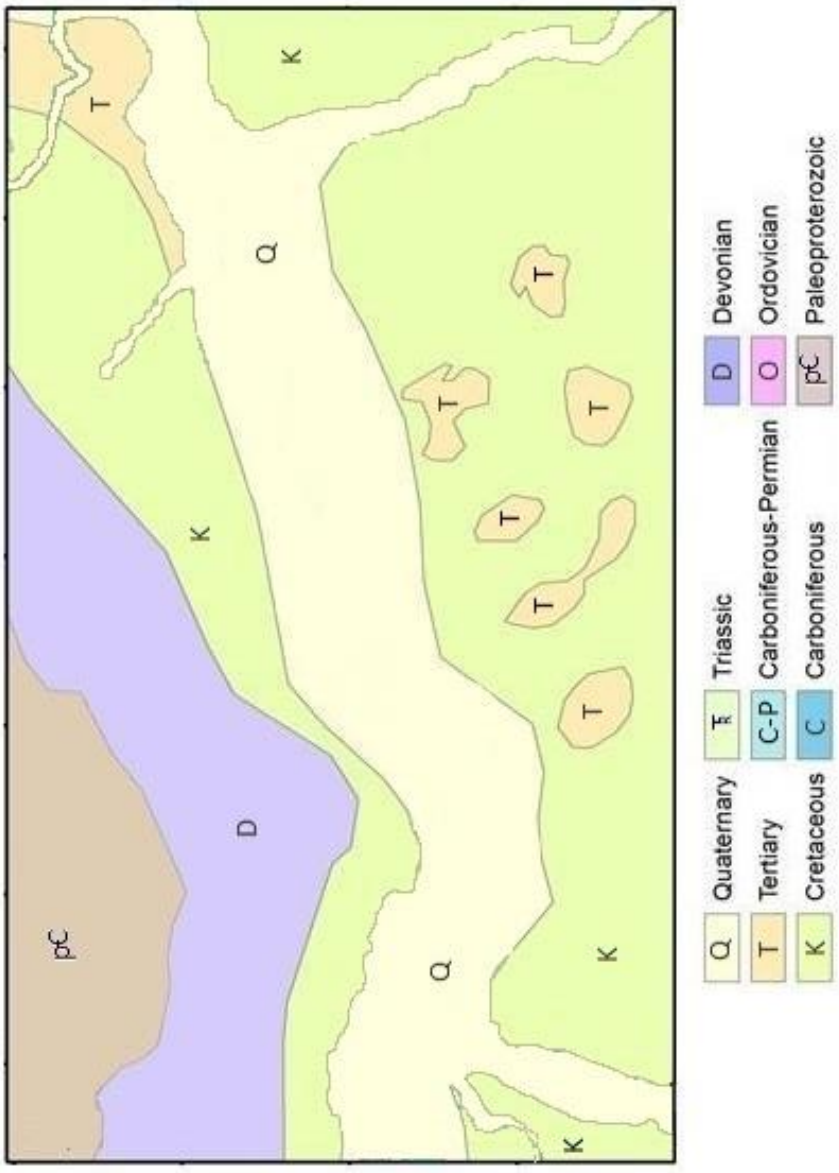

Brazillian Institue of Geography and Statistics (IBGE) (2006)

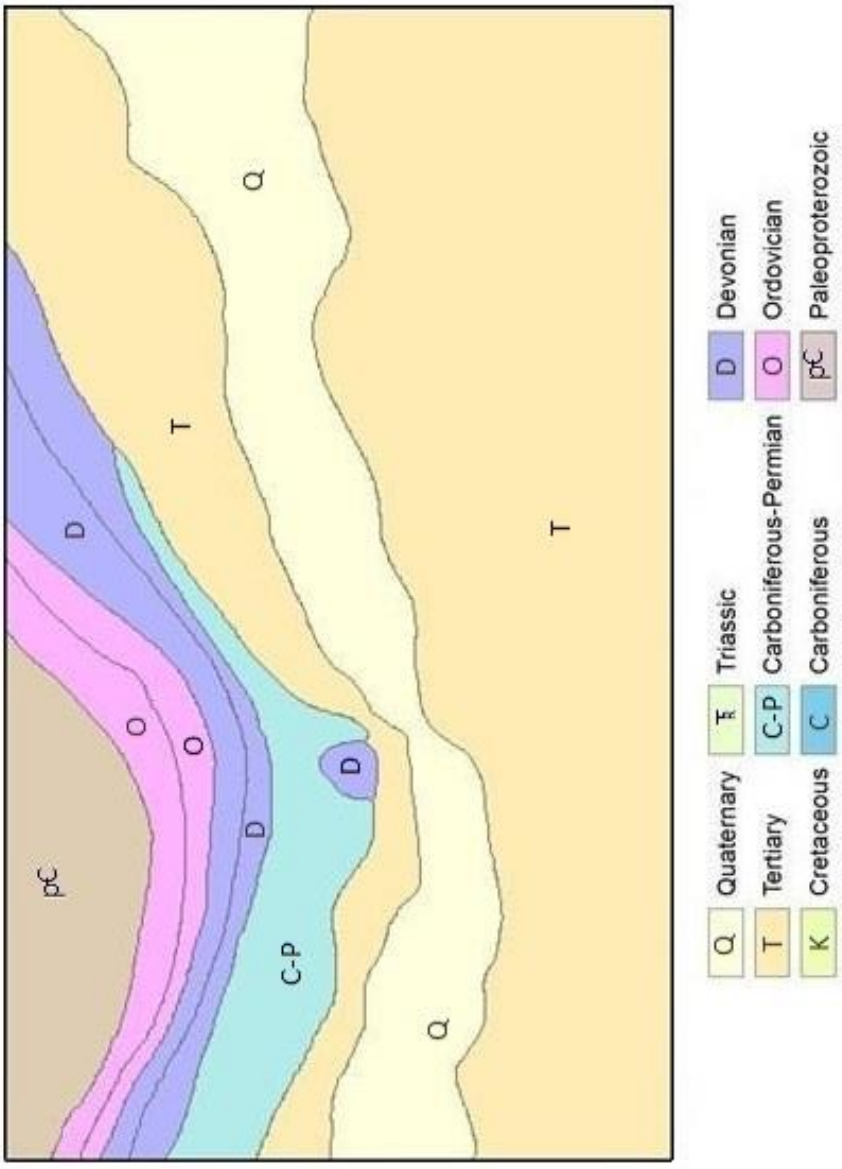

U.S. Geological Survey (2012)

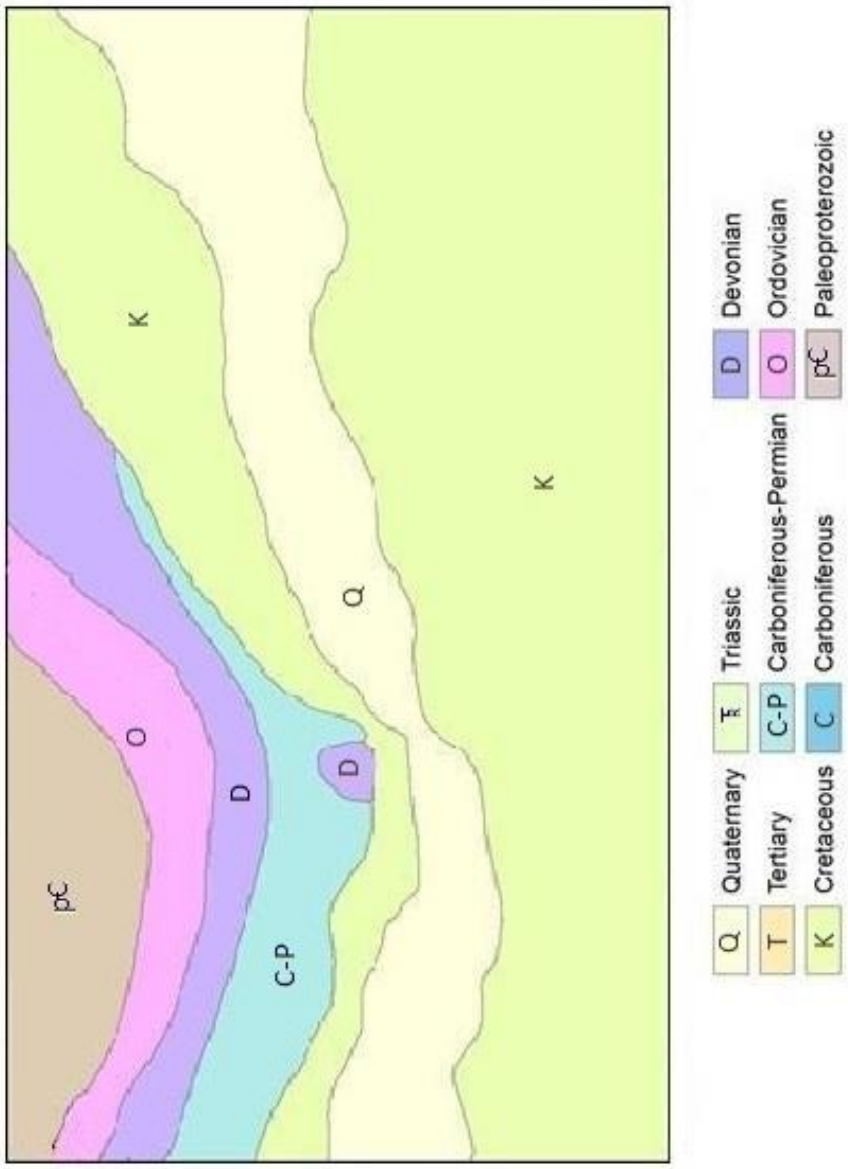

Daemon & Contreiras Geologic Interpretation (1971)

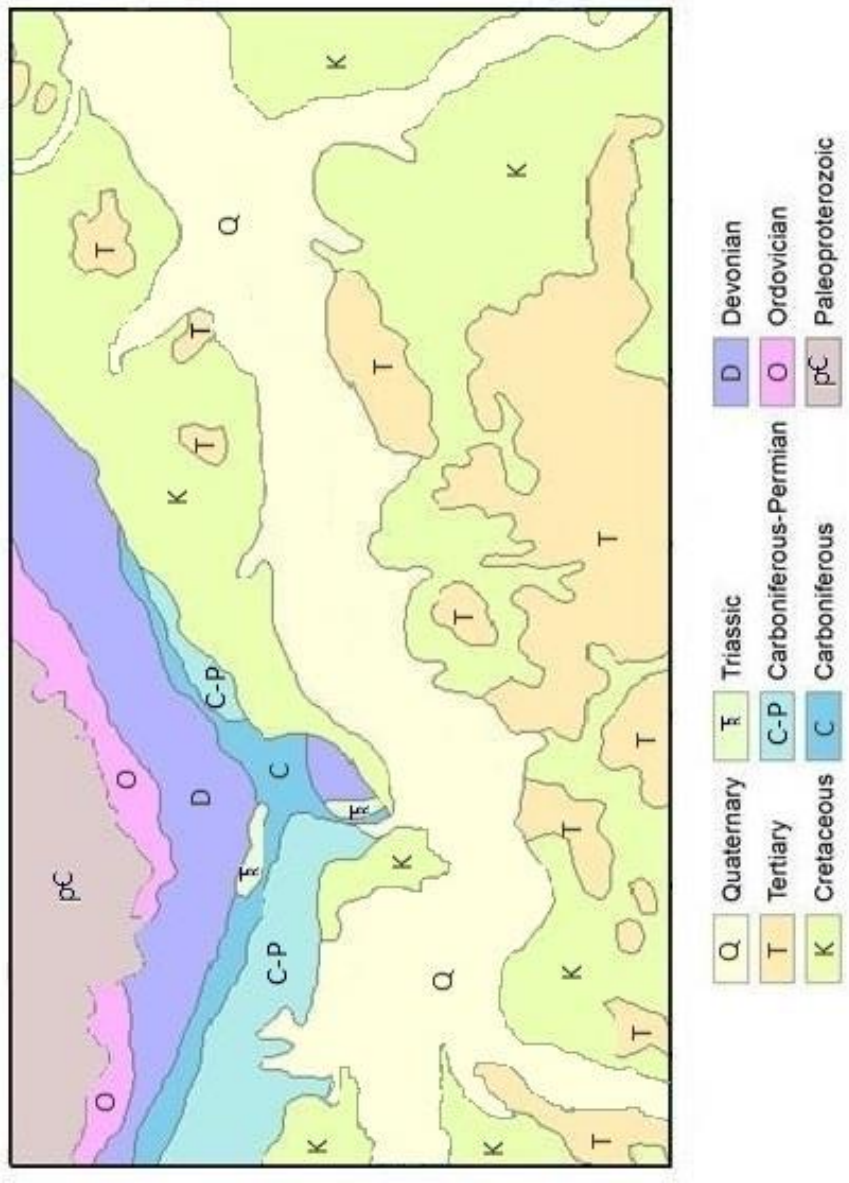

Geological Survey of Brazil (CPRM) (2011)

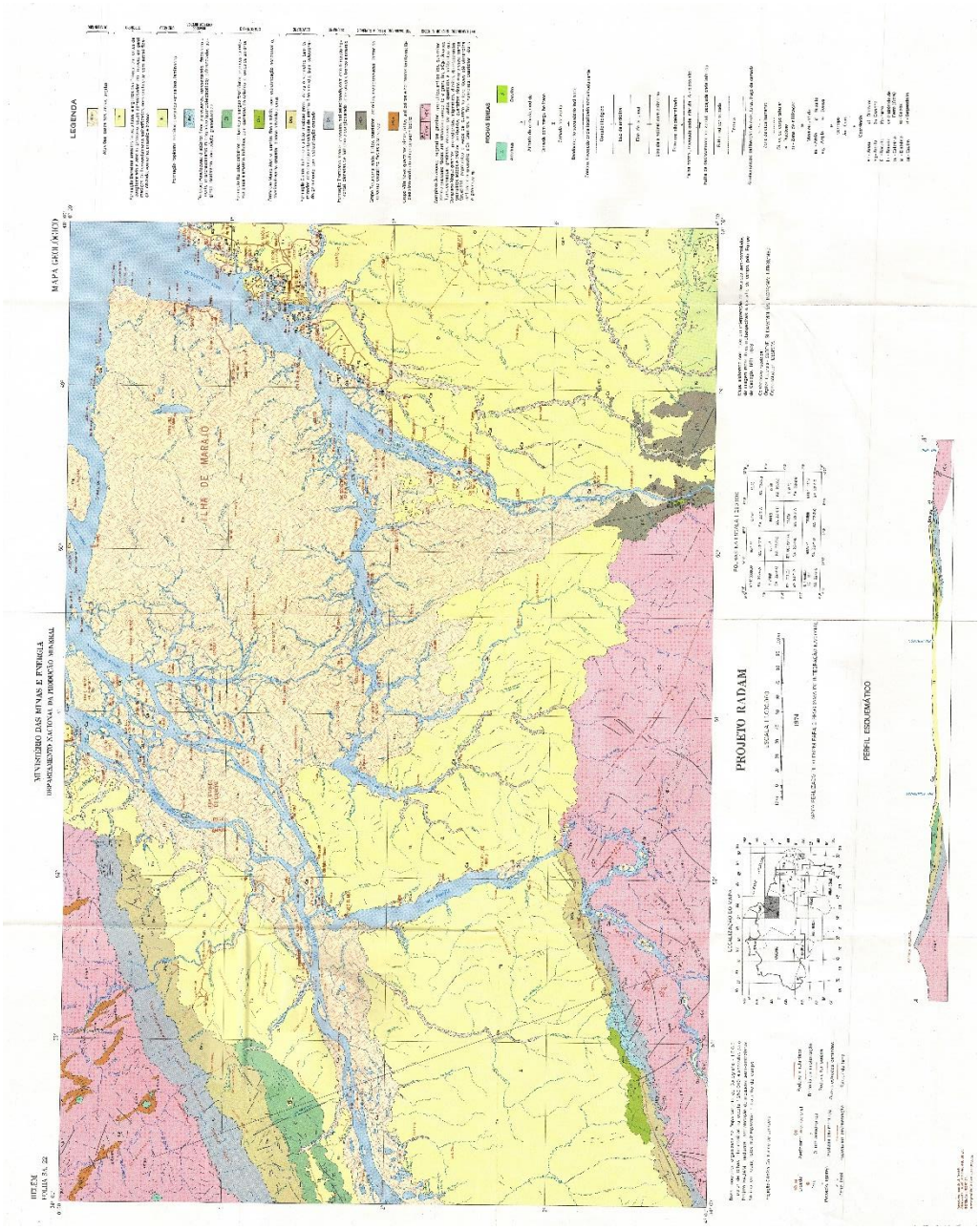

RADAMBRASIL (1974)

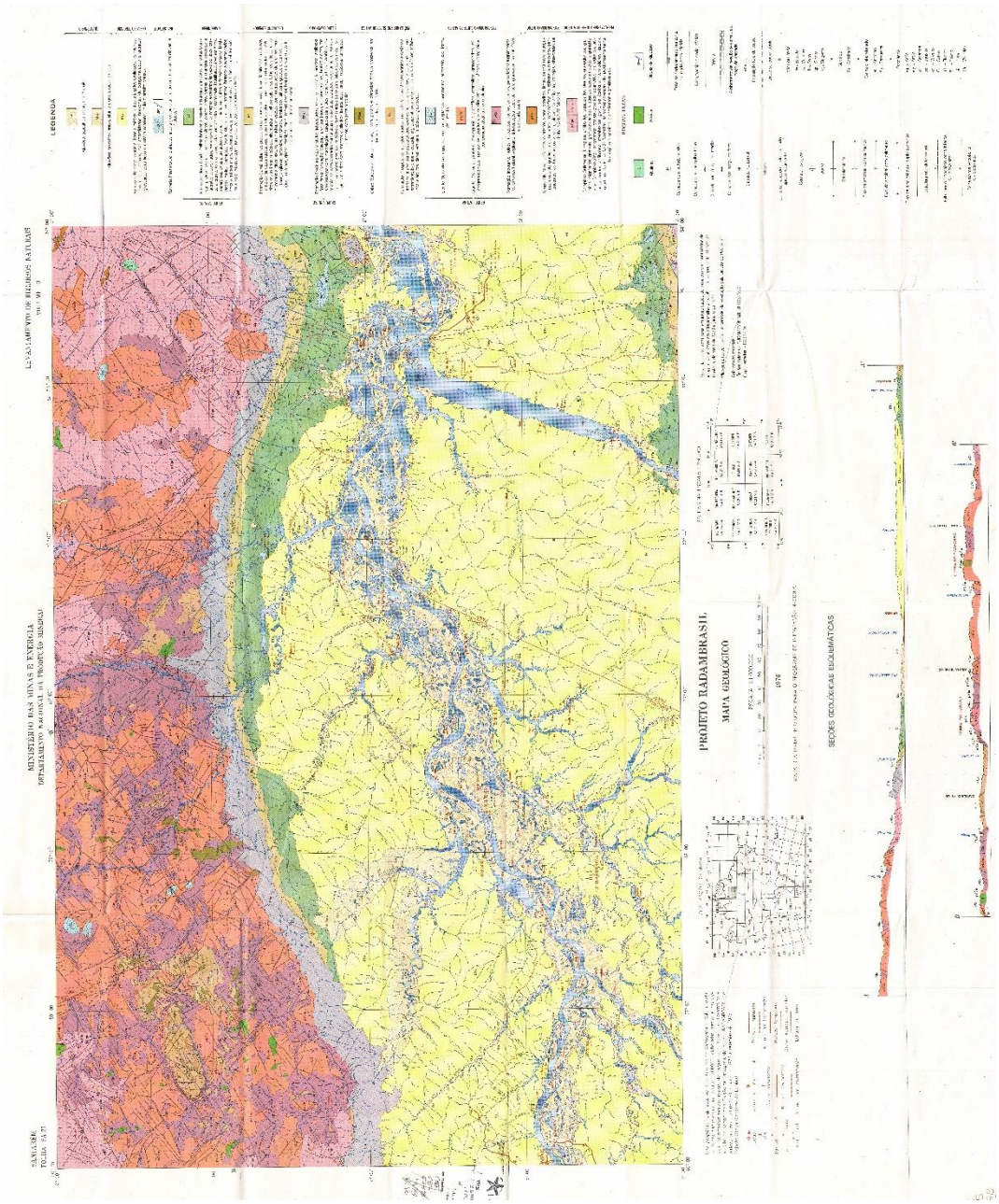

RADAMBRASIL (1976)

Appendix 3 – Geomorphologic Maps

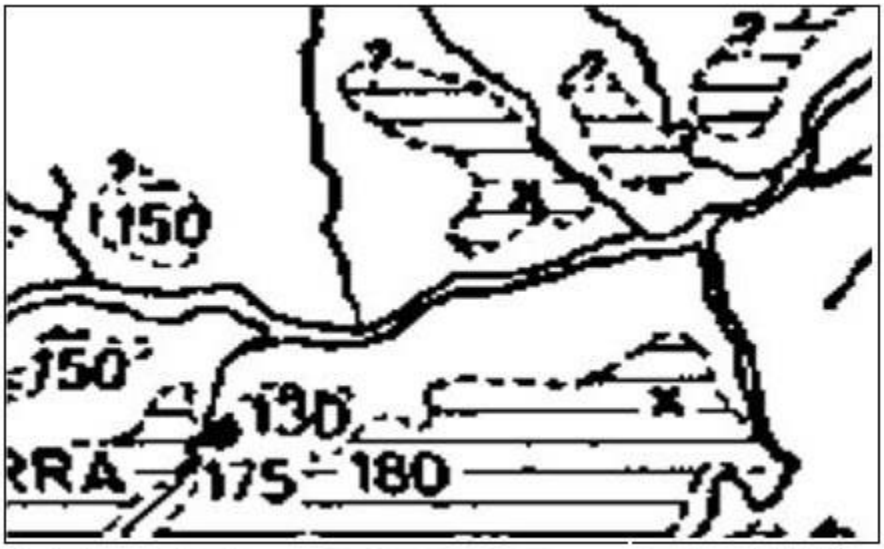

- Amazon Planalto — Sombroek (1966)

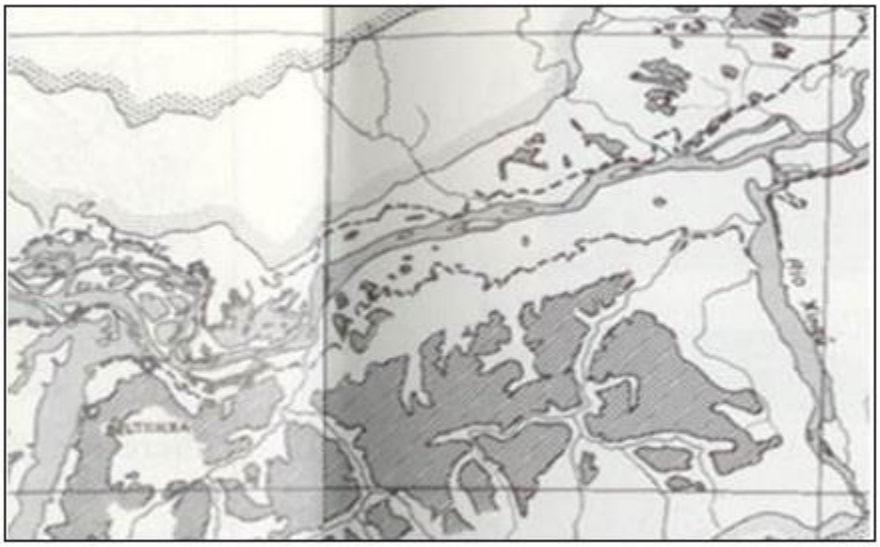

- Belterra Plateau — Klammer (1984)

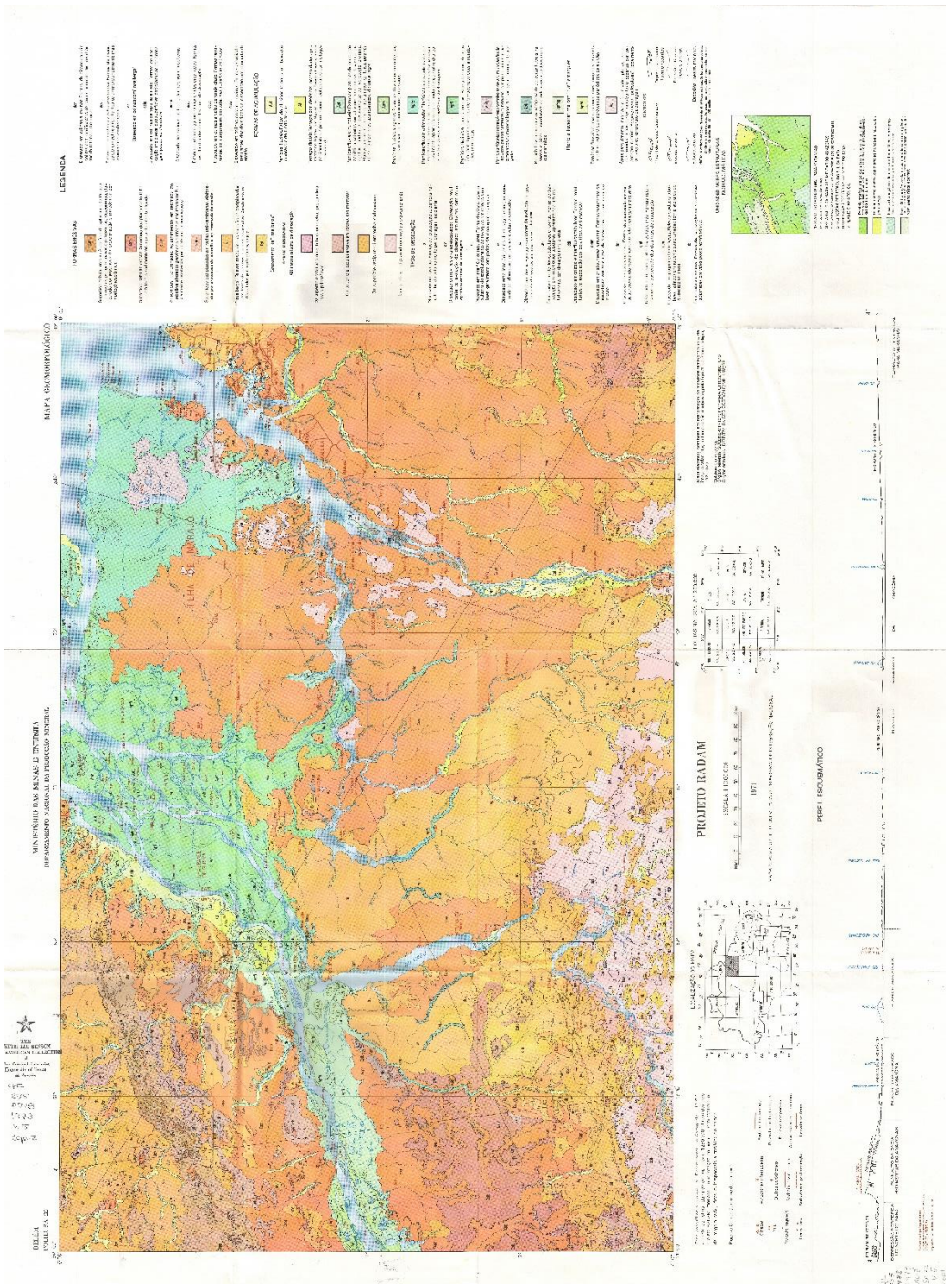

RADAMBRASIL (1974)

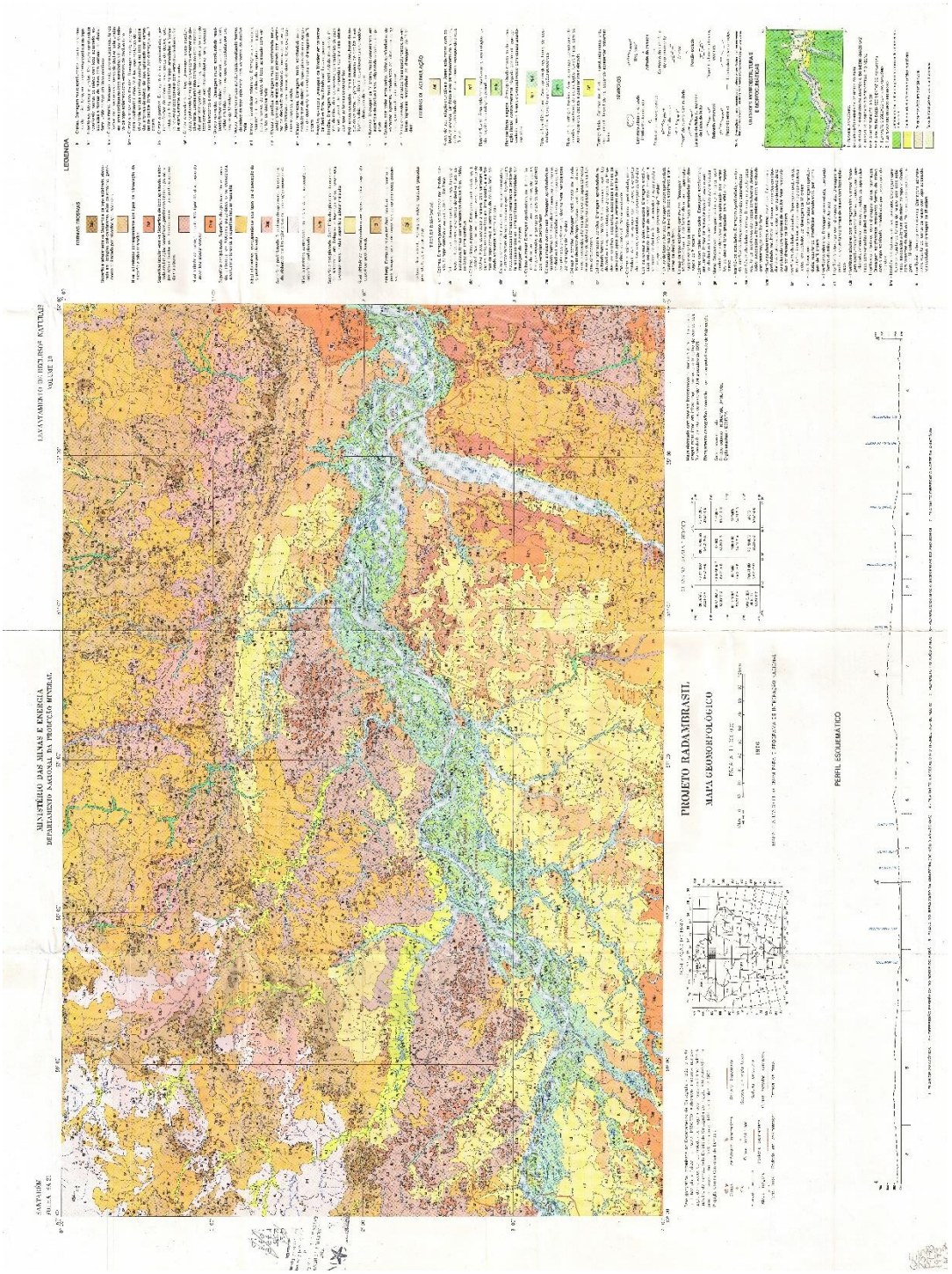

RADAMBRASIL (1976)

References

Ab'Saber, A. N. (1967). Problemas geomorfológicos da Amazônia brasileira. *Atas do Simpósio sobre a Biota Amazônica. Rio de Janeiro, Conselho Nacional de Pesquisa*, 35-67.

Almeida de, F. F. M., Hasui, Y., de Brito Neves, B. B., & Fuck, R. A. (1981). Brazilian structural provinces: an introduction. *Earth-Science Reviews*, *17*(1), 1-29.

Almeida de, F. F., Hasui, Y., & Neves, B. B. D. B. (1976). The upper precambrian of South America. *Boletim IG-USP*, *7*, 45-80.

Antoine, P., Lautridou, J. P., & Laurent, M. (2000). Long-term fluvial archives in NW France: response of the Seine and Somme rivers to tectonic movements, climatic variations and sea-level changes. *Geomorphology*, *33*(3), 183-207.

Baugh, C. A., Bates, P. D., Schumann, G., & Trigg, M. A. (2013). SRTM vegetation removal and hydrodynamic modeling accuracy. *Water Resources Research*, *49*(9), 5276-5289.

Braun, J. (2010). The many surface expressions of mantle dynamics. *Nature Geoscience*, *3*(12), 825-833.

Bridgland, D., & Westaway, R. (2008). Climatically controlled river terrace staircases: a worldwide Quaternary phenomenon. *Geomorphology*, *98*(3), 285-315.

Büdel, J. (1977). *Klima-geomorphologie*. Berlin: Borntraeger.

Campbell Jr, K. E., Frailey, C. D., & Romero-Pittman, L. (2006). The Pan-Amazonian Ucayali Peneplain, late Neogene sedimentation in Amazonia, and the birth of the modern Amazon River system. *Palaeogeography, Palaeoclimatology, Palaeoecology*, *239*(1), 166-219.

Caputo, M. V. (2011). Discussão sobre a Formação Alter do Chão eo Alto de Monte Alegre. *Contribuição à Geologia da Amazônia, Manaus, SBG/Núcleo Norte*, *7*, 7-23.

Carabajal, C. C., & Harding, D. J. (2006). SRTM C-band and ICESat laser altimetry elevation comparisons as a function of tree cover and relief. *Photogrammetric Engineering and Remote Sensing*, *72*(3), 287-298.

Carvalho, T. M. D., & Latrubesse, E. M. (2010). Aplicação de modelos digitais do terreno (MDT) em análises macrogeomorfológicas: o caso da bacia hidrográfica do Araguaia. *Revista Brasileira de Geomorfologia*, *5*(1).

Castleden, R. (1980). Fluvioperiglacial pedimentation: A general theory of fluvial valley development in cool temperate lands, illustrated from western and central Europe. *Catena*, *7*(2), 135-152.

Cordani, U. G., Amaral, G., & Kawashita, K. (1973). The precambrian evolution of South America. *Geologische Rundschau*, *62*(2), 309-317.

Cordani, U. G., & Sato, K. (1999). Crustal evolution of the South American Platform, based on Nd isotopic systematics on granitoid rocks. *Episodes-Newsmagazine of the International Union of Geological Sciences*, *22*(3), 167-173.

Costa, J. B. S., Léa Bemerguy, R., Hasui, Y., & da Silva Borges, M. (2001). Tectonics and paleogeography along the Amazon River. *Journal of South American Earth Sciences*, *14*(4), 335-347.

COSTA, J., Hasui, Y., Bemerguy, R. L., Soares-Junior, A. V., & Villegas, J. (2002). Tectonics and paleogeography of the Marajó Basin, northern Brazil. *Anais da Academia Brasileira de Ciências*, *74*(3), 519-531.

Daemon, R.F. & Contreiras, J.A., 1971. Zoneamento palinologico da Bacia do Amazonas. Soc. Bras. Geol., 3 : 79-88.

Dennen, W. H., & Norton, H. A. (1977). Geology and geochemistry of bauxite deposits in the lower Amazon basin. *Economic Geology*, *72*(1), 82-89.

Dawson, M. R., & Gardiner, V. (1987). River Terraces: The General Model and a Paleohydrological and Sedimentological Interpretation of the Terraces of the Lower Severn. *Palaeohydrology in Practice: A River Basin Analysis. John Wiley and Sons New York. 1987. p 269-305, 6 fig, 2 tab, 57 ref. IGCP Project*, (158).

Day, T. H. (1959). Guide to the classification of the late tertiary and quaternary soils of the lower Amazon Valley. *FAO—55 p. il*.

Emiliani, C. (1957). Paleotemperature analysis of core 280 and Pleistocene correlations. *The Journal of Geology*, 264-275.

Fairbridge, R. W. (1961). Eustatic changes in sea level. *Physics and Chemistry of the Earth*, *4*, 99-185.

Figueiredo, J., Hoorn, C., Van der Ven, P., & Soares, E. (2009). Late Miocene onset of the Amazon River and the Amazon deep-sea fan: Evidence from the Foz do Amazonas Basin. *Geology*, *37*(7), 619-622.

Filizola, N., & Guyot, J. L. (2009). Suspended sediment yields in the Amazon basin: an assessment using the Brazilian national data set. *Hydrological processes*, *23*(22), 3207-3215.

Fisk, H. N. (1944). *Geological investigation of the alluvial valley of the lower Mississippi River* (p. 78). War Department, Corps of Engineers.

Geologico, S., & Brasil–CPRM, D. O. Relatorio Diagnostico Aquifero Alter Do Chao No Estado Do Para Bacia Sedimentar Do Amazonas.

Gorini, C., Haq, B. U., dos Reis, A. T., Silva, C. G., Cruz, A., Soares, E., & Grangeon, D. (2013). Late Neogene sequence stratigraphic evolution of the Foz do Amazonas Basin, Brazil. *Terra Nova*.

Gourou, P. (1949). Observações geográficas na Amazônia. *Revista Brasileira de Geografia*, *11*, 355-408.

Guerra, A.T. (1959) Biblioteca Geografica Brasileira., Conselho Nacional de Geografia, Vol. 15, Rio de Janeiro, Brazil.

Grubb, P. L. C. (1979). Genesis of bauxite deposits in the lower Amazon basin and Guianas coastal plain. *Economic geology*, *74*(4), 735-750.

Hartt, C. F. (1874). *Preliminary Report of the Morgan Expedition, 1870-1871: Report of a Reconnoissance of the Lower Tapajos* (Vol. 1, No. 1). Printed at the University Press.

Hoorn, C. (1994). An environmental reconstruction of the palaeo-Amazon river system (Middle-Late Miocene, NW Amazonia). *Paleogeography, Palaeoclimatology, Palaeoecology, 112(3),* 187-238.

Hoorn, C., Guerrero, J., Sarmiento, G. A., & Lorente, M. A. (1995). Andean tectonics as a cause for changing drainage patterns in Miocene northern South America. *Geology*, *23*(3), 237-240.

Hoorn, C., Wesselingh, F. P., Ter Steege, H., Bermudez, M. A., Mora, A., Sevink, J., ... & Antonelli, A. (2010). Amazonia through time: Andean uplift, climate change, landscape evolution, and biodiversity. *science*, *330*(6006), 927-931.

Irion, G. (1984). Sedimentation and sediments of Amazonian rivers and evolution of the Amazonian landscape since Pliocene times. In *The Amazon* (pp. 201-214). Springer Netherlands.

Irion, G., Müller, J., de Mello, J. N., & Junk, W. J. (1995). Quaternary geology of the Amazonian lowland. *Geo-Marine Letters*, *15*(3-4), 172-178.

Katzer, F. (1903). *Grundzüge der geologie des unteren Amazonasgebietes (des staates Pará in Brasilien)*. M. Weg.

Klammer, G. (1971). Über plio-pleistozäne Terrassen und ihre Sedimente im unteren Amazonasgebiet. *Z. Geomorph*, *15*, 62-106.

Klammer, G., & de Janeiro, Z. R. (1975). Beobachtungen an Hangen im tropischen Regenwald des unteren Amazonas. *Z. Geomorph. NF*, *19*(3), 273-286.

Klammer, G. (1978). Reliefentwicklung im Amazonasbecken und plio-pleistozäne Bewegungen des Meeresspiegels. *Z. Geomorph. NF*, *22*(4), 390-416.

Klammer, G. (1981). Landforms, cyclic erosion and deposition, and Late Cenozoic changes in climate in southern Brazil. *Zeitschrift für Geomorphologie NF*, *25*(2), 146-165.

Klammer, G. (1984). The relief of the extra-Andean Amazon basin. In *The Amazon* (pp. 47-83). Springer Netherlands.

Krantz, D. E. (1991). A chronology of Pliocene sea-level fluctuations: The US Middle Atlantic Coastal Plain record. *Quaternary Science Reviews*, *10*(2), 163-174.

Kroemmelbein, K. (1967). Devonian of the Amazonas basin, Brazil.

Latrubesse, E. M., Stevaux, J. C., & Sinha, R. (2005). Tropical rivers. *Geomorphology*, *70*(3), 187-206.

Latrubesse, E. M. (2012). Amazon lakes. *Encyclopedia of Lakes and Reservoirs*, 13-26.

Latrubesse, E. M. (1997). Paleoenvironmental. Model for the Late Cenozoic of Southwestern Amazon: Paleontology and Geology. *Acta Amazonica*, *27*(2), 103-118.

Latrubesse, E. M., da Silva, S. A., Cozzuol, M., & Absy, M. L. (2007). Late Miocene continental sedimentation in southwestern Amazonia and its regional significance: Biotic and geological evidence. *Journal of South American Earth Sciences*, *23*(1), 61-80.

Latrubesse, E. M., Cozzuol, M., da Silva-Caminha, S. A., Rigsby, C. A., Absy, M. L., & Jaramillo, C. (2010). The Late Miocene paleogeography of the Amazon Basin and the evolution of the Amazon River system. *Earth-Science Reviews*, *99*(3), 99-124.

Latrubesse, E. M., & Restrepo, J. D. (2014). Sediment yield along the Andes: continental budget, regional variations, and comparisons with other basins from orogenic mountain belts. *Geomorphology*, *216*, 225-233.

Latrubesse, E. M., da Silva, S. A., Cozzuol, M., & Absy, M. L. (2007). Late Miocene continental sedimentation in southwestern Amazonia and its regional significance: Biotic and geological evidence. *Journal of South American Earth Sciences*, *23*(1), 61-80.

Leopold, L. B., & Bull, W. B. (1979). Base level, aggradation, and grade. *Proceedings of the American Philosophical Society*, 168-202.

Mackin, J. H. (1948). Concept of the graded river. *Geological Society of America Bulletin*, *59*(5), 463-512.

Maddy, D., & Bridgland, D. R. (2000). Accelerated uplift resulting from Anglian glacioisostatic rebound in the Middle Thames Valley, UK?: evidence from the river terrace record. *Quaternary Science Reviews*, *19*(16), 1581-1588.

Marbut, C. F., & Manifold, C. B. (1925). The topography of the Amazon Valley. *Geographical Review*, *15*(4), 617-642.

Martinelli, L. A., Victoria, R. L., Devol, A. H., Richey, J. E., & Forsberg, B. R. (1989). Suspended sediment load in the Amazon Basin: an overview. *GeoJournal*, *19*(4), 381-389.

Matoshko, A. V., Gozhik, P. F., & Danukalova, G. (2004). Key Late Cenozoic fluvial archives of eastern Europe: the Dniester, Dnieper, Don and Volga. *Proceedings of the Geologists' Association*, *115*(2), 141-173.

Melo, J. H. G., & Loboziak, S. (2003). Devonian–Early Carboniferous miospore biostratigraphy of the Amazon Basin, Northern Brazil. *Review of Palaeobotany and Palynology*, *124*(3), 131-202.

Mendes, A. C., Truckenbrod, W., & César Rodrigues Nogueira, A. (2012). Análise faciológica da Formação Alter do Chão (Cretáceo, Bacia do Amazonas), próximo à cidade de Óbidos, Pará, Brasil. *Revista Brasileira de Geociências*, *42*(1), 39-57.

Merritts, D. J., Vincent, K. R., & Wohl, E. E. (1994). Long river profiles, tectonism, and eustasy: a guide to interpreting fluvial terraces. *Journal of Geophysical Research: Solid Earth (1978–2012)*, *99*(B7), 14031-14050.

Mertes, L. A., & Dunne, T. (2008). Effects of tectonism, climate change, and sea-level change on the form and behaviour of the modern Amazon River and its floodplain. *Large Rivers: Geomorphology and Management, A Gupta (Ed.) John Wiley and Sons: West Sussex, UK*, 115-144.

Mertes, L. A., Dunne, T., & Martinelli, L. A. (1996). Channel-floodplain geomorphology along the Solimões-Amazon river, Brazil. *Geological Society of America Bulletin*, *108*(9), 1089-1107.

Milani, E. J., & Zalan, P. V. (1999). An outline of the geology and petroleum systems of the Paleozoic interior basins of South America. *Episodes*, *22*, 199-205.

Miller, K. G., Kominz, M. A., Browning, J. V., Wright, J. D., Mountain, G. S., Katz, M. E., ... & Pekar, S. F. (2005). The Phanerozoic record of global sea-level change. *science*, *310*(5752), 1293-1298.

Mosmann, R., Falkenhein, F. U., Goncalves, A., & Nepomuceno Filho, F. (1986). Oil and gas potential of the Amazon Paleozoic basins.

Park, E., & Latrubesse, E. M. (2012, December). Mega-pattern Analysis of Suspended Sediments Distribution in the Amazon River Using Multi-temporal Satellite Imageries. In *AGU Fall Meeting Abstracts* (Vol. 1, p. 0975).

Pike, R. J. (2000). Geomorphometry-diversity in quantitative surface analysis. *Progress in Physical Geography*, *24*(1), 1-20.

Potter, P. E. (1997). The Mesozoic and Cenozoic paleodrainage of South America: a natural history. *Journal of South American Earth Sciences*, *10*(5), 331-344.

Räsänen, M. E., Linna, A. M., Santos, J. C., & Negri, F. R. (1995). Late Miocene tidal deposits in the Amazonian foreland basin. *Science*, *269*(5222), 386-390.

Radambrasil, P. (1974). Projeto Radambrasil. *Folha SA*, *22*.

Radambrasil, P. (1977). Projeto Radambrasil. *Folha SC*, *18*.

Riccomini, C., & Assumpção, M. (1999). Quaternary tectonics in Brazil. *Episodes*, *22*, 221-225.

Rodriguez, E., Morris, C. S., & Belz, J. E. (2006). A global assessment of the SRTM performance. *Photogrammetric engineering and remote sensing*, *72*(3), 249-260.

Rossetti, de Fátima., D., Mann de Toledo, P., & Góes, A. M. (2005). New geological framework for Western Amazonia (Brazil) and implications for biogeography and evolution. *Quaternary research*, *63*(1), 78-89.

Saadi, A., Machette, M. N., Haller, K. M., Dart, R. L., Bradley, L., & Souza, A. M. P. D. (2003). *Map and database of Quaternary faults and lineaments in Brazil*. US Geological Survey.

Sakamoto, T., 1960, Rock weathering on the "Terra Firmes" and deposition on "Varzeas" in the Amazon: Tokyo Univ.,Jour. Fac. Sci. v. 12, no. 2, sec. II, p. 155-216.

Salati, E., & Vose, P. B. (1984). Amazon basin: a system in equilibrium. *Science*, *225*(4658).

Schumm, S. A., & Brakenridge, G. R. (1987). River responses. *North America and adjacent oceans during the last deglaciation*, *3*, 221-240.

Simard, M., Pinto, N., Fisher, J. B., & Baccini, A. (2011). Mapping forest canopy height globally with spaceborne lidar. *Journal of Geophysical Research: Biogeosciences (2005–2012)*, *116*(G4).

Sombroek, W. G. (1966). *Amazon soils* (Doctoral dissertation, Centre for agricultural publications and documentation).

Sombroek, W. (2000). Amazon landforms and soils in relation to biological diversity. *Acta Amazonica*, *30*(1), 81-100.

Talling, P. J. (1998). How and where do incised valleys form if sea level remains above the shelf edge?. *Geology*, *26*(1), 87-90.

Thomas, M. F. (1994). *Geomorphology in the tropics: a study of weathering and denudation in low latitudes*. John Wiley & Sons.

Truckenbrodt, W., Kotschoubey, B., & Schellmann, W. (1991). Composition and origin of the clay cover on North Brazilian laterites. *Geologische Rundschau*, *80*(3), 591-610.

Vandenberghe, J. (1995). Timescales, climate and river development. *Quaternary Science Reviews*, *14*(6), 631-638.

Vital, H., & Stattegger, K. (2000). Lowermost Amazon River: evidence of late Quaternary sea-level fluctuations in a complex hydrodynamic system. *Quaternary international*, *72*(1), 53-60.

Vital, H., Stattegger, K., Posewang, J., & Theilen, F. (1998). Lowermost Amazon River: morphology and shallow seismic characteristics. *Marine geology*, *152*(4), 277-294.

Walstra, J., Heyvaert, V. M. A., & Verkinderen, P. (2010). Assessing human impact on alluvial fan development: a multidisciplinary case-study from Lower Khuzestan (SW Iran). *Geodinamica Acta*, *23*(5-6), 267-285.

Waters, M. R. (1985). Late Quaternary alluvial stratigraphy of Whitewater Draw, Arizona: Implications for regional correlation of fluvial deposits in the American Southwest. *Geology*, *13*(10), 705-708.

Westaway, R., & Bridgland, D. (2007). Late Cenozoic uplift of southern Italy deduced from fluvial and marine sediments: coupling between surface processes and lower-crustal flow. *Quaternary International*, *175*(1), 86-124.

Wilson, M., Bates, P., Alsdorf, D., Forsberg, B., Horritt, M., Melack, J., ... & Famiglietti, J. (2007). Modeling large-scale inundation of Amazonian seasonally flooded wetlands. *Geophysical Research Letters*, *34*(15).